Discrete DNA Integration Events During Bridge-Induced Translocation Generate Partial Chromosomal Deletions and Differential Aneuploidy in *Saccharomyces cerevisiae*

Thesis

UNRESTRICTED

Discrete DNA integration events during Bridge-Induced Translocation generate partial chromosomal deletions and differential aneuploidy in *Saccharomyces cerevisiae*

Thesis submitted for the degree of

Doctor of Philosophy

by

Pawan Noel

International Centre for Genetic Engineering and Biotechnology, Trieste, Italy

In accordance with

The Open University, UK

September 2010

Direct Supervisor: Professor Carlo V Bruschi

External Supervisor: Professor Edward J Louis

Date of Submission: 21 July 2010

Date of Award: 15 October 2010

ProQuest LLC.
789 East Eisenhower Parkway
P.O. Box 1346
Ann Arbor, MI 48106 – 1346

Dedicated to

My loving parents

Edwin and Satya

Sister **Soni**

Brother **Sanjeev**

My lovely sweetheart **Irene**

and in loving memory of **Naaniji**

Acknowledgements

It has been a wonderful four-year journey and experience in Trieste since October 2006, when I joined the ICGEB PhD program. Firstly, I would like to thank the institute and all its past and current members who strive to provide excellent training grounds for young emerging researchers, and stand up to the institutional initiative. I am extremely thankful and owe gratitude to my boss, Carlo V Bruschi, who provided me this opportunity in his laboratory. To learn science from him was almost always joyously accompanied by his life experiences (vast range), men's jokes and especially the morning movie trivia to an extent, that I once ironically remarked saying, "Prof.!! ... I don't know about molecular biology, but at the end of my PhD I'll definitely know more about movies". Not being a regular movie watcher myself, we burst into laughter to start our day. The whiteboard aided lessons in lab on classical genetics eg Roman effect, colony sectoring etc will be among the unforgettable memories and moments spent with my humorous Italian PhD guide.

I'm indebted to my ex-boss and current co-supervisor, Ed Louis, for always being extremely helpful in providing essential feedback, support and supervision whenever we have met in Italy or in the UK and throughout the course of my PhD. Second to none, I've had a great start of my experimental career and a super time in the lab during my Master's degree with Marcus Marvin, my great British friend and "Master". I still cant forget the taste of the best Ales we had on a riverside pub once with Pat, and indeed the 26-hour long array printing experiment in Leicester during which all night we shared watching pictures of our hometowns in an attempt to keep awake after a big fat spicy Indian meal. Gianni Litti has been a great person to know and share moments of my brief intermittent Italian speaking attempts.

I cannot find words to thank my dear friend and brother, Amit Dipak Amin, a wonderfully nice and good hearted, hard working intelligent person. We've always had such unforgettable times. I cannot thank him enough for sending me weird and funny email forwards and video links for watching streaming Cricket matches, all to brighten up my days in Trieste while he was dissecting yeast spores in Leicester. Respect to you bro, and God bless you in life wherever you go! Ariful Haque has been a great flatmate and buddy in both Leicester and Trieste and I'm sure he wont forget the first crazy weeks of our lives, when we moved into Trieste.

I want to thank my lab members in Trieste, who have been the daytime family all these four years. I must thank Valentina Tosato for all her initial and continued help with lab matters and discussions. A big thank-you to the ever so patient and gentle Beatrice Rossi, who has always

been available for a chat and discussion and from whom I've learnt many things while we prepared our manuscript. I will miss Fillipo Marcassoli (Pippo) and Andrea Aresu (PBS – Italian abbreviation for Piccolo B*****do Sardo) who have been excellent buddies and wonderful partying companions while they were in Trieste, and Dmitri Nikitin who has been my sole companion in a few but memorable games of pool. I appreciate very much Kreso's (Kresimir Gjuracic) friendliness who borrowed me a great set of DVDs to keep me entertained in the days I was writing all this up and for his time to have short coffee breaks in between. There is one person who I will miss the most and he is my wonderful Polish friend Remigiuz Arnak (Pazzo Polako). I could write page after page about all the stupid and funny things we did together in the lab and after, but I will always cherish every moment of my life that I spent with him. I wish him the best of the best in every aspect of life from the core of my heart! Last but not the least, I have enjoyed working with and teaching my first student Elisa Martelletti, who has been a brilliant, cheerful and hardworking student and I wish her all the best for her future career. I will miss shouting across-the-lab salutations to Patrizia Zori and all chats in which she helped improve my still-broken Italian speaking skills.

My colleagues Sailesh Bajpai, Tibor Pastor and Zulma Suarez will be not only be remembered as people who have been with me from the first day of my life in Trieste, but those who always stood by me in the difficult moments to share comforting and encouraging thoughts. I'm glad to have met Nisha Narayan (now happily Mrs Nisha Pegoraro) who has been such an inspiring personality from both professional and personal perspectives and by whom I've been lucky enough to be called "Bhai". I'm honoured to meet Lawrence Banks who has been really friendly and provided encouragement and it's been great to be neighbors with his lab. I thank Noor Gammoh, Vjeko, "Mr Kazu", David Pim, Miranda Thomas, Vanitha KS and Cristian, Giulia, Iris, Juan and Vittorio Venturi for their friendly gestures in the lab corridors. I must thank Ania, Mircea and Fabio especially for the magnificent time we had hiking up Mt. Triglav, and all the ICGEB football team for out-of-lab fun. Leisure lunch breaks with others and two beautiful friends Elisa Palladino and Francesca Scognamiglio will be missed always.

Some other ICGEB people who truly deserve a thank you are Giorgia Danelon, Tiziana, Carlo Gregori, Antonio Tommasini, Sanjay Pahwah, Suzanne Kerbavcic and Marella Prata. I also thank all other ICGEB colleagues who provided a friendly working atmosphere and have shared a laugh or joke with me. With this, I acknowledge all my friends back home in India and in the UK or abroad, especially Vishal, Vijay, Varun, Yogen, Kuldeep, Manju, Bhopesh, Aman, Sandeep, Mandeep, Samarth, Saurabh, Sushant and Akhilesh who have remotely offered moral support.

The one person, who deserves the biggest thank you and even more, is the love of my life Irene, whom I met here at ICGEB, Trieste (actually in the bus no. 51). I cannot imagine how all these four years would have been without her constant love and care. She has been a pillar of support and kept me on my toes to face challenges purely by love, encouragement, criticism and discussion every single day of this journey. This was complemented by frequent family visits to Padova, where Mamma, Beppe and Arianna gave real relaxed Italian family environment and support. I owe them my respect always.

I cannot pen down, before I express my deepest gratitude to my entire family in India who have been the reason behind this and without whom all this would have been impossible. I've been able to do this because of all the hardwork my parents Edwin and Satya have put in to teach and give unfailing love, care, support, morality, enthusiasm, joy and togetherness all my life. My sister Soni, Sunita didi and brother Sanjeev, along with my cousins Robin and Rohini, have played their part in their own special ways, which I can only be lucky to have, and be really proud of. I sadly miss my grandmother, who passed away while I seeked knowledge, but I'm sure now she is a happy person looking down on me, with all her prayers answered, as I take another step of success.

Lastly, I apologize if I've missed anyone here, but if you've been a friend, companion, peer or acquaintance during my stay in Trieste, I thank you for the very moment you were with me.

Thank you all who have been a part of these unforgettable four years in Trieste.

Abstract

Chromosome aberrations and genome instability have a long history of being associated with human genetic diseases, including cancer. The feasibility to drastically reshape the genome with a single chromosomal translocation also gives this molecular event a powerful capacity to drive evolution. To date, numerous assays have been developed to study gross chromosomal rearrangements (GCRs), although the molecular mechanisms underlying GCRs remain unclear. Here, we have used the Bridge Induced Translocation (BIT) method to induced non-reciprocal translocations in *Saccharomyces cerevisiae* and to provide new insights into DNA integration mediated generation of chromosomal abberations and aneuploidy. We have devised a genetic system to monitor DNA integration events ensuing BIT in real time. Upon BIT induction using engineered linear DNA molecules, this system exploits the cellular homologous recombination machinery to allow reconstruction of individual fluorescent markers GFP and DsRed placed on chromosomes V and III, respectively. Our initial results confirm that targeted DNA integration into sequences placed on yeast chromosomes to allow BIT occurs infrequently in a two step process, resulting mostly in one-sided events scored as a single fluorescent signal.

We have carried out BIT between chromosomes XV and IX in diploid wild type and mutant *S. cerevisiae* strains in an attempt to elucidate the molecular regulation of chromosomal bridging in yeast. In wild type cells, the induction of BIT events was intrinsically biased for preferential integration on chromosome IX. This integration bias was significantly altered in *sgs1*, *mre11* and *esc2* knockout backgrounds. We also noticed that a terminal 36Kbp fragment of chromosome IXL arising after BIT induction was lost not only from the translocation participant chromosome, but also from native chromosome IX. This loss was noticed to be more prevalent in the *sgs1* and *esc2* mutants in whom integration bias was also altered. A similar scenario held true for our observations in *ku70* mutants. Our results suggest that DNA integration during BIT events is under redundant regulation, possibly during DNA replication, and non-reciprocal translocations arising as such may further lead to secondary aberrations when this regulation is compromised.

We also describe at the molecular level, ten morphologically and physiologically different translocants ensuing from the induction of the same BIT event between chromosomes XVI and IX. We have demonstrated that despite their common origin from the integration of the same linear DNA construct, all ten translocation-carrying strains have different phenotypes, ability to sporulate, regulation of gene expression and morphology. Our observations provide insights on how heterogeneous phenotypic variations originate from the same initial genomic event. We show eight different ways in which yeast cells have dealt with a single initial event inducing translocation leading to variable aneuploidies in these cells. Thus despite harboring common translocation breakpoints, we noticed a distinct and separable pattern of chromosomal rearrangements among these translocant strains. Our results are in agreement with the formation of complex rearrangements and abnormal karyotypes described in many leukemia patients, thus confirming the modelistic value of the yeast BIT system for mammalian cells.

Contents

List of Abbreviations

AML	Acute Myeloid Leukaemia
ARMs	At-risk motifs
ATP	Adenosine Tri-Phosphate
5-FOA	5-Fluororotic Acid
BER	Base Excision Repair
B/F/B	Breakage Fusion Bridge
BIR	Break Induced Replication
BIT	Bridge Induced Translocation
bp	Base Pair
BME	β-Mercapto-Ethanol
CENs	Centromeres
CF	chromosomal fragments
CI	Chloroform Isoamyl alcohol
CIN	Chromosome instability
CHEF	Clamped Homogenous Electric Field
CML	Chronic Myeloid Leukaemia
CVF	Chromosomal fragmentation vector
DAPI	4',6-diamidino-2-phenylindole
DDR	DNA damage response
DIG	Digoxygenin
DNA	Deoxyribonucleic Acid
DNA-PK_{cs}	Deoxyribonucleic Acid Protein kinase catalytic subunit
dNTPs	Deoxyribonucleoside Triphosphates
DSB	Double-Strand Break
DSBR	Double Strand Break Repair
DsRed	*Discosoma* species red fluorescent protein
dsDNA	Double Stranded DNA
E. coli	*Escherichia coli*
EDTA	Ethylenediaminetetraacetic Acid
FRT	Flp-recognition target
FoSTeS	Fork Stalling Template Switching
G418	Geneticin
GFP	Green florescent protein
GIN	Genome Instability
GC	Gene conversion
GCRs	Gross Chromosomal Rearrangements
HCl	Hydrochloric Acid
hDNA	heteroduplex Deoxyribonucleic Acid
HR	Homologous Recombination
IAA	Isoamyl alcohol
Ig	Immunoglobulin
Kbp	Kilo Base Pair
LB	Luria Broth
LCRs	Low copy repeats
LiAc	Lithium acetate

LINEs	Long interspersed repeat elements
LOH	Loss of Heterozygosity
mM	mile-molar
MMR	Mismatch Repair
MMS	Methyl methane sulfonate
MRX/MRN complex	Mre11-Rad50-Xrs2/ Mre11-Rad50- Nbs2 complex
NER	Nucleotide Excision Repair
NHEJ	Non-Homologous End Joining
NLS	Nuclear Localisation Signal
ORF	Open reading frame
PCNA	Proliferating Cell Nuclear Antigen
PCR	Polymerase Chain Reaction
PEG	Polyethylene Glycol
PFGE	Pulsed field gel electrophoresis
PIKK	Phosphatidylinositol 3′ kinase-like kinase
QPCR	Quantitative polymerase chain reaction
rDNA	Ribosomal Deoxyribonucleic Acid
REC	Recombination Execution Checkpoint
RF	Replication Fork
RFC	Replication Factor C
RG-BIT	Red Green Bridge Induced Translocation
RNA	Ribonucleic Acid
ROS	Reactive Oxygen Species
RPA	Replication Protein A
RT-PCR	Reverse-transcriptase Polymerase Chain Reaction
rpm	rotations per minute
S. cerevisiae	*Saccharomyces cerevisiae*
SDS	Sodium Dodecyl Sulphate
SDSA	Synthesis Dependent Strand Annealing
SIC	Single Isolated Colony
SINEs	Short interspersed repeat elements
snRNAs	small nuclear Ribonucleic Acid
SSA	Single Strand Annealing
SSC	Sodium Chloride and Sodium Citrate
ssDNA	Single Stranded DNA
TAR	Transcription Associated Recombination
TELs	Telomeres
TNR	Trinucleotide repeats
tRNA	transfer RNA
TBE	Tris-Borate EDTA
TE	Tris-HCl EDTA
UV	Ultra-Violet light
YPD	Yeast Peptone Dextrose
μg	microgram
μM	micromolar
μl	microliter

Introduction

1.1 Genome integrity and maintenance:

Genomes are under constant assault from exogenous and endogenous DNA damaging agents. Nevertheless, all normally dividing cells must accurately replicate and repair their genomes before transmitting them into daughter cells. Failure to do so usually results in the accumulation of mutations and the generation of gross chromosomal rearrangements (GCRs) often leading to aneuploidy, cell death or neoplastic transformation in higher eukaryotes. To avoid such detrimental consequences, processes like DNA replication, damage sensing and repair, and cell cycle progression are tightly coordinated in order to prevent harmful mutations and unrepaired damage from being passed on into daughter cells. To this end, eukaryotes have evolved regulatory and surveillance mechanisms such as cell-cycle checkpoints, which safeguard the genome by sensing damage and triggering repair and thus ensuring faithful replication, segregation and transmission of chromosomes during cell divisions. In humans, defects in these intricately coordinated pathways preserving genome integrity are usually associated with numerous pathological disorders, cancer susceptibility syndromes, premature aging and various inherited diseases.

1.2 Genome instability: forms, causes and consequences:

Genetic instability (GIN) generally refers to a temporal or persistent state of mutational events, many times leading to the generation of gross genomic rearrangements. Genomic instability manifests itself in forms ranging from simple mutations to complex chromosome rearrangements. Additionally, accumulation of these

genetic aberrations over time as ongoing genome instability is associated with many human cancers (HOEIJMAKERS 2001). A diverse plethora of DNA lesions including base modifications and breaks arise in genomes due to three major causes (**Figure 1.1**). Environmental exposure to ultraviolet light from the sun, ionizing radiation and genotoxic compounds cause alterations in the DNA structure leading to mutations if left unrepaired. Normal cellular metabolism involving oxidative respiration and lipid peroxidation can generate more than 100 identified by-products, posing a permanent and integral threat to genome integrity from within. These include reactive oxygen species (ROS) such as hydroxyl radicals, hydrogen peroxide and superoxide anions (FINKEL and HOLBROOK 2000). Additionally, spontaneous hydrolysis and deamination of chemical bonds in DNA can lead to conversion of cytosine, adenine and guanine into miscoding bases such as uracil, hypoxanthine and xanthine (LINDAHL 1993).

Instability leading to mutations like nucleotide substitutions, insertions and deletions is often linked to errors occurring during replication, like replication slippage, a process during which the replicon is confronted by repetitive sequences. This can lead to expansion and contraction of repeat elements, and instability of this type is implicated in more than 40 neurological, neurodegenerative and neuromuscular human disorders (PEARSON *et al.* 2005). Alternatively, such instability can arise upon impairment of mismatch repair (MMR), base excision repair (BER) and nucleotide excision repair (NER) pathways, which correct damages at the level of single DNA bases. MMR defects in humans often lead to sporadic and colorectal cancers, whereas, NER defects have been associated with diseases like xeroderma pigmentosum, Cockayne syndrome and trichothiodystrophy (LEHMANN 2001). On the other hand, genetic instability in the form

of GCRs such as chromosomal translocations, deletions, duplications or inversions lead to changes in the genetic linkage of DNA fragments. Such rearrangements often result under circumstances of increased or defective homologous recombination (HR) mediated events. Alternatively, mutagenic repair of DNA damage by the non-homologous end-joining (NHEJ) pathway can lead to deletions and chromosome fusions by simple ligation of broken DNA molecules. Defects in these various repair pathways have been associated with elevated rates of GCR formation and several human syndromes, some of which are listed in **Table 1.1**. Furthermore, GIN can arise as a consequence of telomere dysfunction, a process leading to breakage/fusion/bridge (B/F/B) cycles that result in DNA amplification and large terminal deletions (BAILEY and MURNANE 2006; MURNANE 2006).

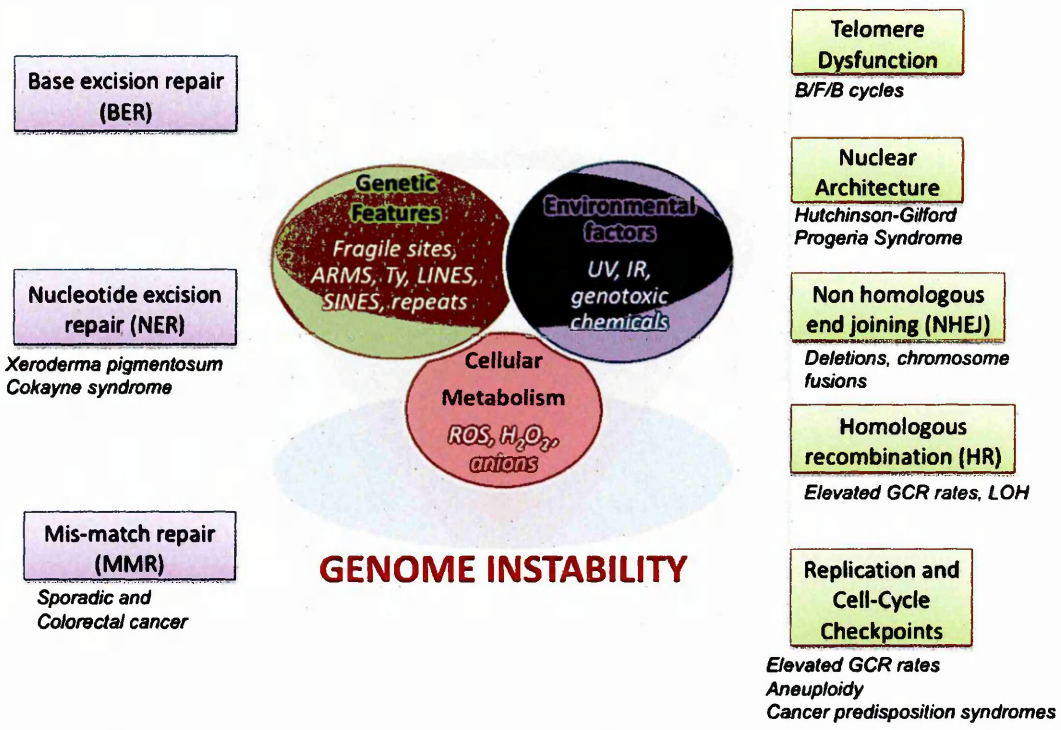

Figure 1.1 Genome instability is caused by a variety of exogenous and endogenous factors responsible for inducing DNA damage. Defects and deregulation of molecular mechanisms involved in DNA metabolism processes causes increased rates of GCR formation and is implicated in the occurrence of many human genetic disorders.

Besides the role of various *trans* acting genes and pathways involved in recombination and repair mechanisms, *cis* acting intrinsic genomic features such as fragile sites and highly transcribed regions have also been associated to high levels of genome instability. For instance, transcription associated recombination (TAR); a phenomenon by which transcription of a certain DNA sequence increases its frequency of recombination has been associated with increased formation of GCRs (AGUILERA 2002; AGUILERA and GOMEZ-GONZALEZ 2008). Moreover, sequence features in the human genome such as: micro and minisatellite repeats, trinucleotide repeats (TNRs), short interspersed repeated elements (SINEs), long interspersed repeated elements (LINEs), inverted repeats, mirror repeats, segmental duplications and dispersed repetitive elements are naturally prone to be unstable due to increased rates of recombination between them (BATZER and DEININGER 2002). Similar sequence features known as at-risk motifs (ARMs) have also been identified in *S. cerevisiae* and are often associated with the generation of chromosomal rearrangements. Such features like inverted repeats, homonucleotide runs, short distance repeats, minisatellites and triplet repeats can give rise to non-canonical DNA structures and thus increase the likelihood of mutations and recombination (GORDENIN and RESNICK 1998). Along the same lines, homologous recombination between Ty elements flanked by long terminal repeat (LTR) sequences is a major source of genetic variation in *S. cerevisiae* (ARGUESO et al. 2008; MIECZKOWSKI et al. 2006). Recently, the role of the nuclear architecture in establishing local higher order chromatin structure, chromatin dynamics as well as the spatiotemporal organization of repair machineries and the sequence elements involved, are emerging as key factors in the maintenance of genome integrity (MISTELI and SOUTOGLOU 2009).

1.3 Aneuploidy, chromosomal rearrangements and cancer:

An alteration in the karyotype of a species seen as variations in euploid chromosome number is known as aneuploidy. Frequently, aneuploidy leads to major developmental defects and has detrimental effects on cellular and organism physiology and fitness. Aneuploidy is often associated with sterility, tumour formation and disease. Polyploidy, on the other hand, refers to a condition of having a chromosome number that is a multiple of more than two times the haploid content. This genetic condition is frequently found in nature and generally does not result in detrimental consequences. Cells can become aneuploid in two major ways: either by errors originating during mitosis leading to whole chromosome loss or gain; or via rearrangements leading to changes in chromosome structure like deletions, amplifications, inversions or translocations.

Moreover, chromosome instability (CIN) leading to genomic rearrangements is caused by defects in chromosome missegregation during mitosis. This can occur due to faults in mitotic checkpoint (or spindle assembly checkpoint) and sister chromatid cohesion functions. Additionally it can occur as a result of improper (merotelic) attachment of kinetochores to spindle pole microtubules, a condition when a single kinetochore binds to both spindle poles (CIMINI 2008), or upon assembly of multipolar spindles. Mutations and deregulation of mitotic checkpoint components has been reported in a subset of human cancers, including types of leukaemia as well as ovarian, colorectal, breast and lung cancer. Aneuploidy resulting from such deregulation is a hallmark genetic feature of solid human tumours. (KOPS *et al.* 2005; WEAVER and CLEVELAND 2006). In humans, it is well established that solid tumours are aneuploid, but whether aneuploidy is

the cause or an effect of tumorigenesis is still hotly debated (HOLLAND and CLEVELAND 2009).

In 1914, Theodor Boveri proposed the somatic mutation theory for cancer, suggesting that genetic alterations acquired within a single cell can lead to the development of cancer by clonal expansion. His work on sea urchin embryos concluded that loss or gain of chromosomes led to abnormal development and lethality. In 1970, Parry and Cox reported the generation of rare but viable aneuploid spores from triploid yeast strains, showing tolerance of aneuploidy in *S. cerevisiae* (PARRY and COX 1970). Just an year later, stable chromosome III disomes were constructed and characterised in budding yeast (SHAFFER *et al.* 1971). Over the next few decades, aneuploidy associated with decreased fitness was also reported and studied in organisms like *Drosophila melanogaster*, the fruit fly; *Datura stramonium*, the jimson weed; *Caenorhabditis elegans,* maize, rice and *Arabidopsis thaliana* (TORRES et al. 2008). Reduction in fitness is thought to be associated with an imbalance of protein stoichiometry, reduction in gene dosage, and higher energy demands on DNA replication, transcription and protein synthesis required for additional chromosomes. Consistent with this it has more recently been reported that aneuploid *Saccharomyces cerevisiae* strains exhibit increased sensitivity to conditions affecting transcription and translation (TORRES *et al.* 2007).

In the 1950s, several scientists discovered that virtually all tumour cell lines had chromosome aberrations, and postulated that chromosomal abnormalities were an effect and not a cause of cancer. This view changed in 1959, when Peter Nowell and David Hungerford indentified a chromosomal abnormality known as the Philadelphia or Ph chromosome, and associated it with a single human cancer type, chronic myeloid

leukaemia (CML). Several years later in 1973, the Philadelphia chromosome was characterized as a reciprocal translocation between chromosomes 9 and 22. Shortly after, a reciprocal translocation involving chromosomes 8 and 21 was reported in acute myelogenous leukaemia (AML) patients and another translocation between chromosomes 8 and 14 was associated with Burkitt's lymphoma (ROWLEY 2001). Since then, chromosomal translocations have been found to be a hallmark of a plethora of haematopoietic malignancies like leukemias and lymphomas. To a lesser extent, they are also reported in several epithelial carcinomas, sarcomas and tumours (NAMBIAR *et al.* 2008). Most commonly, translocations mediate their effect by the generation of fusion proteins at the breakpoint, like in the case of Ph chromosome, where recombination between *c-ABL* and *BCR* genes result in the expression of a tyrosine kinase fusion protein (GOLLIN 2007). The genes that are often involved in chromosome translocation in cancer are often proto-oncogenes, and thus give rise to fusion oncogenes. Presently, about 358 gene fusions involving 337 different genes have been reported and described in human hematologic malignancies and sarcomas (MITELMAN *et al.* 2004; MITELMAN *et al.* 2007). Reciprocal translocations have been reported to result in gene fusions often associated with leukemias (BARR 1998; PANE *et al.* 2002). Alternatively, chromosome translocations can lead to the juxtaposition of regulatory elements (promoter or enhancer) of one gene with the coding region of a proto-oncogene, thus deregulating its expression (GASPARINI *et al.* 2007; ROWLEY 2001). Non-reciprocal translocations on the other hand can lead to a process called loss of heterozygosity (LOH) of tumour suppressor genes, thereby contributing to tumorigenesis (YEH *et al.* 2002). LOH basically refers to the loss of a functional allele of a gene in cells, which is already in a heterozygous condition. Furthermore, non-disjunction in meiosis-I, which is caused by failure to separate sister

chromatids, can lead to germline chromosomal abnormalities such as the human trisomy 21 (Down Syndrome). On the other hand, in somatic cells, recombination between low copy repeats (LCRs) and palindromic sequences have been reported to contribute to GCR formation (KURAHASHI *et al.* 2009a). Recently, the role of low copy repeats in mediating deletions and duplications, in addition to that of palindromic sequences in mediating translocations, has been reported in human diseases (KURAHASHI *et al.* 2009b). Moreover, certain forms of cancer have a clear chromosomal determinism and may be associated with genome instability seen as GCRs (SHAW and LUPSKI 2004), similar to those that can be modelled in *Drosophila* (EGLI *et al.* 2004) and in yeast cells (WAGHMARE and BRUSCHI 2005).

To date over 45000 human neoplasms have been reported to harbour cytogenetic aberrations. Numerous genes and chromosomes have been identified at the translocation breakpoints and thus provide important diagnostic markers for a plethora of different cancers. However, the mechanisms by which chromosomal translocations arise in diseased cells, or by which they are suppressed in healthy ones, remain unclear.

1.4 Suppression of genome instability: cell cycle checkpoints and DNA damage response:

The maintenance of genome stability is of critical significance for the normal growth and survival of all cells. Consistent with this, a vast array of human cancers and genetic diseases are often associated with increased genetic instability. Over the years, it has become increasingly clear that tumorigenesis is driven by genome instability, which emanates from chromosomal DNA damage and errors made during DNA replication, recombination and repair machineries. In healthy cells, the levels of GIN are kept to a

minimum level by genome surveillance mechanisms involved in the sensing and repair of a variety of DNA lesions. Eukaryotic cells have evolved redundant and extensive mechanisms to counteract and eliminate lesions arising from exogenous and endogenous assault. Additionally, the method of repair usually depends on the type of the lesion and the stage of the cell cycle at which the lesion occurs. Thus, genome maintenance is carried out ubiquitously throughout the cell cycle by a concerted effort of relevant cell cycle checkpoints and DNA damage response pathways. The classical DNA damage checkpoint mediates cell cycle arrest upon damage in the G_1 and G_2 phases of the cell cycle. The replication and intra-S checkpoints respond to damage that occurs during the S phase, causing cell cycle arrest and suppression of late firing replication origins in response to blocked DNA replication. The spindle assembly or mitotic checkpoint functions during mitosis in response to spindle damage causing mitotic arrest. Subsequently, checkpoint-signalling leads to damage repair, which can be carried out by HR mediated processes predominantly during S-phase or via NHEJ in the absence of a donor template. Studies of *S. cerevisiae* checkpoint genes have revealed that mutations in replication checkpoint functions greatly enhance the rate of GCR formation. Contrary to this, mutations of genes required for G_1 and G_2 checkpoints or the mitotic spindle checkpoints had little or no effect (KOLODNER *et al.* 2002).

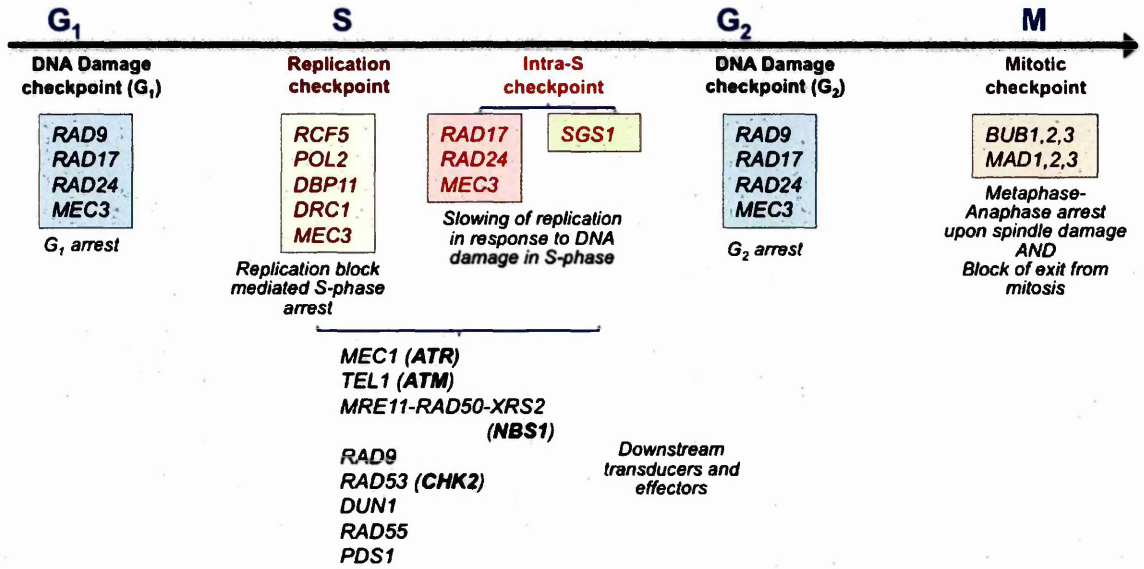

Figure 1.2 *Saccharomyces cerevisiae* DNA damage, replication and mitotic checkpoints. The different stages of the cell cycle are represented above the horizontal arrow, with relevant checkpoints mentioned at those stages below. A sub-set of genes that function in each checkpoint branch are grouped and the effect of each checkpoint is listed below the gene complexes. Below the three checkpoint branches that function in S-phase, are listed some of the genes, which function as downstream signal transducers or effector targets. In bold are represented human homologues of the yeast counterpart. [Adapted from (KOLODNER *et al.* 2002)]

1.4.1 Replication checkpoints and genome instability:

Apart from environmental and metabolic assaults, mitotically dividing cells are confronted by a huge task to duplicate their entire set of chromosomes. During this process, they must eliminate harmful mutations and repair any damage to DNA before its duplication, as failure to do so may result in cell death. To prevent this from happening, eukaryotic cells have evolved checkpoints throughout the cell cycle. Essentially, these mechanisms mediate their effect in response to damaged or incompletely replicated DNA by arresting the cell division cycle, giving cells time to repair damage and thus coordinating replication, repair, chromosome segregation and cell-cycle progression (FOIANI *et al.* 2000). In humans, many checkpoint components are known tumour suppressors and most checkpoint genes are evolutionarily conserved, highlighting the

importance of these genome surveillance mechanisms in the maintenance of genome integrity.

In nature, DNA is most vulnerable to damage during synthesis by replication, which is a major source of endogenous DNA breaks. These breaks are usually generated when causative agents such as DNA adducts, tightly bound proteins or secondary structures in DNA stall replication fork (RF) progression driven by a functional replisome complex. Replication can resume upon removal of such obstacles, or alternatively, RFs might even be delayed to coordinate fork progression and repair. Among the cellular checkpoints, the S-phase checkpoint (or replication checkpoint) and the intra-S-checkpoint respond to RF stalling and damage in the form of ssDNA gaps and double strand breaks (DSBs) (COBB *et al.* 2005; SOGO *et al.* 2002). In *S. cerevisiae*, mutations in replication checkpoint genes *RFC5*, *DPB11*, *MEC1*, *DDC2*, *MEC3*, *RAD53*, *CHK1*, *PDS1* and *DUN1* have been reported to cause significant increase in GCR rates. However, mutations in DNA damage and mitotic checkpoint genes *RAD9*, *RAD17*, *RAD24*, *BUB3* and *MAD3* are reported to have little effect on the rate of spontaneous GCR formation. Additionally, *TEL1* mutations in combination with mutations that cause higher rates of GCR increased the rates of chromosomal translocations (MYUNG *et al.* 2001b). Furthermore, genetic analysis of replication and recombination defective mutants for genes such as *RFA1*, *RAD27*, *MRE11*, *RAD50* and *XRS2* suggests multiple pathway suppression of GCRs. Mutations in these genes that have pleiotropic roles in DNA replication and repair increased the rate of GCR formation by 600-5000 fold (CHEN and KOLODNER 1999). In response to errors during replication, the replication checkpoint function in suppressing GIN seems to be mediated through regulation of cell cycle progression by modulating DNA repair,

maintaining stalled replication forks to restart DNA synthesis and establishment of sister chromatid cohesion. At the same time, two redundant branches of the intra-S checkpoint, one requiring *RAD17* and *RAD24*; and the other requiring *SGS1*, mediate slow cell cycle progression and reduced rates of replication. Additionally, with regard to spontaneous GCR rates, a synergistic interaction between individual branches of the intra-S checkpoint or the replication checkpoint has been reported (MYUNG and KOLODNER 2002). This observation stems from highly elevated rates of GCR formation in strains bearing combined mutations that inactivated both S-phase checkpoints and downstream effectors. Besides maintaining low levels of genome instability, DNA damage checkpoint and recombination defects also lead to increased loss of chromosomes in diploid cells. This loss is further enhanced synergistically in cells defective for both checkpoint and recombination functions (KLEIN 2001). Thus, synergistic interactions between redundant checkpoint functions initiating cell cycle delay or arrest, and recombination functions that mediate repair, keep the levels of GIN to a minimum in healthy cells, and thereby maintain the integrity of chromosomes. Notably, in yeast, mutations in most of the checkpoint genes results in elevated rates of GCR formation, and human homologues of many of these genes are mutated in cancer susceptibility syndromes.

Saccharomyces cerevisiae gene	Human homologue	Function	GCR rate	Disorder
MEC1	*ATR*	Transducer kinase	High	Seckel Syndrome
TEL1	*ATM*	Transducer kinase	High	Ataxia telangiectasia
MRE11	*MRE11*	HR and NHEJ	High	Ataxia telangiectasia-like disease
XRS2	*NBS1*	HR and NHEJ	High	Nimegen breakage syndrome
RAD53	*hCHK2*	Effector kinase	High	Li-Fraumeni syndrome
SGS1	*BLM / WRN / RTS*	RecQ helicase	High	Bloom, Werner or Rothmund Thompson syndrome
DPB11	*TOPBP11*	Polymerase ε subunit, checkpoint mediator	High	Not known
RCF1-5	*RCF1-5*	Clamp loader, checkpoint sensor	High	Not known
PDS1	*PTTG1*	Mitotic arrest	High	Not known
RAD9	*Not known*	Damage-checkpoint mediator	High	Not known
RAD24	*RAD17*	RFC-like, S-phase checkpoint	High	Not known
DDC1-RAD17-MEC3	*RAD9-RAD1-HUS1*	PCNA-like complex	High	Not known
ELG1	*Not known*	RFC-like	High	Not known
DUN1	*Not known*	Effector kinase	High	Not known

Table 1.1 A list of several checkpoint genes, mutations in which are known to cause increased GCR rates in *S. cerevisiae*, with human homologues implicated in various cancer predisposing syndromes.

1.4.2 DNA Damage Response (DDR):

In section 1.2 we have described some of the major kinds of DNA lesions that arise due to cellular and environmental factors. Intrinsically, DNA damage might accumulate due to defects in molecular pathways that carry out genome surveillance functions including DNA damage sensing, signalling and repair, which act to maintain the integrity of the genome throughout the cell cycle. Inefficient or inaccurate repair of lesions due to defects in such pathways lead to increased mutation rates and formation of chromosomal aberrations. In particular, inadequate repair of lesions like DNA-double strand breaks (DSBs) generally ensues into a broad spectrum of mutations and genome rearrangements like deletions, inversions, and chromosomal translocations. Mitotic DNA double-strand breaks are the most genotoxic and cytotoxic lesions of a cell and can lead to the

generation of unbalanced reciprocal or non reciprocal translocations (BRADBURY and JACKSON 2003). Failure to repair can often lead to catastrophic consequences like cell death via triggering apoptosis. However, at the molecular level, DSB mediated rearrangements drive evolution by generating genetic variation and can also be beneficial for the organism. For instance in mammals, programmed DSBs during V(D)J recombination are the basis of immunoglobulin (Ig) gene diversity (MAIZELS 2005). In *S. cerevisiae,* programmed DSBs are created by the *HO* endonuclease during mating-type switching.

The presence of DSBs triggers cellular responses to coordinate cell cycle progression and efficient repair. In budding yeast, three responses have been characterized as G_1/S, intra-S and G_2/M DNA damage checkpoints. In this regard, molecular signals have been characterized that identify and mark the sites of damage, leading to checkpoint activation, which ensues in a signal transduction cascade to activate DNA repair pathways or apoptosis. This signalling and sensing of damage, and transduction to effector functions that carry out repair, is collectively known as the DNA damage response. In addition to these core components of DDR, a special class of non-catalytic molecules called mediators or adapters are known to facilitate signalling by promoting physical interaction between other proteins.

1.4.2.1 The DNA-Damage Checkpoint:

A major component of DDR is the DNA damage checkpoint, which is activated and arrests the cell cycle in response to damage until repair is complete. This checkpoint is essential to prevent segregation of broken chromosomes that can lead to aneuploidy, chromosome loss or formation of nonreciprocal translocations.

In eukaryotes, all aspects of the DNA damage checkpoint depend on two central proteins belonging to the phosphatidylinositol 3′ kinase-like kinase (PIKK) family, *ATM* (Ataxia Telangiectasia Mutated) and *ATR* (Ataxia Telangiectasia Mutated and Rad3-related) (ABRAHAM 2001). In *S. cerevisiae* they are known as *TEL1* and *MEC1*, respectively. Mec1 forms part of the sensor mechanism that detects damage in the form of single stranded DNA (ssDNA). Mec1-mediated Rad9 activation then relays the signal to downstream transducing and effector kinases like Rad53 and Chk1 (MA *et al.* 2006; SWEENEY *et al.* 2005). These in turn amplify the checkpoint signal and regulate the cell cycle machinery to mediate arrest. The recruitment of Mec1/ATR to DNA is carried out by of the partner protein Ddc2/ATRIP (PACIOTTI *et al.* 2000). At ssDNA regions generated at a DSB, the recruitment of Mec1/Ddc2 complex requires the ssDNA binding complex RPA (ZOU and ELLEDGE 2003; ZOU *et al.* 2003). In budding yeast, ssDNA generation at DSBs occurs via the 5′ to 3′ exonuclease activity of the MRX (Mre11/Rad50/Xrs2) complex, as well as other, recently identified exonucleases (HARRISON and HABER 2006). In the absence of Sae2 and Mre11, DSBs have been reported to be processed by the Sgs1-Top3-Rmi1 complex and Exo1 or Dna2, but with a much lower efficiency (MIMITOU and SYMINGTON 2008; ZHU *et al.* 2008).

In *Saccharomyces cerevisiae*, the discovery of *RAD9*-dependent coordination of cell cycle progression and DNA damage response marked the first finding which led to identification and characterization of other checkpoint functions (WEINERT and HARTWELL 1988). Later, it was reported that gene products of *RAD17*, *RAD24*, *MEC3* and *DDC1* (collectively known as the Rad24 group) are specifically required at an early stage for damage recognition and processing of DNA lesions (WEINERT 1998).

Supportingly, physical interaction between Mec3 and Ddc1 *in vivo* and dependency on Rad17 for this interaction has also been reported (PACIOTTI *et al.* 1998). Rad24 on the other hand is related to Replication Factor C (RFC), which is a protein complex that binds to template-primer junctions during replication and loads proliferating cell nuclear antigen (PCNA) clamp onto DNA followed by recruitment of replicative DNA polymerases like Polε (WAGA and STILLMAN 1998) (refer to **Figure 1.3**). The structural similarity of Rad17 and PCNA further strengthens the analogy between role of RFC and PCNA in replication and that of Rad24 and Rad17/Mec3/Ddc1 in DNA damage response.

Moreover, Rad9 is phosphorylated in a Mec1-dependent manner and this modification also requires Tel1 and the Rad24 group of proteins. However, Mec1-dependent phosphorylation of Rad53, Dun1, Pds1 and Rpa1 are believed to function downstream of Rad9 and Ddc1 phosphorylation by Mec1. Furthermore, Rad9 and Ddc1 are required with Mec1 to enable Rad53 phosphorylation, while Mec1 is required for phosphorylation of Rad9 and Ddc1, suggesting that the checkpoint response pathway is more complex rather than being simply linear. Once activated by Mec1, Rad9 and Rad24 complex, the Rad53 kinase plays a central role in checkpoint response by modulating the activity of target proteins by their subsequent phosphorylation (see **Figure 1.3**). For instance, Rad53 and Mec1 are required for Dun1 phosphorylation, which in turn leads to the transcriptional induction of many repair genes. Anaphase inhibitor Pds1 on the other hand, is activated by hyper-phosphorylation in a Mec1-, Rad9- and Chk1- dependent manner, but does not require Rad53 activity. Finally, delayed bud emergence and entry into S-phase post DNA damage in G_1 requires Rad53-dependent transcriptional inhibition

of the G_1 cyclins (*CLN1* and *CLN2*), by inactivation of a transcriptional regulator Swi6 required for their expression (FOIANI *et al.* 2000; LONGHESE *et al.* 1998).

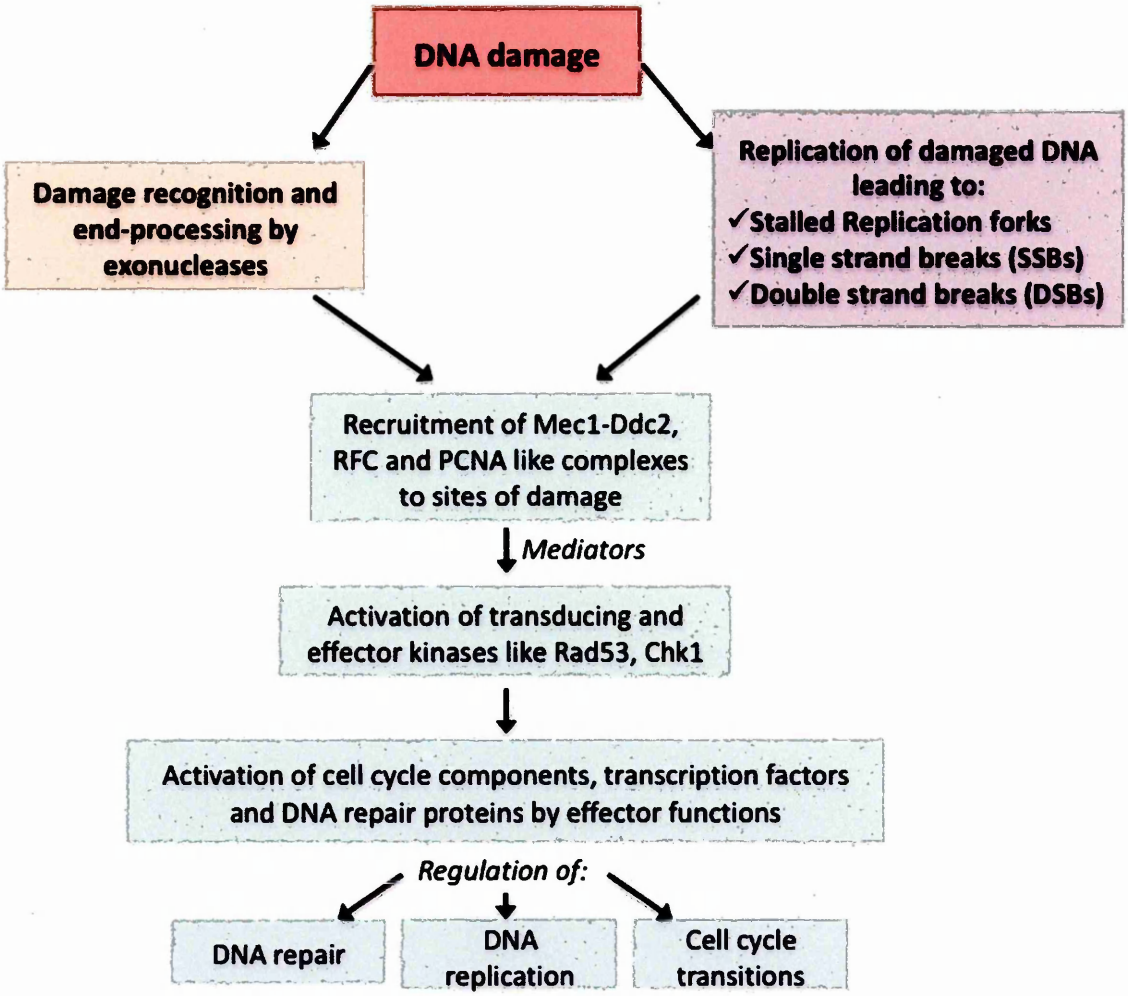

Figure 1.3 Schematic representation of DNA damage checkpoint activation in *S. cerevisiae* DNA lesions detected during replication or recombinational repair lead to recruitment of Mec1-Ddc2 and RFC-like (Rad24-RFC2-5). The latter in turn loads the PCNA-like (Rad17-Mec3-Ddc1) next to the Mec1-Ddc2 complex. Mec1 then phosphorylates and activates downstream transducing and effector kinases like Rad53 and Chk1 via specific mediators. Activated effector functions then mediate transcriptional response of specific targets, and depending on the stage of the cell cycle and the DNA lesion, further regulate replication and repair and cause arrest. [Adapted from (LONGHESE *et al.* 2003)]

The checkpoint PIKK, Tel1/ATM is recruited to free DSBs via its interaction with the MRX/MRN complex, where it binds to a common motif on the C terminus of Xrs2/Nbs1. In contrast to the Mec1-Ddc2 complex, which binds RPA coated ssDNA, the Tel1-MRX complex binds to blunt ended or minimally processed DSBs. In budding yeast, Tel1 plays a minor role in checkpoint signalling at unprocessed DSBs, but in the absence of Mec1, transmits the signal to Rad53. However, in G_1-arrested cells where resection and Mec1 contribution is minimal, Tel1 plays a major role in the phosphorylation of histone H2A around the break to form γ-H2AX. In mammalian cells, where unresected DSBs persist longer, ATM plays major role in triggering resection and activation of the ATR.

1.4.2.2 S-phase and intra-S checkpoints:

Stalling of replication forks can occur due to dNTP pool depletion or in response to DNA damage confronted during DNA synthesis, leading to the activation of the S-phase checkpoint. The RFC-like (Rad24, Rfc2-5) and PCNA-like (Rad17-Mec3-Ddc1) complexes play a minor role in checkpoint activation during the S phase of the cell cycle. In response to DNA damage during replication, the intra-S phase checkpoint blocks initiation of DNA replication from late-firing origins, maintains stalled forks in a state to restart replication after damage repair; and prevents spindle elongation and thereby entry into mitosis. In *S. cerevisiae* proteins like Polε, Dpb11, Mrc1 and Tof1, which localise at replication forks regulate these responses in conjunction with the Mec1-Ddc2 complex and Rad53 (LONGHESE *et al.* 2003). The mediator protein Mrc1, a Rad9 counterpart has been implicated in activating Rad53 specifically during replication stress (ALCASABAS *et al.* 2001). Apart from this response, a RecQ helicase, *SGS1* solely regulates a second

branch of the intra-S checkpoint independently of Rad17 and Rad24 group of proteins (**Figure 1.2**). Moreover, stalled forks have been associated with increased binding of replicative DNA polymerases α and ε, which requires the activity of Sgs1 and Mec1. Such polymerase association is propose to be mediated by Sgs1, whereby it resolves aberrant structures at the fork to maintain ssDNA, thus providing substrates for RPA and Mec1 (COBB *et al.* 2003; FREI and GASSER 2000).

Eventually, both the replication and intra-S checkpoints converge in their signalling cascades to trigger the phosphorylation and activation of Rad53, leading to block of replication initiation from late-firing origins and maintaining the integrity of stalled forks to resume replication after DNA repair.

1.4.2.3 DNA Repair Pathways:

Cells have evolved numerous pathways for the repair of a variety of DNA lesions. The choice of the repair pathway to be utilized for repair depends on the nature of the break and on the cell cycle stage at which the lesion is detected. DSBs occurring in S and G_2 phases are repaired by homologous recombination (HR) using the intact sister chromatid as donor template. However, as cells that progress into G_2/M, chromosomes get compacted and condensed making non-homologous end-joining (NHEJ) mediated ligation of broken ends as the preferred pathway for repair. Additionally, a DSB can be stabilised in the genome by *de novo* telomere addition (PENNANEACH *et al.* 2006; PUTNAM *et al.* 2004), or can be joined to a DSB on another broken chromosome formed during breakage fusion breakage cycles (**Figure 1.4**).

With regard to HR mediated pathways of repair, DSBs can be repaired by at least three distinct mechanisms: gene conversion (GC), when homology is present for both ends of the DSB; break induced replication (BIR), when only one end of the DSB has an available homologous donor; or by single strand annealing (SSA), when a DSB is flanked by repeated sequences (**Figure 1.4**). The choice of repair pathway to be used depends on the stage of the cell cycle, homology status, nature and context of the DSB ends. Moreover, recent research suggests that this control of choice is regulated by the so-called recombination execution checkpoint (REC). The choice of repair pathway occurs before DNA synthesis initiates during repair, and is dependent on the location and orientation of the homologous sequence to be used for repair. In this context, Sgs1, a RecQ family helicase has been implicated to play a major role in regulating the choice of repair pathway (JAIN *et al.* 2009).

Earlier studies examined the frequency of spontaneous recombination between homologous *LEU2* alleles places at allelic locations (at same places on homologous chromosomes), and that on ectopic locations (elsewhere in the genome between non-allelic positions). They concluded that both kind of events occurred at near equal rates during mitosis regardless of where the two interacting homologous sequences were placed in the genome (LICHTEN and HABER 1989). On the contrary, meiotic recombination between such allelic or non-allelic homologous sequences occurred at similar rates but was largely influenced by the genomic location of the sequences involved (JINKS-ROBERTSON and PETES 1985; JINKS-ROBERTSON and PETES 1986; LICHTEN *et al.* 1987). Furthermore, similar work done by Agmon *et al.* in *S. cerevisiae* sheds light on HR mediated repair of an artificially *HO*-induced single DSB, when more

than one homologous donors are present on the same chromosome as the DSB or elsewhere in the genome (AGMON *et al.* 2009). Observations from this study suggest that homologous sequences present on the same chromosome are readily preferred as donors in comparison to those located on an ectopic/different chromosome. Moreover, ectopic donors may be more readily used with increase in size, although never as efficiently as intra-molecular donors.

1.4.2.3.1 Eukaryotic Homologous Recombination (HR):

Homologous recombination is the exchange of genetic information between allelic sequences and it plays indispensable roles in both meiotic and mitotic cells. HR can occur between alleles present on homologous chromosomes or between DNA repeats present on either homologous or heterologous chromosomes. Mitotic recombination can further occur via multiple mechanisms like double strand break repair (DSBR), synthesis-dependent strand annealing (SDSA), single strand annealing (SSA) or break induced replication (BIR). In meiosis, HR accounts for the generation of genetic diversity among gametes by mediating exchange of genetic information between paternal and maternal alleles. In the first meiotic division, HR ensures the critically correct segregation of homologous chromosome pairs. On the other hand, in mitotic cells, HR indispensably maintains genome integrity by promoting efficient repair of deleterious lesions such as double strand breaks (DSBs), inter-strand crosslinks and the repair of damaged/collapsed replication forks to resume normal cell division. Such repair mediated by HR has been implicated in the avoidance of cancer predisposition in humans (PRADO *et al.* 2003; SAN FILIPPO *et al.* 2008).

The first model for the repair of a double strand break, called the DNA double strand break repair (DSBR) model, was based on the observation of yeast cells transformed with a linear plasmid carrying homologous sequences to those of yeast chromosomal DNA (SZOSTAK *et al.* 1983). During DSBR, the broken ends of the chromosome are first processed by endonucleases to give rise to single stranded 3′ overhangs. This ssDNA is then coated with recombinases like Rad51 to form the nucleoprotein filament, which invades the homologous chromosome to copy genetic information. Strand invasion is accompanied by D-loop formation followed by DNA synthesis accompanied by D-loop migration. Finally, specialized enzymes called resolvases accomplish the resolution of Holliday junctions formed by interacting DNA strands. Recombination can result in the transfer of genetic information from homologous DNA molecule to the broken DNA by a process called gene conversion, and/or in crossing over, a process involved in the reciprocal exchange of DNA fragments between chromosomes. The DSBR model explains meiotic recombination related observations in fungi, but not that of mitotic recombination. This is because during mitosis, most DSB repair occurs by gene conversion whereas meiotic HR is associated with crossover formation. The formation and resolution of a double Holliday junction recombination intermediate is central to the DSBR model of DSB repair (WYMAN and KANAAR 2006).

The synthesis-dependent strand-annealing (SDSA) model is very similar to the DSBR model especially in the initial steps of DSB end processing and strand invasion, but is not associated with crossover formation. However, the second end of DSB, rather than being captured by the recombination intermediate, is displaced after DNA synthesis and reanneals with the ssDNA tail on the other DSB end (**Figure 1.4** ahead).

A more mutagenic HR pathway called single strand annealing (SSA) can be employed for repair if a DSB occurs between closely repeated sequences. This pathway does not require strand invasion or a donor molecule as a template for synthesis but requires end processing to form ssDNA tails that can anneal with each other at the repeated sequence. The terminal 3′ overhangs adjoining the repeat sequences are excised and the remaining gaps are ligated to complete repair, although with a loss of DNA sequence leading to deletions.

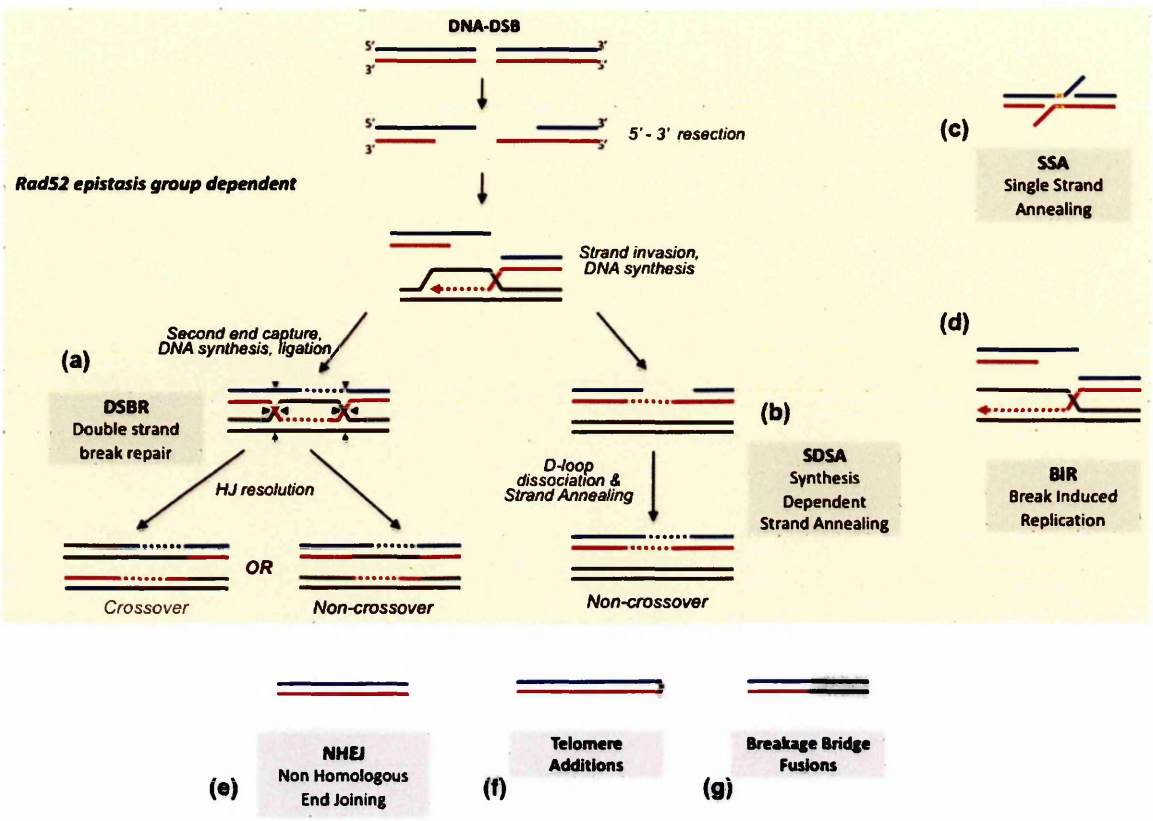

Figure 1.4 Pathways of DNA DSB repair in eukaryotes. Rad52 epistasis group dependent pathways require end processing to generate 3′ overhangs, which become substrates for recombinases, a prerequisite for strand invasion and homology search on a suitable donor followed by DNA synthesis. The resolution of Holliday junctions (HJ) can occur in discrete ways leading to crossover or non-crossover products as in DSBR (**a**); or exclusively non-crossover products as in SDSA (**b**). Some pathways require only some components of the Rad52 group to initiate repair by SSA (**c**), when DSBs occur between repeat sequences. Single ended DSBs are repaired by BIR (**d**), during which DNA synthesis proceeds to the chromosome termini. Simple ligation of DNA ends by NHEJ (**e**); *de novo* telomere additions (**f**); and chromosome fusions (**g**) can heal and rescue DNA breaks independently of Rad52 epistasis group.

1.4.2.3.2 Break Induced replication (BIR):

In some cases, only one end of the DSB is used to initiate repair by a process called break induced replication (BIR). This might occur at a collapsed replication fork after encountering a single strand gap or nick and converting it into a DSB on one sister chromatid. Alternatively single ended breaks can form at telomeres that have lost their protective subtelomeric repeats. In these cases, a single DSB end can invade a homologous sequence to initiate unidirectional DNA synthesis, which can proceed till the end of the chromosome arm. The DNA polymerase δ subunit, Pol32 is uniquely required for BIR to initiate replication at broken or stalled RFs and at damaged telomeres (LYDEARD *et al.* 2007). When BIR occurs between homologous chromosomes, it can result in large-scale LOH of chromosomal regions spanning several hundred kilobases. Alternatively, multiple invasion and dissociation into dispersed repeat sequences via template switching during BIR can lead to complex genome rearrangements (SMITH *et al.* 2007).

1.4.2.3.3 Non Homologous End Joining (NHEJ):

The NHEJ repair pathway is conserved from bacteria to humans. In human cells it seems to be the preferred pathway for DSB repair, whereas in *S. cerevisiae*, HR is more prevalent. In the absence of a donor molecule available for gene conversion mediated DSB repair, as in G1 and G2 phases of the cell cycle, broken DNA ends can be readily healed by simple ligation of broken ends following end processing. Thus, NHEJ occurs independently of the presence of homologous sequences at DSB ends. It requires a conserved set of proteins, including the Ku70/80 heterodimer, DNA protein kinase catalytic subunit (DNA-PK_{CS}), DNA ligase IV (Lig4) and *XRCC4* (Lif1). The

MRX/MRN complex plays end-processing roles in both HR and NHEJ pathways. During NHEJ, in concert with the Ku70/80 heterodimer, the MRX/MRN complex serves an additional role to promote bridging and alignment of broken ends (DALEY *et al.* 2005). This is followed by Ku/DNA-PK_{CS} mediated recruitment of (Lig4) DNA ligase IV / (Lif1) *XRCC4* complex to facilitate repair.

1.4.2.3.4 The Rad52 epistasis group of HR genes:

The eukaryotic HR machinery is fundamentally conserved over evolution from yeasts to mammals, although certain additional factors that mediate HR are specifically found in higher eukaryotes. Genes of the *RAD52* epistasis group (SYMINGTON 2002) play a central role in HR and repair processes. This group of genes includes *RAD50*, *RAD51*, *RAD52*, *RAD54*, *RDH54* or *TID1*, *RAD55*, *RAD57*, *RAD59*, *MRE11* and *XRS2*. Homologous recombination is mediated by a special class of enzymes known as recombinases, which are conserved from bacteria to humans. Recombinases mediate the pairing and exchange of DNA strands during HR. The most well studied bacterial recombinase is the *E. coli* RecA, the eukaryotic orthologues of which are Rad51 and Dmc1. The Rad51 recombinase mediates HR reactions in mitotically dividing somatic cells, whereas Dmc1 on the other hand is exclusively active during meiosis and does so in concert with Rad51. A significant amount of sequence homology is shared between Rad51 and bacterial RecA, especially the residues encoding DNA binding and ATP hydrolysis functions. Rad51 assembles both on single-stranded DNA (ssDNA) and double stranded DNA (dsDNA) filaments to form a right-handed helical polymer, which can span thousands of base pairs, with each helical turn of monomers covering 18-19 nucleotide base pairs (OGAWA *et al.* 1993). Homologous DNA pairing and strand exchange is mediated by the

presynaptic filament, which consists of single stranded DNA coated with Rad51 and Dmc1. Both Rad51 and Dmc1 hydrolyze ATP when bound to DNA, although, this ATP hydrolysis is required for dissociation of recombinase molecules from DNA rather than for the assembly of the presynaptic filament (CHI *et al.* 2006). The Rad55/Rad57 heterodimer stimulates strand exchange by stabilizing the binding of Rad51 to single-stranded DNA. Moreover, the assembly of the presynaptic filament is competitively interfered by the tightly bound ssDNA binding protein RPA, the removal of which is enhanced by recombination mediators like Rad52 in *S. cerevisiae* and *BRCA2* in humans. Rad52 shares some biochemical features with Rad59 and both have overlapping functions in non-conservative pathways of repair like BIR and SSA. Other DNA-dependent ATPases like Rad54 and Rdh54 further promote homologous pairing and strand exchange by modifying the topology of DNA. These DNA motor proteins also play roles in recycling the recombinases by mediating their removal from duplex DNA formed after strand invasion. (SAN FILIPPO *et al.* 2008; SYMINGTON 2002).

1.5 *Saccharomyces cerevisiae*: a model for studying genome instability:

1.5.1 The organism and its biology:

The most extensively studied unicellular eukaryotic model organism for biological studies is *Saccharomyces cerevisiae*, commonly known bakers' or budding yeast. The oldest records refer to its use for beer brewing in Babylonia around 6000 BC, for grape cultivation in Georgia and for dough leavening in Egypt. However, since the last few decades, starting around 1960, *S. cerevisiae* has been exhaustively exploited as an experimental system for molecular biology and genetics. The mere ease of handling,

growth and maintenance of yeast cells and a short life cycle renders them as an invaluable tool for biological research. Additionally, yeast cells unlike most other microorganisms exist in both haploid and diploid states. Diploid strains of yeast can divide either mitotically by budding and give rise to daughter cells, or they can undergo meiosis under nutrient starvation giving rise to four haploid ascospores, which are encapsulated in a sac like structure known as the ascus. *Saccharomyces cerevisiae* strains can be stably maintained either as heterothallic haploids or diploids, or as homothallic diploids. Yeast cells have two mating types, *a* and α, and in both haploid and diploid cells is determined by a single *MAT* locus on chromosome III. Haploid cells can further undergo mating-type switching from *a* to α, or vice-versa. However, all strains used for this study here are diploid *MAT a/α*. Each diploid *S. cerevisiae* cell is ovoid in shape and is around 4μm × 6μm. Mitotic cells divide by budding giving rise to daughter cells, and each mother can bud nearly 20 times before it reaches replicative senescence. The cell cycle is divided into G1, S, G2 and M phases and in wild type strains, each mitotic cycle lasts about 90 – 100 minutes.

The haploid nuclear genome of the budding yeast *Saccharomyces cerevisiae* was completely sequenced in 1996 and consists of sixteen linear chromosomes encompassing ~ 12.07 mega base pairs of genetic information (GOFFEAU *et al.* 1996). Recent figures define 6607 open reading frames (ORFs) corresponding to 70% of the nuclear genome and nearly 73.9% of total ORFs represent protein coding genes with known functions. In addition, the yeast genome contains around 150 ribosomal RNA genes located as large tandem arrays of ~ 9.1 Kbp on chromosome XII (PETES 1979). Some other major sequence features include the 16 centromeres (CENs) one on each chromosome, 32

telomeres (TELs) one on each end of the chromosome, in addition to 40 small nuclear RNAs (snRNAs) and 275 tRNA genes distributed randomly over the genome. The mitochondrial genome on the other hand contains 28 ORFs as well as 24 tRNA genes. The *S. cerevisiae* chromosomes vary in size from the smallest being chromosome I (~230 Kbp), and the largest being chromosome XII, which is 1.09 Mbp without rDNA but can get closer to 2 Mbp with the rDNA arrays, making it run aberrantly on CHEF gels. In contrast to higher eukaryotes, most of the relatively small sized yeast chromosomes can be separated individually and others as doublets using pulsed field gel electrophoresis (PFGE). Unlike the human genome; the yeast genome is rather compact with short intergenic stretches of DNA sequence of an average length of 400 base pairs. Many *S. cerevisiae* chromosomes contain large alternating domains of GC-rich and GC-poor sequences. As a general rule, ORFs are more GC-rich compared to sequence features, such as promoters and terminators, which are AT-rich. Furthermore, previous work in our laboratory demonstrates the promoters and terminators are more recombinagenic than the more GC-rich ORFs (GJURACIC *et al.* 2004). Notably, since the availability of the complete yeast genome sequence and deletion mutants for all but some of the essential genes, *S. cerevisiae* has been extensively used as an important tool for understanding the regulation of eukaryotic cell biology. Furthermore, around 40% of the human genes involved in heritable diseases have homologues in yeast, which makes it an excellent model system to understand and provide insight into the molecular intricacies of human pathologies.

1.5.2 GCR assays in yeast:

In around the last three decades, several *S. cerevisiae* systems have been used as models to study genome rearrangements. These methods have aimed at understanding DNA recombination and repair, suppression of genome instability by multiple pathways, and to provide further insights into the molecular pathways leading from DSBs to GCRs. Since the early 1980s, there have been several reports, which suggest that recombination between dispersed repeated or duplicated DNA sequences play roles in generation of gene instability and chromosomal aberrations (CHALEFF and FINK 1980; JACKSON and FINK 1981; KLEIN and PETES 1981; ORR-WEAVER *et al.* 1981; ROEDER *et al.* 1980; ROEDER and FINK 1980; SCHERER and DAVIS 1980). In all such studies, DNA sequences under investigation were introduced into specific chromosomal loci by yeast transformation methods (ORR-WEAVER *et al.* 1981). Initially, recombination between alleles placed on non-homologous chromosomes III and XII provided a means to induce reciprocal and non-reciprocal translocations (MIKUS and PETES 1982). Later, a yeast strain carrying translocation between *URA2* site on chromosome X and *HIS3* site on chromosome XV was constructed by mitotic recombination between engineered sequences (POTIER *et al.* 1982). Others used yeast strains carrying *his3* alleles on non-homologous chromosomes to study gene conversion and crossing over between dispersed repeat elements, resulting in a reciprocal translocation (SUGAWARA and SZOSTAK 1983b). This method was then proposed as a general method for constructing chromosomal translocations (SUGAWARA and SZOSTAK 1983a). A couple years after, others demonstrated that during meiosis, recombination between repeated yeast genes on non homologous chromosomes occurs frequently (JINKS-ROBERTSON and PETES 1985), and can also lead to the generation of chromosomal translocations (JINKS-ROBERTSON and

PETES 1986). Others reported that recombination between dispersed homologous sequences on different chromosomes (ectopic recombination), and that between parental homologs (allelic recombination), happened at similar frequencies during mitosis in *S. cerevisiae* (LICHTEN and HABER 1989).

Inversion of large chromosomal segments by transforming *S. cerevisiae* cells with two bridging constructs was performed to perturb synapsis, generating dicentric or acentric chromosomes (DRESSER *et al.* 1994). The transformation of yeast cells with a chromosomal fragmentation vector (CFV) produced chromosomal fragments (CF) containing altered orientation of centromere and subtelomeric sequences with or without the loss of targeted chromosome, following DSB processing by break-copy duplication (MORROW *et al.* 1997). A year later, it was demonstrated that a chromosomal DSB produced by homing *HO* endonuclease could be repaired by BIR, leading to a NHEJ mediated reciprocal translocation (BOSCO and HABER 1998). Later, a genetic assay engineered on the left arm of chromosome V was exploited to measure the rate of the loss of *CAN1* or *URA3* markers. This followed mapping, sequencing and characterizing the breakpoints of selected rearrangements such as translocations, interstitial deletions, chromosome fusions and terminal deletions (CHEN and KOLODNER 1999). Similar assays were also engineered for loss of other markers on chromosomes III and XV (HACKETT *et al.* 2001; MYUNG *et al.* 2001b). The *CAN1* genetic marker in conjunction with others has been used to determine rate of chromosome loss and mitotic recombination in diploid yeast cells (KLEIN 2001). Other systems are based on loss of hemizygous or heterozygous *URA3* markers on chromosomes III or V, and detect GCRs mediated by repeated sequences such as retrotransposon Ty elements and mating-type loci (UMEZU *et al.* 2002).

Various systems exploiting site-specific recombinases have been used to induce GCR mediated genome instability. For instance, a *cre* site-specific recombination based system targeting pre-engineered *loxP* sites has been developed to generate reciprocal translocations (DELNERI *et al.* 2003). Other GCR assays to study telomere additions have been developed in which site-specific DNA DSBs near telomeres are created using the *HO* endonuclease. Such *HO* based systems have also been utilized to produce reciprocal translocations mediated by NHEJ when two DSBs are created on separate chromosomes (YU and GABRIEL 2004). Similarly, I-*SceI* induced DSBs on different mobile P-elements of *Drosophila* have been used to create translocations (EGLI *et al.* 2004).

The work described above describes a large number of genetic systems have been developed to study GCR mediated genome instability in yeast and other model organisms. However, these experimental systems require pre-engineering of tester strains to allow the induction of GCR formation at specific genetic loci. Here, in this study we use a simple yeast system developed for diploid cells, which allows induction and selection of non-reciprocal translocations between any two pre-defined loci without any prior modification of cells.

1.5.3 The Bridge- Induced Translocation (BIT) system:

In context to GCRs and to further elucidate the molecular mechanisms underlying the suppression of genome instability, we here, exploit the genetic applicability of the budding yeast, *Saccharomyces cerevisiae* as a cellular model organism. Members of our group have previously pioneered the experimental feasibility of inducing non-reciprocal translocations between any two desired loci on two different yeast chromosomes. They have accomplished this using a linear DNA construct bearing a selectable marker (KAN^R)

flanked by sequence homology targeting two chosen loci on different chromosomes (TOSATO *et al.* 2005).

Upon correct integration on both sides, this *KAN*^{R} linear DNA construct acts as a molecular bridge between the two chosen loci, thereby resulting in the formation of an aberrant translocated chromosome (**Figure 1.5**). Translocation harboring recombinants will be referred to as *"translocants"* throughout this study. Moreover, this Bridge-Induced Translocation (BIT) results in the formation of discrete free-ended DNA fragments, the fate of which is described and characterized further in the results chapters. Since chromosomal bridging is observed in cancers, and mammalian cells have been shown to recruit extrachromosomal DNA to repair a DSB (DELLAIRE *et al.* 2002; LIN and WALDMAN 2001a; LIN and WALDMAN 2001b), chromosomal translocations in eukaryotic mitotic cells might occur via a BIT like mechanism.

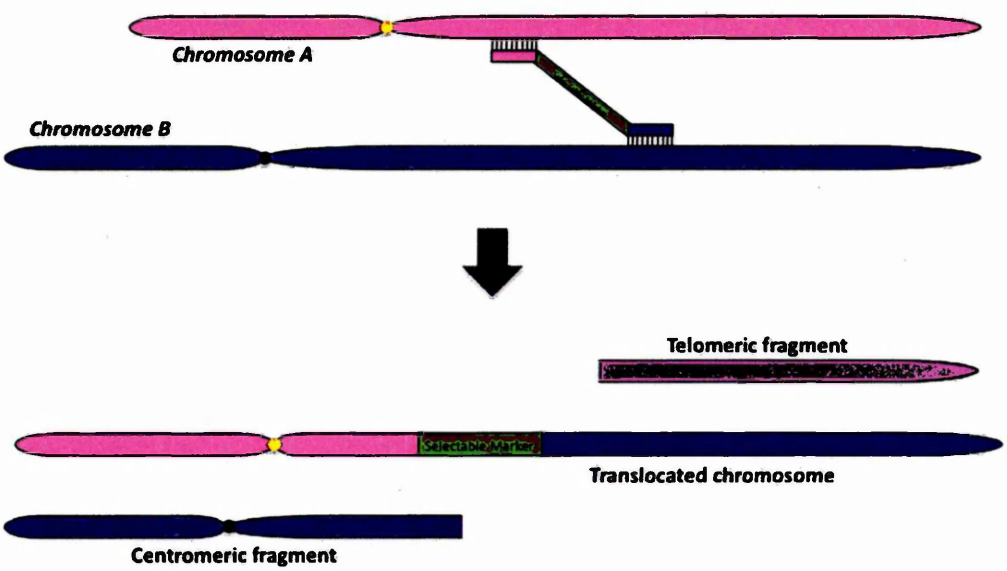

Figure 1.5 Schematic depiction of Bridge Induced Translocation (BIT) in *S. cerevisiae*. Chromosomal bridging by targeted homologous recombination on separate chromosomes results in the formation of aberrant translocated chromosome and chromosomal fragments, which might or might not carry a centromere.

Thus, this straightforward technique could provide important extrapolations to higher eukaryotic and mammalian cells by serving as a model to induce and study genome rearrangements in them.

1.5.4 Targeted integration of extrachromosomal DNA in yeast:

The targeted introduction of exogenous DNA into yeast cells has proven to be a highly valuable and efficient tool in genome manipulation and function elucidation. Since the introduction of yeast transformation in the late 1970s (HINNEN *et al.* 1978), gene replacement using artificially synthesized linear DNA constructs (SCHERER and DAVIS 1979), and insertional mutagenesis employing plasmids bearing homologous sequence to the targeted locus, has been performed (ORR-WEAVER *et al.* 1981). Moreover, both strategies of genome manipulation depend on the homologous recombination system in yeast cells. Earlier, yeast genes were disrupted using plasmids carrying a fragment of the targeted gene to facilitate HR between plasmid and chromosomal DNA. Recombination frequency was greatly enhanced when such plasmids were linearised at the region of homology (ORR-WEAVER *et al.* 1981). This kind of "ends-in" method of gene disruption introduces exogenous DNA within the target site, without deleting the target gene itself. Insertional mutagenesis of this type has been proposed to be analogous to DSBR, during which integration of broken plasmid into chromosomal DNA occurs by gene conversion associated with crossing over (ORR-WEAVER *et al.* 1981). On the other hand, gene replacement or deletion strategies in yeast (ORR-WEAVER *et al.* 1983) utilize recombinant linear DNA, which bears a selectable marker flanked by sequences at its termini that are homologous to those flanking the target gene on the chromosome. The "ends-out" type of gene targeting involves HR between sequences at the ends of the linear targeting DNA

and those flanking the target gene, which facilitates the replacement of the target gene with the selectable marker (**Figure 1.6**).

Figure 1.6 **(a)** "Ends-in" model of integrative recombination resulting in gene disruption using plasmids linearised within the homologous target they carry, and **(b)** Gene replacement by "ends-out" type of targeted recombination using linear DNA.

Introduction of linearised plasmid DNA in yeast usually results in efficient recombination into sequences homologous to the ends of the linear molecule. Although, transformation of *S. cerevisiae* cells with linear exogenous DNA results in a surprisingly low frequency of gene replacement, despite possessing an efficient homologous recombination system. This could possibly be associated with rapid degradation of histone-free naked DNA by cellular nucleases, or alternatively, the process itself might be inherently inefficient. Other factors influencing such events could be the mere competence of certain cells to take up exogenous DNA from the environment, or even the amount or copies of exogenous DNA that might have been taken up by an individual cell.

Two opposing views of gene targeting by linear duplex DNA have arisen from studies in yeast. Earlier work shows that linear fragments of DNA are assimilated into targeted regions by the formation of heteroduplex DNA (hDNA) over the entire region between the fragment and the targeted chromosomal sequence (**Figure 1.7a**). This

happens by single strand assimilation of the fragment over this region, whereby one or the other strand of the linear duplex DNA is assimilated into the recipient chromosome (LEUNG *et al.* 1997). These studies support single strand assimilation of fragments ranging from 2 to 4 Kbp in length, provided they carry no more than two mismatches to the targeted chromosomal region. More recently others have demonstrated that the frequency of homologous integration by ends-in targeted recombination employing a linearised vector for gene targeting is increased by the inactivation of *HDF1* (yKU70) and *SGS1*, which have roles in DSB processing and repair (YAMANA *et al.* 2005).

The second view suggests separate strand invasions during gene replacement employing linear fragments, which carry distant regions of homology flanking a selectable marker (**Figure 1.7b**). During this, hDNA is formed at two separate chromosomal locations where homologous sequences located at the ends of the linear duplex DNA interact with those on the chromosome. This initiates two independent strand invasions and subsequent resolution at the two ends to facilitate gene replacement (LANGSTON and SYMINGTON 2004).

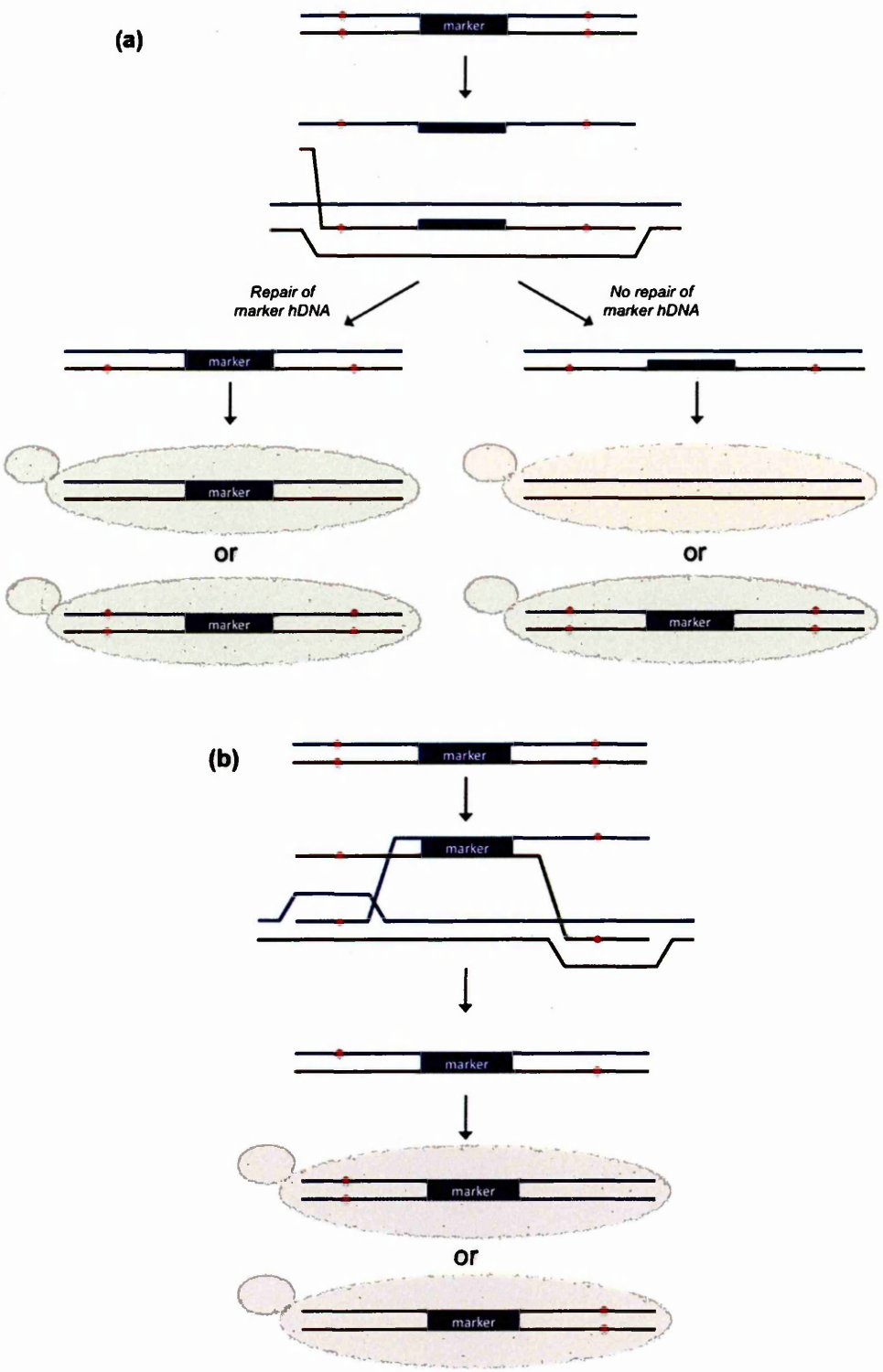

Figure 1.7 Gene targeting models: **(a)** Single strand assimilation – with and without mismatch correction, **(b)** Independent strand invasion and resolution at both ends of linear duplex DNA. Shaded ovals represent cell genotypes arising from replication of either DNA strand after targeted integration. Small red dots represent mismatches in homologous sequences carried on the targeting DNA.

Other studies in yeast have tried to overcome the limitations of transformation-based introduction of linear DNA molecules for gene targeting. Instead, pre-engineered strains have been developed in which linear fragments of DNA can be excised/liberated endogenously from extrachromosomal (HAVIV-CHESNER *et al.* 2007) or chromosomal (LEUNG *et al.* 1997) locations to act as targeting molecules on other chromosomal targets. Most often these fragments are reported to become captured by DSBs utilizing the NHEJ pathway for repair, whereas excision site have been reported to be repaired by SSA as per experimental conditions provided.

The BIT model for translocation induction is clearly based on targeted assimilation of exogenous DNA into distinct loci on separate yeast chromosomes. This is different from previous studies, which report gene targeting and linear DNA integration on single chromosomes in yeast. Besides, gene replacement and integrative mutagenesis, two independent groups have used methods that rely on co-transformation of linear DNA molecules that can interact among them in addition to the target chromosomal sequence. For example, tandem arrays of linearised plasmid have been reported to integrate into the chromosome carrying homologous sequence, provided transformation was carried out using excess DNA (PLESSIS and DUJON 1993). A similar mutagenesis system referred to as the "*delitto perfetto*" or perfect deletion requires *in vivo* interaction of overlapping integrative recombinant oligonucleotides (IROs) followed by its integration into the target chromosomal sequence (STORICI *et al.* 2001).

In contrast, the BIT system provides the first such model system to study homologous DNA targeting on separate DNA molecules. Interestingly, the frequency of the occurrence of such an event targeting loci on two different chromosomes is relatively

much lower (1-8%) than a standard gene knockout event (50-70%) that targets loci on the same DNA molecule. This suggests that possibly intra-molecular deletions are well tolerated by yeast cells in contrast to inter-molecular rearrangements. Such tolerance might involve suppression mechanisms that keep GCR levels to a minimum in cells, or might depend merely on the frequency due to locality of targeted loci within the cell nucleus. In short, the infrequency of chromosomal bridging points to possible regulatory mechanism(s), which represses gross chromosomal rearrangements or rather Bridge Induced Translocations in this case.

1.6 Aims and objectives:

Translocations between non-homologous chromosomes are some of the most severe genomic aberrations that often lead to malignant transformation in higher eukaryotes. In humans they have been associated to hematological cancers such as myelogenous leukemias but also to lymphomas, solid tumors and recently, to mesenchymal and epithelial cancers. Despite this diagnostic significance, very little is known about the molecular mechanisms by which translocations occur or remain suppressed in healthy cells. Numerous assays have been developed to broaden the understanding of the formation and regulation of chromosome abberations. The "Bridge Induced Translocation" system has been recently developed by our group, as described above. This method has been employed to investigate the multiple molecular mechanisms and pathways that might be involved during a translocation event in *Saccharomyces cerevisiae*.

To this end, here in this report, I have utilized the BIT methodology to generate a series of translocant strains derived from parental wild type strains. Initial attempts have

focused on the detection and visualization of BIT events in real time using fluorescence reconstruction by targeted integration directed on chromosomes V and III. This was followed by attempts to elucidate the timing of linear DNA integration at targeted loci on the same two chromosomes. In these experiments we have tried to address whether BIT-targeting events are sequential, or simultaneous events, at the two targeted loci in question. Chapter 3 of the results section describes the experimental setup and observations in these lines of investigation.

Keeping in mind the suppression of GCR rates in wild type cells, and the low frequency of BIT events generating non-reciprocal translocations, I have generated a series of diploid mutants that carry deletions of a few important candidate genes that have well established roles in the maintenance of genome stability and integrity. The list of these genes includes recombination and repair factors like *MRE11, KU70, ELG1*, in addition to DNA damage and S-phase checkpoint functions like *TEL1, SGS1, MRC1, ESC2*. Following mutant construction, these strains were subjected to the BIT induction between the promoter regions of *ADH1* and *SUC2* genes located on chromosomes XV and IX, respectively. Such experiments have aimed at understanding the genetic control and regulation of targeted BIT events *in vivo*. Furthermore, the fate of chromosomal fragments generated after BIT formation has been studied using CHEF and southern hybridization strategies. Results described in Chapter 4 provide an elaborate description of observations and some interesting findings in this context.

Similarly, another set of translocant strains have been generated between chromosomes XVI and IX, targeting *SSU1* terminator and *SUC2* promoter loci, respectively. These set of translocants harboring the same translocation breakpoints have

been characterized from physiological, morphological and genomic point of views. Expression patterns of some genes along the translocated chromosome and those located at other genomic locations were elucidated using QPCR strategies. The nature of diverse aneuploidies arising after BIT formation in these translocants has also been characterized at the chromosomal level. Observations described in results Chapter 5 provide descriptive analysis of these translocation bearing yeast strains, and reveal the complexity of chromosomal rearrangements ensuing the BIT process in these modified cells. Such complex genomic rearrangements seen in yeast may play a role as key evolutionary forces, reshaping and remodeling genomes. This could then be followed by selection and adaptation into specialized cells or even neoplastic transformation, as observed in mammalian cancer cells.

Materials and Methods

2.1 Growth media and growth conditions:

All *S. cerevisiae* strains were cultured and maintained at 30 °C with aeration in a shaking incubator set at 200 rpm for liquid cultures. Yeast extract Peptone Dextrose (YPD) medium [1 % yeast extract (Difco, Detroit, MI); 2 % (w/v) Bacto-peptone (Difco, Detroit, MI); 2 % (w/v) glucose] was used for non-selective growth. For preparation and use of all solid media, 2% (w/v) agar was added. Geneticin G418 (Gibco, Rockville, Md.) was added at a final concentration of 200 μg/ml, for selection of kanamycin resistant transformants. Similarly, for selection and growth of all hygromycin resistant transformants, Hygromycin B (Invitrogen) was added at a final concentration of 200 μg/ml. Growth density of all strains in liquid medium was monitored using a haemocytometer at the required timepoints. Sporulation of yeast strains was carried out by overnight preculture in sporulation media II containing 0.05 % glucose and then for 3-7 days in sporulation media III (potassium acetate 1 %). All *E. coli* strains used were cultured in luria broth (LB) media at 37 °C.

The standard growth conditions for RT-PCR were as follow: cells were cultured in 100 ml baffled flasks with 10 ml medium in a shaking incubator at 30 °C and 160 rpm. After 18 hours of pre-culturing in YPD the cells were washed with sterile water and inoculated (10^5 cells ml^{-1}) in 250 ml flasks containing 20 ml of fresh YPD medium. After 16 hours of growth, cells were centrifuged and then resuspended in 1 ml sterile water. A volume corresponding to 0.3-0.5 OD_{600} of these suspensions were then transferred to new 250 ml flask containing 15 ml of fresh YPD (glucose 2%). Cultures were further incubated for an additional 3 hours and then harvested for total RNA extraction.

2.2 Strains and plasmids:

Two diploid *Saccharomyces cerevisiae* strains San1 and PAW1 were used as recipient strains to induce the translocation between chromosomes XV and IX. All double knockout mutants were generated in the BY4743 (*MAT*a/α *his3Δ1/his3Δ1 leu2Δ0/leu2Δ0 LYS2/lys2Δ0 met15Δ0/MET15 ura3Δ0/ura3Δ0*) background of PAW1, which was also used as the reference strain throughout this work. The San1 strain was obtained by mating Fas20 a, *ade1, ade2, ade8, can1*^{R}, *leu2, trp1, ura3-52* (BRUSCHI and HOWE 1988) and YPH250 **a**, *ade2-101, leu2-D1, lys2-801a, his3-D200, trp1-D1 ura3-52* (ATCC 96519). This strain harbors the GFP and RFP fluorophores at the *arg4* locus on chromosome VIII (WAGHMARE *et al.* 2003). All SUSU translocants were derived from the San1 parental strain.

The SAD translocants are all derivatives of PAW1 and they were obtained using the BIT methodology (TOSATO *et al.* 2005)). The BIT construct was amplified using the primers Fw(XVI) and Rev(IX) reported in **Table 2.3**. Transformants were selected as Kan^{R} strains and the presence of the translocation between the *SSU1* and *SUC2* loci was detected by PCR and Southern blot analyses. The two diploid mutant strains San1-*DBP1/dbp1::KANMX4* and San1-*GUT2/gut2::KANMX4* used in CHEF experiments are both derivatives of San1 and they were obtained using the standard PCR-based gene knockout technique. DFDBP1 (forward) and RKANDBP1 (reverse) primers were used for DBP1 deletion cassette amplification; GUT2DFw (forward) and GUT2DrevNEW (reverse) for GUT2 deletion cassette amplification.

The *Escherichia coli* strain XL1-blue MRF' D(*mrcA*)183 D(*mrcCB-hsdSMR-mrr*)173 *endA1, supE44, thi-1, recA, gyrA96, relA1, lac* (F'*proAB lacIqZ* DM15 Tn10

[*Tet*^{r}*J*]^c (Stratagene, La Jolla, CA) was used for routine plasmid preparation. Plasmid pFA6-KanMX4 containing the *KANMX4* gene (OKA *et al.* 1981), was used as template for the amplification of the SUSU- BIT and SAD-BIT constructs, and plasmid pNP001 derived from pAG32 backbone was used as a PCR template to synthesize the RG-BIT construct. Oligonucleotide sequences of primers used for construction of the PAW1 strain and pNP001 plasmid are listed in **Table 2.2**.

2.3 Microscopy and Staining:

2.3.1 *Light microscopy:*

Cell density of all cultures was calculated based on cell counts obtained using a haemocytometer or alternatively measured using a spectrophotometer. Light microscopy was also used for observation of cellular phenotypes of all knockout mutants and translocant cells.

2.3.2 *Fluorescence imaging:*

Detection of GFP and/or DsRed markers was carried out using an Axiovert® 100M confocal microscope. Samples taken from cultures at late exponential phase were spotted on glass slides and spread in order to air dry and fix the sample. A small drop (~8μl for a 10μl sample) of mounting medium for fluorescence without DAPI was placed on the dried sample and covered with a clean glass slide, which was then sealed on the borders to proceed for detection using microscopy.

2.3.3 *DAPI staining*:

A single isolated colony was inoculated in 100 ml baffled glass flask containing 10 ml YPD medium and incubated at 30 °C. After 16, 40 or 72 hours of growth, 1ml of the culture was harvested and the cells were washed once with ddH_2O. A drop of this suspension was then fixed on a slide and stained with DAPI solution (Vectashield mounting medium for fluorescence with DAPI, Vector Laboratories, Inc. Burlingame, CA). The morphology of cells and nuclei was monitored by fluorescence microscopy using a Leica DMLB fluorescence microscope equipped with a CCD computer-driven camera at 60X and 100X magnifications. The images were processed using Adobe Photoshop Elements 3.0 (Adobe Systems, Inc., San Jose, CA).

2.4 Preparation of total Genomic DNA from *S. cerevisiae:*

Overnight cultures of yeast strains were set up in 10 ml of YPD or SD at 30 °C. Cells were sub-cultured back in 50 ml of fresh YPD equilibrated at 30 °C to a cell titre of 2×10^6 cells.ml^{-1}. Incubation was continued until a cell titre of 2×10^7 cells.ml^{-1} to 3.6×10^7 cells.ml^{-1} was attained. Cells were harvested by centrifugation at 4000 rpm for 5 minutes. The cells were washed in 1 ml of sterilised distilled water and resuspended in 0.5 ml of solution A (1.2 M sorbitol; 0.2 M Tris-HCl, pH 8.5; 0.02 M EDTA; 0.1% BME: β-mercapto-ethanol). Fifty microliters of 10 mg.ml^{-1} Zymolyase (Saekagaku, Japan) was added and cells were incubated at 37 °C for 25 minutes in a shaker till sphaeroplasting was complete. Sphaeroplasting was checked microscopically, as sphaeroplasted cells appear phase dark and do not refract light at the cell periphery. Sphaeroplasted cells were harvested in 1.5 ml snap-top tubes by centrifugation at 13000 rpm for 2 minutes and were resuspended in 50 µl of 1 M sorbitol. Half a milliliter of solution B (50 mM Tris-HCl, pH

7.5; 100 mM NaCl; 100 mM EDTA; 0.5 % SDS) was then added to the cell suspension. Twenty microliters of 10 $mg.ml^{-1}$ Proteinase 'K' and 5 µl of 10 $mg.ml^{-1}$ RNase 'A' were then added and the cell suspension was incubated at 65 °C for 2 hours. Phenol, chloroform and isoamyl alcohol (IAA) solution was prepared in the ratio of 25:24:1 (v/v). Half a milliliter of phenol/chloroform/isoamyl alcohol solution was then added to each sample in 2 ml Eppendorf® phase-lock gel (PLG) tubes and mixed by inverting tube several times. Lower organic and upper aqueous phases were separated by centrifugation at 13000 rpm. This was repeated again with 0.5 ml of phenol/chloroform/isoamyl alcohol and finally with 0.5 ml of chloroform/IAA (CI) in a ratio of 24:1 (v/v). The supernatant from the PLG tubes was transferred to fresh 1.5 ml snap-top tubes and 1 ml of absolute ethanol was added to precipitate the DNA. The DNA was pelleted by centrifugation at 13000 rpm and washed with 70 % ethanol. After air-drying the DNA pellet at room temperature, it was resuspended in 100 µl of sterile distilled water. Concentration of DNA was determined using UV spectrophotometer.

Alternatively, genomic DNA extractions were performed using the Wizard Genomic DNA purification Kit (Promega, Madison, WI).

2.5 Lithium Acetate (LiAc) transformation of *S. cerevisiae* (GIETZ *et al.* 1992)**:**

Transformation of *S. cerevisiae* was performed either by the LiAc method as per the EUROFAN protocol for PCR-based gene replacements (WACH *et al.* 1994) or with the Sphaeroplast method following instructions reported in *"Methods in Yeast Genetics"* (KAISER *et al.* 1994).

Yeast strains to be transformed were cultured overnight in 5 ml of YPD or SD and the cell titre was determined and diluted to a concentration of 2×10^6 cells.ml^{-1}. Incubation was continued until a cell titre of 2×10^7 cells.ml^{-1} to 3.6×10^7 cells.ml^{-1} (late exponential phase) was attained. Cells were harvested by centrifugation at 4000 rpm for 5 minutes and the supernatant was discarded. The cells were first washed in 1 ml of sterile distilled water and then in 1 ml of 1×TE-100 mM lithium acetate (pH 7.5). After each wash the cells were harvested by centrifugation at 13000 rpm and the supernatant was discarded. Finally, the cells were resuspended in 1×TE-100 mM lithium acetate (pH 7.5) at a cell concentration of 2×10^9 cells.ml^{-1}. Salmon sperm DNA at a concentration of 1 mg.ml^{-1} was boiled for 5 minutes and then kept on ice immediately to keep it single stranded.

For each transformation, 50 µl of the cell suspension was mixed with 300 µl of 50 % PEG3350, 50 μl of 1 mg.ml^{-1} salmon sperm DNA and 5-10 μg of transforming DNA. A negative control excluding the transforming DNA, and a positive control using plasmid harboring an appropriate selectable marker were also set up. This cell suspension mixture was incubated at 30 °C for 30 minutes and then at 42 °C for 15 minutes. The cells were resuspended in 1 ml of YPD and incubated at 30 °C for at least 90 minutes if selecting for a positive antibiotic resistance marker. Cells were then harvested by centrifugation at 13000 rpm and resuspended in 1×TE buffer (pH 7.5) or sterile ddH_2O. The transformation suspension was then plated on selective media and spread using sterile glass beads or plastic cell spreaders. Plates were then incubated at 30 °C for about 3 to 5 days till growing colonies were observed.

2.6 PCR-based gene-disruption by marker recycling:

A PCR-based technique was employed to generate gene disruption cassettes using specific primers, bearing 40 bp of homologous sequence to the target gene to be disrupted. A 2-micron DNA-based marker recycling system for multiple gene disruption in *Saccharomyces cerevisiae* (STORICI et al. 1999) was employed to construct knockout mutants of several genes in the diploid strain PAW1. Homozygous deletions for individual genes were performed in tandem by providing the second deletion homology internal to the first one. A series of isogenic plasmids pGKG, pHKH, pXKX; all containing a KANMX4 resistance marker flanked by variants of FRT (*Flp* recognition target) sequences, were utilized as templates for the synthesis of gene disruption constructs. Each PCR verified replacement of any locus in question, by a KANMX4-FRT construct, was followed by induction of KANMX4 pop-out to leave a distinct FRT-scar of 108bp. Pop-out events were induced by growth on media without selection for kanamycin resistance for 3-5 days. Cells were plated at a dilution of 1×10^3 cells/ml and colonies arising from these plates were replica plated on G418 containing plates to select for pop-out clones that were unviable on selective media. PCR parameters were set up at 94 °C for 3 minutes (initial denaturation); 30 cycles of 94 °C for 30 seconds, 55 °C for 30 seconds, 68 °C for 1 minute; final extension at 68 °C for 4 minutes and 16 °C forever. Fifty micro liter PCR reactions were set up using 50 ng of appropriate plasmid as initial template DNA. PCR products obtained from these reactions were purified by gel extraction (Quiagen Gel Extraction Kits) and used as transforming DNA for LiAc-based transformation of yeast strains. The oligonucleotide sequences for gene-disruption primers are shown in **Table 2.1**.

2.7 Semi-quantitative RT-PCR analyses:

Total RNAs were isolated from cells using the SV Total RNA Isolation System (Promega, Madison, WI) or the Total Quick RNA kit (Talent, Trieste, Italy). Equal amounts of total RNA (1 μg) were then employed to synthesize the total cDNA in a 25 µl reaction mixture using the AMV Reverse Transcriptase in the presence of RNase Inhibitor (Promega, Madison, WI) according to the manufacturer's instructions. Semi quantitative PCR was performed with GoTaq polymerase (Promega, Madison, WI) using a limiting number of cycles (20 – 23 cycles). A Sprint Hybaid Thermocycler device was employed for PCR cycling. Thermal-cycling parameters were as follows: after an initial denaturation at 95 °C for 5 minutes, samples were subjected to a cycling regime of 22-23 cycles at 95 °C for 30 seconds, 50 °C for 30 seconds and 72 °C for 1 minute. At the end of the final cycle, an additional extension step was carried out for 7 min at 72 °C.

RT-PCR results were quantified using a laser-scanning densitometry (UltroScan XL, Pharmacia LKB) and the intensity of each band (area) was calculated as the average of three different measures. The housekeeping gene *HSC82*, located on chromosome VIII, was used to normalize the data. Data presented in **Figure 5.5** are averages and standard errors from at least three independent determinations in which the final values are the expression level of each gene normalized with respect to its expression in the San1 control strain considered as unit.

2.8 Hydrolyzing probe based Quantitative PCR:

We have also used fluorescently labeled oligonucleotide probes and gene specific primer pairs for the copy number determination in experiments described in Results

Chapter 4. The sequence of probes and oligonucleotide pairs are listed in **Table 2.4.** Genomic DNA from samples to be used as template for such PCR reactions was diluted 100 fold from stocks generated using genomic DNA extraction kits. The optimum concentration of template DNA, primer pairs and fluorescently labeled probe needed for quantification experiments were standardized by PCR. For each sample, each PCR reaction was performed in triplicate, in addition to those carried out in tandem with probes specific for *ACT1*, acting as an internal control for a gene copy number of two. All reactions were prepared in JumpStart™ Taq ReadyMix™ for Quantitative PCR mastermix. Gene specific primers and labeled probes were designed and provided by Sigma Aldrich. A Bio-Rad CFX96 PCR detection system was employed to obtain quantitative measurements from each reaction.

2.9 Contour-clamped Homogeneous Electric Field (CHEF) analysis:

The agarose cell plugs were prepared as described in KAISER *et al.*, (1994) using proteinase K (Sigma-Aldrich, St. Louis, MO) at the final concentration of 20 mg/ml. Chromosomal separation was performed in 1% pulse-field certified agarose gel (BioRad, Richmond, CA) by electrophoresis using the CHEF DR-II apparatus (BioRad, Richmond, CA) set at 200 V for 24 hours with an initial switching time of 60 seconds and a final time of 120 seconds. Alternatively the same was set at 200 V for 16 hours with an initial switching time of 60 seconds and a final time of 120 seconds followed by 200 V for 8 hours with an initial switching time of 90 seconds and a final time of 120 seconds. Chromosomal DNA was then depurinated and denatured prior to transfer onto a positively charged nylon membrane (Hybond N+, GE healthcare, Piscataway, NJ) by

capillarity or using a vacuum manifold for nucleic acid transfer (BioRad, Richmond, CA).

2.10 Southern Hybridization and DIG-Probe synthesis:

Chromosomal DNA was fixed on nylon membranes by baking at 80 °C for at least 90 minutes. Pre-hybridization and hybridization using appropriate reagents was performed at 68 °C and detection with DIG labeled probes was performed using CDP star as a chemiliuminiscent substrate. Hybridization probes were labeled using the polymerase chain reaction digoxygenin (PCR-DIG) probe synthesis kit (Roche, Basel, Switzerland) and were amplified from genomic DNA using the following primers listed in **Table 2.5**.

2.11 Molecular biology techniques:

Standard recombinant DNA techniques were carried out essentially according to (SAMBROOK *et al.* 1989). Plasmid mini-preparations were obtained using the Wizard plus SV kit (Promega, Madison, WI). Restriction enzymes and biochemicals, obtained from New England Biolabs (Beverly, MA), were used as described by the manufacturer.

Name of Oligonucleotide	Oligonucleotide Sequence 5'-3'
HDF1 F	ATGCGCTCAGTCACTAATGCATTTGGCAATAGTGGAGAACaaaaataggcgtatcacgag
HDF1 R	TTATATATTGAATTTCGGCTTTTTATCAAAGGGCTTCTTTtcgatgataagctgtcaaac
HDF1 F2	TTAACGATCAAGTGGATGAAACAGGTTATAGGAAGTTTGAaaaaataggcgtatcacgag
HDF1 R2	TATTTAGCCTTTGGATGATTGGATCTTCTGACTTCTCAGAtcgatgataagctgtcaaac
deltaKU70 2nd INT Fw	ATCCATGAAGGAATTTTGTTTTGCATTGAACTATCAGAGACaaaaataggcgtatcacgag
deltaKU70 2nd INT Rev	TCTAAAATTTTATTTCGTATATAATATAGTTTCCTTAAAGAtcgatgataagctgtcaaac
Ku70 F1	AGATCGGGCGTTCGACTCGC
Ku70 Rev*	CAAGTGATCATTTGTCTATGGTGTG
MRE11 F1 delta	ATGGACTATCCTGATCCAGACACAATAAGGATTTTAATTAaaaaataggcgtatcacgag
MRE11 R1 delta	CTATTTTCTTTTCTTAGCAAGGAGACTTCCAAGAATATCCtcgatgataagctgtcaaac
MRE11 F2 delta	CTACAGATAATCATGTGGGTTACAACGAAAATGATCCCATaaaaataggcgtatcacgag
MRE11 R2 delta	GTCTTTGGCGTCCTTGATGCTCTTCCTTTTCCCCTTCTGGtcgatgataagctgtcaaac
MRE11 F1	AGAGTTCACAAGCAAGCCTG
MRE11 R2	AACAAAAGAGCAAAGGCTGG
TEL1 Fw1 delta	ATGGAGGATCATGGGATTGTAGAAACTTTAAACTTTCTATaaataggcgtatcacgaggc
TEL1 Rev1 delta	TTAATAAAAAGGTGACCATCCCATATATATAACACTCAAAgcatcgatgataagctgtca

TEL1 Fw2 delta	CATCAACAAAAATCAAAGAGAGAAACAATGCTTTAGATGAaaataggcgtatcacgaggc
TEL1 Rev2 delta	TTTGATGGATCCGTGGCTTGCTGAATCAAATCTTGTACGCgcatcgatgataagctgtca
TEL1 Fw	ATTATGAGCGTGATAGGAGG
TEL1 Rev	TTGGCTCAGAATTTACGGGC
SGS1 Fw1 DELTA	CACAAGGCGGTAATGGTGACGAAGCCGTCACATAACTTAAGaaataggcgtatcacgaggc
SGS1 Rev1 DELTA	AGAATGCTTTGGCGAATGGTGTCGTAGTTATAAGTAACACTATTAgcatcgatgataagctgtca
SGS1 Fw2 DELTA	GACAAAGATTTCGTATTCCAGGCTATCCAAAAGCACATCgataggcgtatcacgaggccc
SGS1 REV2 DELTA	CCTTGTACCTGATTTGCTGCTTGTGGTATTTTTGGGTAATcatcgatgataagctgtcaaac
SGS F1	GATATACGGATCAATAGAGGG
SGS R2	GCGAGGATCATGAAAAATACG
SGS F2 NEW	TGAGTACATACCCATTATGTTG
SGS F2	AACTGAGCAATGTGCACACCA
ELG1 Fw1 delta	ATGAAAAGGCACGTGTCTTTATCTGATATATTGACAGGAAAataggcgtatcacgaggccc
ELG1 Rev1 delta	TTATTTGTTCTTTGAAAAGCCTGAGTGCAAATGCTCCCATcatcgatgataagctgtcaaac
ELG1 Fw2 delta	GTGAGAAGACAAGATGCTCTACAGATTACCATCGATGACgataggcgtatcacgaggccc
ELG1 Rev2 delta	CACGACTATGCTCGGATCAGCGTTGAACCATACGTTTTTCcatcgatgataagctgtcaaac
ELG1 up	CCAAACGCGTAACGTTAGCG
ELG1 down	GCTTAATGCAAGGTTGCAGA

ESC2 F1 delta	ATGACCGGTGATTCCAGAAGCATCAGCGAACCCTCAATTAtaggcgtatcacgaggcc
ESC2 R1 delta	CAATCAATAATGACATCAACCATGTCTTCATCTTCCATATatcgatgataagctgtcaaac
ESC2 F2 delta	TAATAGGCAAAGTGTCATAGTTGACTCTAAAGTCACGGTAtaggcgtatcacgaggcc
ESC2 R2 delta	CCTGATCGGCTATACACTCATTCATGTCCAATTCATCATGatcgatgataagctgtcaaac
ESC2 F1	CAGCATGCCTATGAATTCCC
ESC2 R1	ATGTTGTTCCTTTGCGTCGC
ESC2 F2	ATATCGCGAGTTTGAATCCG
ESC2 R2	CAAGAAAACTATAGCCGAGG
MRC1 F1 delta	ATGGATGATGCCTTGCATGCTTTGTCCTCGTTGACTGCAAtaggcgtatcacgaggcc
MRC1 R1 delta	TAATTATCAAAGCTATCTTGTCCGCTTTCAAAAAGTTTATatcgatgataagctgtcaaac
MRC1 F2 delta	AGAAGAGAACTACCACCTACAAAAAAGTTGCTGTTCCCATtaggcgtatcacgaggcc
MRC1 R2 delta	ATGGTCATGGTGGTAGCGGTGGCTCCCTTCAGTTTTCCTCatcgatgataagctgtcaaac
MRC1 F1	GACGCGTCATGAAGAGATAG
MRC1 R1	CGATTTAATGTGGCATTGGC
MRC1 F2	AGATACATCACTAGTTGGCG

Table 2.1 A list of all the oligonucleotides used for gene knockout experiments and subsequent verification. Nucleotides in capital letters represent the genome sequences targeted for the knockout, whereas, those in small letters represent sequence homologous to the template plasmids used for amplification by PCR.

Name of Oligonucleotide	Sequence of oligonucleotide 5'-3'
GEA2-URA3 Fw	ATGTTAATTACCTTTTTTGCGAGGCATATTTATGGTGAAGaaaaataggcgtatcacgag
GEA2-URA3 Rev	ATGGACCCTGAAACCACAGCCACATTAACCTTCTTTGATGgccatggaacaggtagtttt
GFP Reconstruction Fw	**TTTTAGATCT**AAATTTATTTGCACTACTGGAAAACTACCTGTTCCATGGC
GFP Reconstruction Rev	**TTTTAGATCT**tcgatgataagctgtcaaac
GEA2 F2	TGAAACTAGGGAAGACAAGC
YEL020C-B F2	GACACAGTCTGTGAAACATC
LEU2-NFS1 Fw	AGACGAAACTATATACGCAATCTACATACATTTATCAAGAaaaaataggcgtatcacgag
LEU2-NFS1 Rev	CGTTGAGCCATTAGTATCAATTTGCTTACCTGTATTCCTTttggtcaccttcagcttcac
RFP Reconstruction Fw	**TTTTACTAGT**CCTACGAGGGCCACAACACCGTGAAGCTGAAGGTGACCAA
RFP Reconstruction Rev	**TTTTACTAGT**tcgatgataagctgtcaaac
Ty1 Downstream	ATTACAGCCCTCTTGACCTC
NFS1 F2	TTATCCAGGGTGTGTTAACG
HYG Fw	AGCTGAAGCTTCGTACGCTG
HYG Rev	ATACGACTCACTATAGGGAG
H1	AGCTATTTACCCGGAGGACA
H2	CTCTATCAGAGCTTGGTTGA

R-G BIT Fw	AAATTTATTTGCACTACTGG
R-G BIT Rev	CCTACGAGGGCCACAACACC
R-G BIT Fw *	AAATTTATTTGCACTACTGGAAAAC
R-G BIT Rev *	CCTACGAGGGCCACAAC
RFP int	TTGGAGCCGTACTGGAACT
GFP int	CATTGAACACCATAAGAGAAAG
TetR F2	GCATTATATGCACTCAGCGC
Leu2 Promoter	ATAGGTGGTTAGCAATCGTC
TIM9 Fw	ATGGACGCATTGAACTCCAAAG
TIM9 Rev	CTACACGTTCGCTATGCTTCAAGAA
Tim9 Ext F	TACCTCGCCAGAACCAAGTA
Tim9 Ext R	TATATATACGCCAGTACACC
RIP1-YEL023C Fw	ATCTGCATGTATTTATAATTAACGAAACTATTTATCTTCCaaaaataggcgtatcacgag
RIP1-YEL023C Rev	GTGAAATCTTCTGCTTCTGGACATCAATATTCAAATACAGgccatggaacaggtagtttt
RIP1 F2	AAGGGACCTGCCCCCTTAAA
YEL023C F2	TGGACTGGGATAGTAATTCC

YEL023Cdelta GFP recons	ATGGATAGCTTCAATTATATTCATGGAAAATATAAAAAAATTCGAGCTCGTTTTCGACAC
NFS1delta DsRed recons	ATGTTGAAATCAACTGCTACAAGATCGATAACAAGATTTGTTTAGCTTGCCTTGTCCC
YEL023C Ext F	TGGTAATGGCCCTCCTGTTG
NFS1 Ext F	CGGTCGCTGACAAATAGTAA
RIP1-YEL023C Forward	GTGAAATCTTCTGCTTCTGGACATCAATATTCAAATACAGaaaaataggcgtatcacgag
RIP1-YEL023C Reverse	ATCTGCATGTATTTATAATTAACGAAACTATTTATCTTCCgccatggaacaggtagtttt
URA3 Promoter	TTGAAATTTTTTTGATTCGGTAAT
URA3 Ter/pGKGE::GFP	TTAGTTTTGCTGGCCGCATCTTCTCAAATATGCTTCCCAGtcgatgataagctgtcaaac
ChrV/ΔGFP Probe Fw	TGCTTTACTAAGTCATCGCG
ChrV/ΔGFP Probe Rev	gccatggaacaggtagtttt
ChrIII/ΔDsRed Probe Fw	CCTCAACATAACGAGAACAC
ChrIII/ΔDsRed Probe Rev	ttggtcaccttcagcttcac
R-G BIT Fw 70	agagggtgaaggtgatgcaacatacggaaaacttaccctAAATTTATTTGCACTACTGGAAAAC
R-G BIT Rev 70	tcgagatcgagggcgagggcgagggccgccCCTACGAGGGCCACAACACC

Table 2.2 A list of all the oligonucleotides used in work described on Results chapter 3.

Name of Oligonucleotide	**Sequence of oligonucleotide 5'-3'**
Adh1 Fw 63 newW	GATAGTTGATTGTATGCTTGGTATAGCTTGAAATATTGTGCAGAAAAAGAAACAAGGAAGAAAGgtcgacggatccccgggttaa
Fw XVI (*SSU1*)	TCTCAGTATATTTTGCTGCTTTCCTTCATATGTATATATATCTATTTACATATTACAGAAgtcgacggatccccgggttaa
Rev IX (*SUC2*)	CTTTGCTGGGGGAGCGAGAACTACGCTAGGACAACAACTCCCATACGGTAAATGTCTTAGTATGtccgcgcgttggccgattcat
K1	acaatcgatagattgtcgcac
K2	actcgtcactcatggtgatt
Adh Up	ATTAACGACAAAGACAGCACC
Adh3	GTTAGCTCTAACGTATCTGGTA
DUR3R	AATTTGGAAGCATGCGCCAG
SSU1 Fw	CGGAGCTTTCCATTTGGAAT
SUC2 Rev New	CCTGGACGTGGGGTCGATTA
SUC2 FW New	ATAGGGGCTTAGCATCCACA

Table 2.3 A list of all the oligonucleotides used in the work described in Results chapter 5.

Name of Oligonucleotide	Oligonucleotide Sequence 5'-3'
SDL1-P	ACAACCAGGTGGAAGTTTCAAATC
SDL1 sense	TTTACGTTAAGCATGAGAT
SDL1 antisense	AATTAAGTGCCATCGATC
BRX1-P	ATTGCTTGACATTGCCTTGCTTC
BRX1 sense	CAGGAAAGAGCAAAGATAA
BRX1 antisense	TCTACTCGAAATCAGAAGA
ACT1-P	TTGCCGGTGACGACGCTCCTC
ACT1 sense	TGCTTTGGTTATTGATAACGGTTCTG
ACT1 antisense	GCTTCATCACCAACGTAGGAGTC
CDC33-P	CGTCCCGTCACTTCATTCCAAACTG
CDC33 sense	GATAAATCTGAGTCGTGGTCTGATC
CDC33 antisense	GTAATCTGATTTCAATGGTAGTTCGTG
KANr-P	TTCCAGACTTGTTCAACAGGCCAGC
KANr sense	TTGCATTCGATTCCTGTTTGTAATTG
KANr antisense	ACGACTGAATCCGGTGAGAATG
MUC1-P	ACCACCGCTCCTGCTACACCAACCA
MUC1 sense	TACCACTACATCTAGCACTTCCG
MUC1 antisense	ATGGAGTGGTGTCGTGATGAG

Table 2.4 A list of all the oligonucleotides used in the quantification of chromosomal loci on chromosomes XV and IX located by probe based QPCR. Each probe and primer pair set for each locus is represented separately.

Name of Oligonucleotide	Oligonucleotide Sequence 5'-3'	Application
PEP4 Fw	TCACTGAAGGTGGTCACGAT	Probe synthesis for *PEP4*
PEP4 Rev	CCATCGAACTTGCCAAATGC	
CFD1 Fw	AACAGGAGATAGGCGTTCCT	Probe synthesis for *CFD1*
CFD1 Rev	GGAATATCTCAGCTCCTCTG	
KAR1 Fw	TCAATCAGCGATATACACAGTTTCG	Probe synthesis for *KAR1*
KAR1 Rev	TCCTTTGAATCGGTATCGTCTTTTA	
MUC1 Fw	ATTCCAACCACTTACCTAACCACAA	Probe synthesis for *MUC1*
MUC1 Rev	TTCCAAGAACCTTGATATTAGCAGC	
RRD1 Fw	ATCTACACAGCATCAAAACGGAAA	Probe synthesis for *RRD1*
RRD1 Rev	CGACTGGTTTTGATGGCTTAGTAAA	
SDL1 FW sgd	ATGAAAAGACACCTTTGATTCGTCA	Probe synthesis for *SDL1*
SDL1 REV sgd	GCTCCTGCACTTTGAATTTTCTTTA	
South SUC2 Fw	TACTAACATGGCAGCATGC	Probe synthesis for *SUC2*
South SUC2 Rev	CGACGGCATTAGCAAAGCTT	

Cdc33Fw	ATTGATGAAGACGACTCCCA	Probe synthesis for *CDC33*
Cdc33Rev	GGTGCGTCTTTCATACCTTG	
Alg6Fw	GTTAAAGCAATGGCACTCCG	Probe synthesis for *ALG6*
Alg6Rev	AGTACCACTTAGAAAGCGGT	
Elg1Fw	ACAGCTTCAATTGGCTTCACA	Probe synthesis for *ELG1*
Elg1Rev	CCAAACGCGTAACGTTAGCG	
BRX1 Fw	CGGATTATTGCCTCATTCCAG	Probe synthesis for *BRX1*
BRX1 REV	TCTTACGACGTTTGGCGAAAC	
Kanfw	GGTGCGACAATCTATCGACGA	Probe synthesis for *KANMX4*
Kanrev	AGAAATCACCATGAGTGACGA	
HIS5fw	TTAGAGCATGCTGTGTTCCC	Probe synthesis for *HIS5*
HIS5rev	ACTCTGCTGTTGCATATGTC	

Table 2.5 A list of all the oligonucleotides used in the PCR amplification of Digoxigenin labeled probes used in the CHEF and Southern hybridization experiments

Name of Oligonucleotide	Oligonucleotide Sequence 5'-3'	Application
SSU1RTfw	TGGTATGATCTCGCAGTCTGTCTAG	RT-PCR of *SSU1*
SSU1RTrev	AAAGGCATAGAATTGACCAACAAA	
SUC2RTfw	GATCCTTCCAAATCTTATTGGGTC	RT-PCR of *SUC2*
SUC2RTrev	CATGTTCACAGATCCTAGAGCGTTA	
GLR1fw	TCTGATGGGTTCTTTAGATTGGAAG	RT-PCR of *GLR1*
GLR1rev	AGTAACCAATTCTTCTGCGCTAGTC	
GSH1fw	GCCAAAGACGTACAAGATAAAGTCC	RT-PCR of *GSH1*
GSH1rev	TTTCAGCTCCTAAAAAGGATGTCAA	
CLB1_For	TAGAGCAGGATGACCAGAAAAAGTT	RT-PCR of *CLB1*
CLB1_Rev	TCGTCGTGAATAGTAGATCCAACAA	
VMR1Fw	TTACTATCATCCCTCAGGAC	RT-PCR of *VMR1*
VMR1Rev	TTGCTTCAAAAGCTCTAGGC	
CdcFw	CCCAGTCTTACATCCAGACCAATAC	RT-PCR of *CDC48*
CdcRev	GATGCTTTCATTTGCTGTGAGTATG	
YCFw	TCCACCTCAAACACAAACTATCAA	RT-PCR of *YCA1*
YCRev	TACTTACCAGCCAATTCTTTCCTCA	
CAR1fw	GGAAAGTTGAAAATGGAGAAGGACT	RT-PCR of *CAR1*
CAR1rev	TACAATAAGGTTTCACCCAATGCAC	
MUC1Fw	ATTCCAACCACTTACCTAACCACAA	RT-PCR of *MUC1*

MUC1Rev	TTCCAAGAACCTTGATATTAGCAGC	
RRD1Fw	CCAGGTCCTAGAAGGTATGGTAACC	RT-PCR of *RRD1*
RRD1Rev	CGACTGGTTTTGATGGCTTAGTAAA	
GAL4fw	CCTCGAGAAGACCTTGACAT	RT-PCR of *GAL4*
GAL4rev	ATGGTCGGGAGCCTGTTAAC	
DAL4fw	CAGAGACTTGAAACCGGTTG	RT-PCR of *DAL4*
DAL4rev	GCATACCATACTATAGCCAT	
Hsc 82 For	TACATGAGGACACTCAAAACAGAGC	RT-PCR of *HSC82*
Hsc 82 Rev	TAATCAACTTCTTCCATCTCGGTGT	

Table 2.6 A list of all the oligonucleotides used in the RT-PCR analysis of genes located along the translocated chromosome and at other genomic locations in SUSU translocants.

Results (Part 1) – The Red-Green BIT system

The Bridge Induced Translocation system provides an excellent means to induce non-reciprocal translocations in *Saccharomyces cerevisiae* cells without prior modification and to study the molecular mechanisms and consequences of such chromosomal aberrations (NIKITIN *et al.* 2008; TOSATO *et al.* 2005). Here, we have attempted to engineer a genetic system for the visualization of BIT events in real time. This system is based on reconstitution of two different fluorescent markers on two separate yeast chromosomes upon BIT induction and subsequent detection of DNA integration on either chromosome in the form of fluorescent signals. To this end, we have genetically engineered a yeast strain named PAW1 containing truncated fragments of GFP and DsRed markers on chromosomes V and III, respectively. We have integrated these exogenous fragments into carefully chosen intergenic sequences, so as to minimally compromise normal cell homeostasis. We then engineered a plasmid to be used as a PCR template for amplification a novel BIT inducing construct, which provides homologous sequences for the reconstitution of full length GFP and DsRed upon correct integration on either chromosome and subsequent selection of transformants conferring hygromycin resistance.

Using such a genetic tool, we have aimed at elucidating the timing of BIT-inducing linear-DNA integration into targeted loci of yeast and selection of transformants and translocant cells by fluorescence. We propose that such a system will allow rapid and efficient screening of targeted events by direct visualization and in monitoring the real-time dynamics of linear DNA constructs undergoing HR at chromosomal loci.

3.1 Construction of the PAW1 strain:

A truncated sequence of GFP was initially integrated on chromosome V within the intergenic region of genes *GEA2* and *URA3* in *S. cerevisiae* strain BY4743. Notably, the *URA3* ORF bears a homozygous deletion in this strain (BRACHMANN *et al.* 1998). This fragment was amplified from the plasmid pGKGE::*URA3*P-NLS-tetr-GFP using oligonucleotides bearing 40bp of homologous sequence to the site of integration. The amplified and purified construct was then integrated using the STIK methodology (WAGHMARE *et al.* 2003) that involves the pop-out of the KAN^R selectable maker flanked by FRT (*Flp* recognition target) sequences, following the integration process (**Figure 3.3**). In other words, the integrated fragment bears the *URA3* promoter, the NLS sequence, *TETr* gene and the first 169 nucleotides of the coding sequence of GFP. The remaining sequence of GFP terminated by the *ADH1* terminator was cloned into the *BglII* site of pAG32, just upstream the promoter of the HYG^R marker as described further.

We have discovered that integration of the *URA3*P-NLS-tetr-truncatedGFP construct leads to the formation of jagged-edge colonies in the engineered strain (**Figure 3.2**). To investigate this phenotype further, we noticed the presence of the *TIM9* ORF, encoded about 170bp downstream the integration site. *TIM9* encodes a mitochondrial inter-membrane space protein, which forms a complex with Mrs11p/Tim10p that mediates import and insertion of a subset of polytopic inner membrane proteins and may prevent aggregation of incoming proteins in a chaperone-like manner. We hypothesized that the strong *URA3* promoter of the ΔGFP construct was driving the over-expression of *TIM9* or alternatively leading to the formation of a fusion protein between the engineered construct and *TIM9*. This might be due to the lack of a stop codon in the truncated GFP

construct. To test our hypothesis, we performed a reverse transcriptase-PCR on this strain. Our results show that although the expression of *TIM9* is not altered in this strain in comparison to the wild type BY4743 strain, we did however notice the presence of a transcriptase read-through into the *TIM9* ORF (**Figure 3.1**).

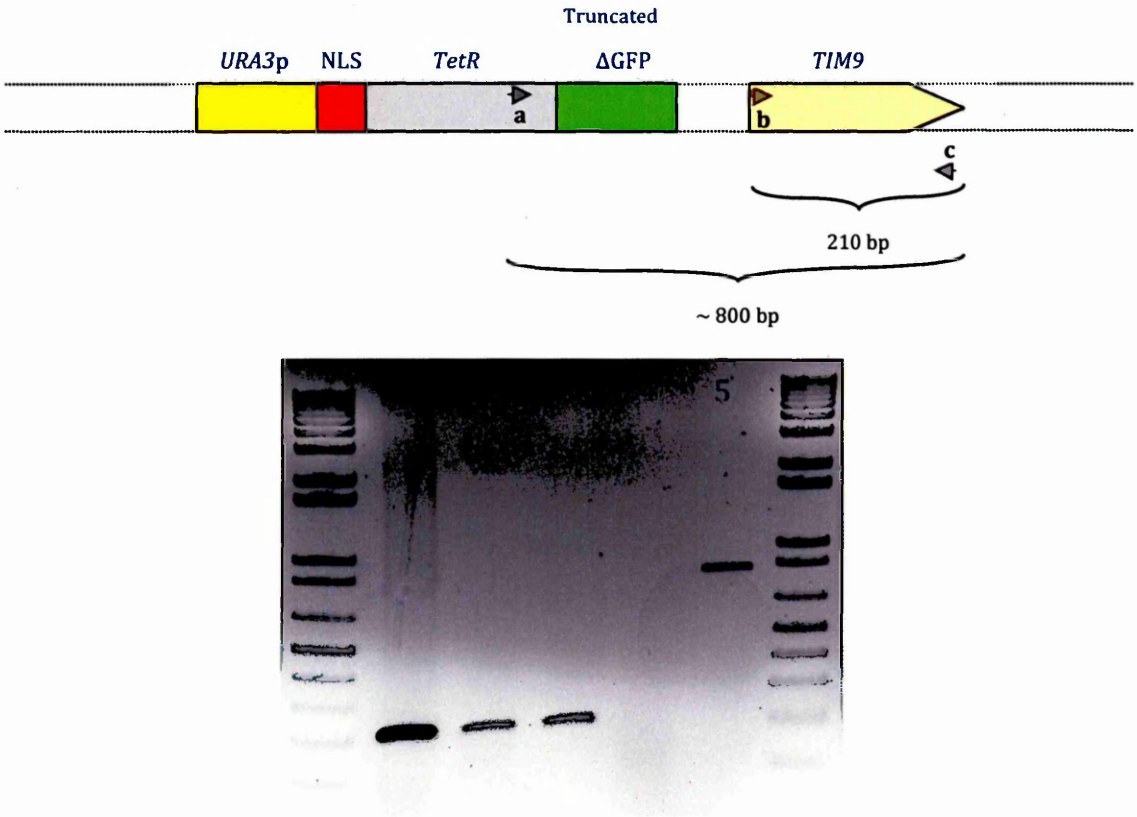

Figure 3.1 (top): Cartoon representation of the *URA3*P-NLS-tetr-truncated GFP construct integrated upstream the *TIM9* ORF. Here, **a, b** and **c** represent position of oligonucleotide primers used in RT-PCR, **(bottom):** 0.8% agarose gel electrophoresis showing:

Lane 1: Amplicon produced with **b** and **c** primers and genomic DNA of BY4743 as template.

Lanes 2 and 3: Amplicons generated with **b** and **c** primers and cDNA templates derived from BY4743 and strain carrying integration of the truncated GFP construct.

Lane 4: BY4743 cDNA with primers **a** and **c**.

Lane 5: Amplicon generated by **a** and **c** primers with cDNA of strain carrying integration of the truncated GFP construct.

So we hypothesized that a novel fusion protein between the ΔGFP construct and *TIM9* might be expressed in this strain, which is possibly toxic/lethal to the cells, concomitantly leading to the formation of jagged-edge colonies. However, upon sequencing the cDNA-derived amplicon, we discovered that this was not the case. In fact, this seems to be a read-through event possibly leading to the formation of a toxic mRNA transcript. Further investigation in these lines was beyond the scope of this work. Thus, we decided to choose a new locus for the integration of our truncated GFP construct to prevent any alteration in the overall homeostasis of the cell. This new locus of targeted integration was chosen in the inter-genic region between the *RIP1* and *YEL023C* genes on chromosome V.

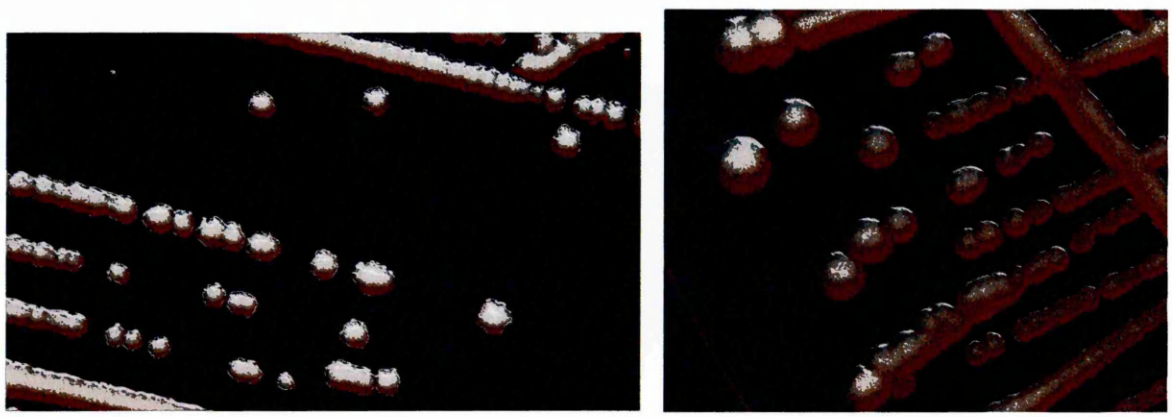

Figure 3.2 Phenotype of strains seen as jagged-edge colonies produced by cells bearing an integration of the *URA3*P-NLS-tetr-truncatedGFP construct (left), and normal round shape colonies formed by cells carrying integration of the *LEU2*P-truncatedDsRed construct (right).

In a similar fashion as described above, a truncated fragment of the DsRed gene carrying the first 151bp of coding sequence was integrated on chromosome III in the intergenic region between *LEU2* and *NFS1* genes. This fragment was amplified from the

plasmid pXKXE::*LEU2*P-DsRed using primers bearing 40bp of homology to the site of integration. The integration event was followed by the pop-out of the *KAN*^{R} selectable marker flanked by FRT sequences. Colonies formed after integration at this locus were round in shape as were the colonies formed by the wild type strain BY4743 (**Figure 3.2**). The remaining sequence of DsRed encompassing coding sequence from 112 to 680 bp was cloned into the *SpeI* site of pAG32, just downstream the terminator of the *HYG*^{R} marker.

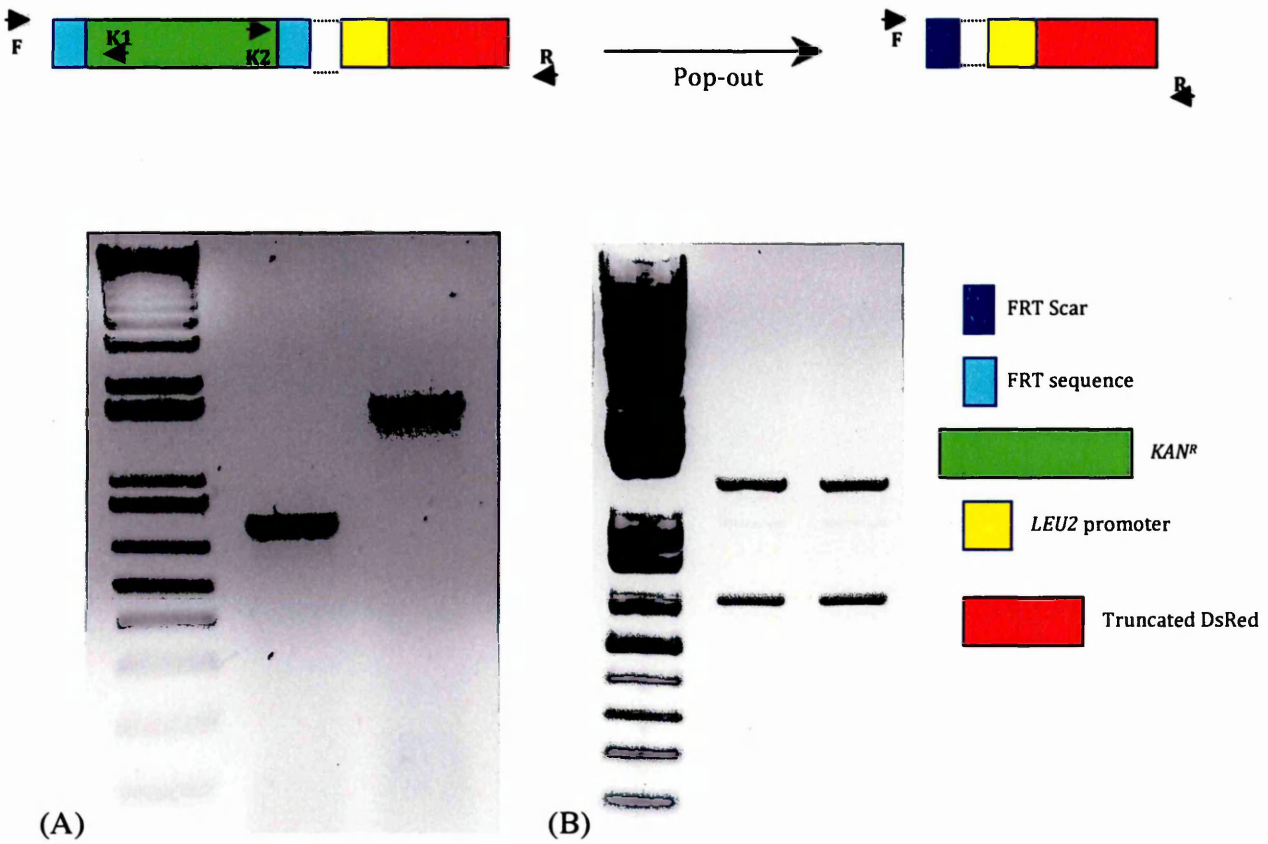

Figure 3.3 (top) Cartoon representation of *KAN*^{R} excision by a pop-out event resulting in the formation of a FRT-scar. (**A**) 0.8% agarose gel electrophoresis showing correct integration of the *LEU2P*-truncated DsRed construct integrated using the STIK system. Lanes 1 and 2 show amplicons generated by F-K1 and K2-R primer pairs, respectively. (**B**) Lanes 1 & 2 are identical; the top band represents amplicon generated with F & R primers confirming integration of *LEU2P*-truncated DsRed construct and pop-out of *KAN*^{R}. The lower band represents amplicon generated by F and R primers on wild type chromosome of diploid strain BY4743.

3.2 Construction of pNP001 vector for RG-BIT synthesis:

The linear DNA construct to be used in this experiment was amplified using plasmid pNP001, which has the pAG32 backbone. This plasmid was constructed by cloning a PCR-generated fragment of GFP carrying coding sequence from 133 to 717 bp followed by the *ADH1* terminator into the *BglII* site of pAG32, which is just upstream the promoter of the HYG^R marker. Similarly, a PCR-generated fragment of DsRed bearing the coding sequence from 112 to 680 bp was cloned into the *SpeI* site of pAG32, just downstream the terminator of the HYG^R marker. **Figure 3.4** below shows the restriction profile of pNP001 generated with *BglII* and *SpeI* endonucleases to confirm the successful cloning of PCR-generated fragments bearing incomplete coding sequences for GFP and DsRed genes. Both cloned fragments bear the fluorophores of their corresponding fluorescent markers, such that they reside on the linear DNA construct. Integrated fragments on the genome were not fluorescent by themselves and only upon correct integration of the construct on either side would a fluorescent signal be noticed. We have named this linear DNA construct as RG-BIT cassette.

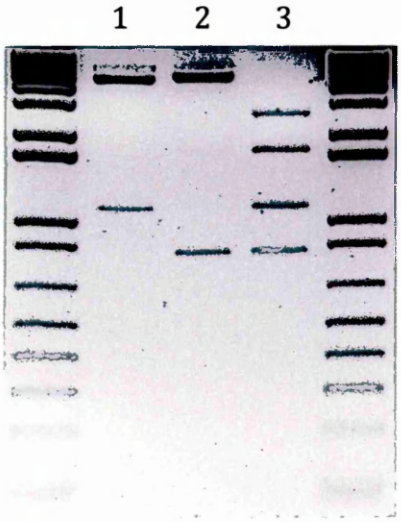

Figure 3.4 Restriction digestion profile of plasmid pNP001 generated by digestion with:

Lane 1: Digestion with *BglII* showing the remaining portion of GFP cloned into the *BglII* site of pAG32.

Lane 2: Digestion with *SpeI* enzyme showing the remaining sequence of DsRed cloned into the *SpeI* site of pAG32.

Lane 3: Double digestion of plasmid pNP001 with both *BglII* and *SpeI* enzymes showing presence of both fragments cloned into pAG32.

3.3 GFP and DsRed reconstitution in PAW1:

The *S. cerevisiae* strain generated by integrating truncated fragments of GFP and DsRed on chromosomes V and III respectively was named as PAW1 (ΔGFP between *RIP1* and *YEL023C*; ΔDsRed between *LEU2* and *NFS1*). The plasmid constructed by cloning the remaining sequences of both the fluorescent markers as mentioned above, was used as a template to PCR amplify the RGBIT cassette, and was named pNP001.

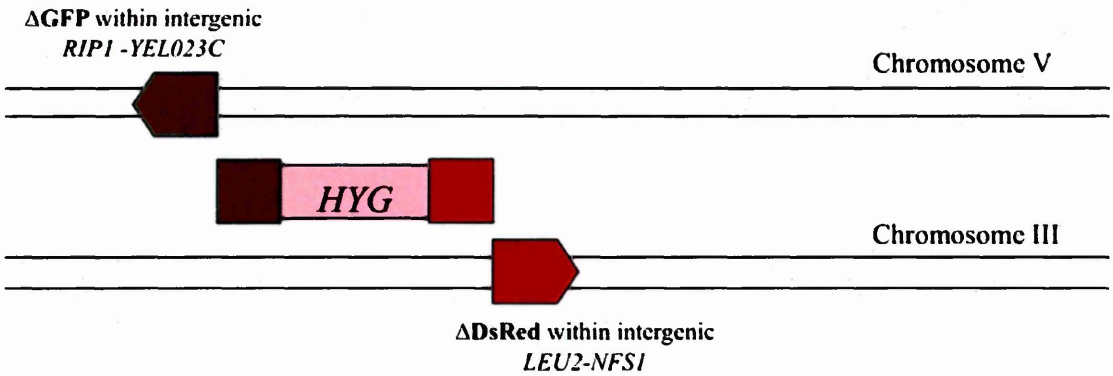

Figure 3.5 A schematic representation of the Red-Green BIT (RG-BIT) system, for targeting the reconstitution of GFP and DsRed on chromosomes V and III, respectively.

Using this genetic system (**Figure 3.5**), we first tested the feasibility of the reconstitution of each fluorescent marker on either chromosome, separately, before attempting a double reconstitution by BIT induction. Using a linear DNA construct generated to target each specific chromosome we carried out the reconstitution of an individual fluorescent marker and concomitant deletion of an adjacent ORF. Thus, we successfully reconstituted GFP on chromosome V with concomitant deletion of an adjacent *YEL023C* ORF. In a similar way DsRed was reconstituted on chromosome III with concomitant deletion of *NFS1* (**Figure 3.6**). Once the reconstitution events were

tested feasible, the yeast strain PAW1 was transformed with the RGBIT cassette to induce a translocation accompanied with the reconstitution of both GFP and DsRed markers. Among 104 hygromycin resistant transformants obtained by several transformations, 3 were integrants on chromosome V with GFP reconstitution, whereas only one was an integrant on chromosome III with DsRed reconstitution. Our results indicate that HR mediated targeting of exogenously introduced non-yeast sequences seems to occur at very low rates. A possible speculation at least under the current experimental setup might be that a high GC base content of the introduced non-yeast sequences disfavors an open DNA context at these sites, thereby discouraging HR at the same. This aspect has been discussed further in Chapter 6.

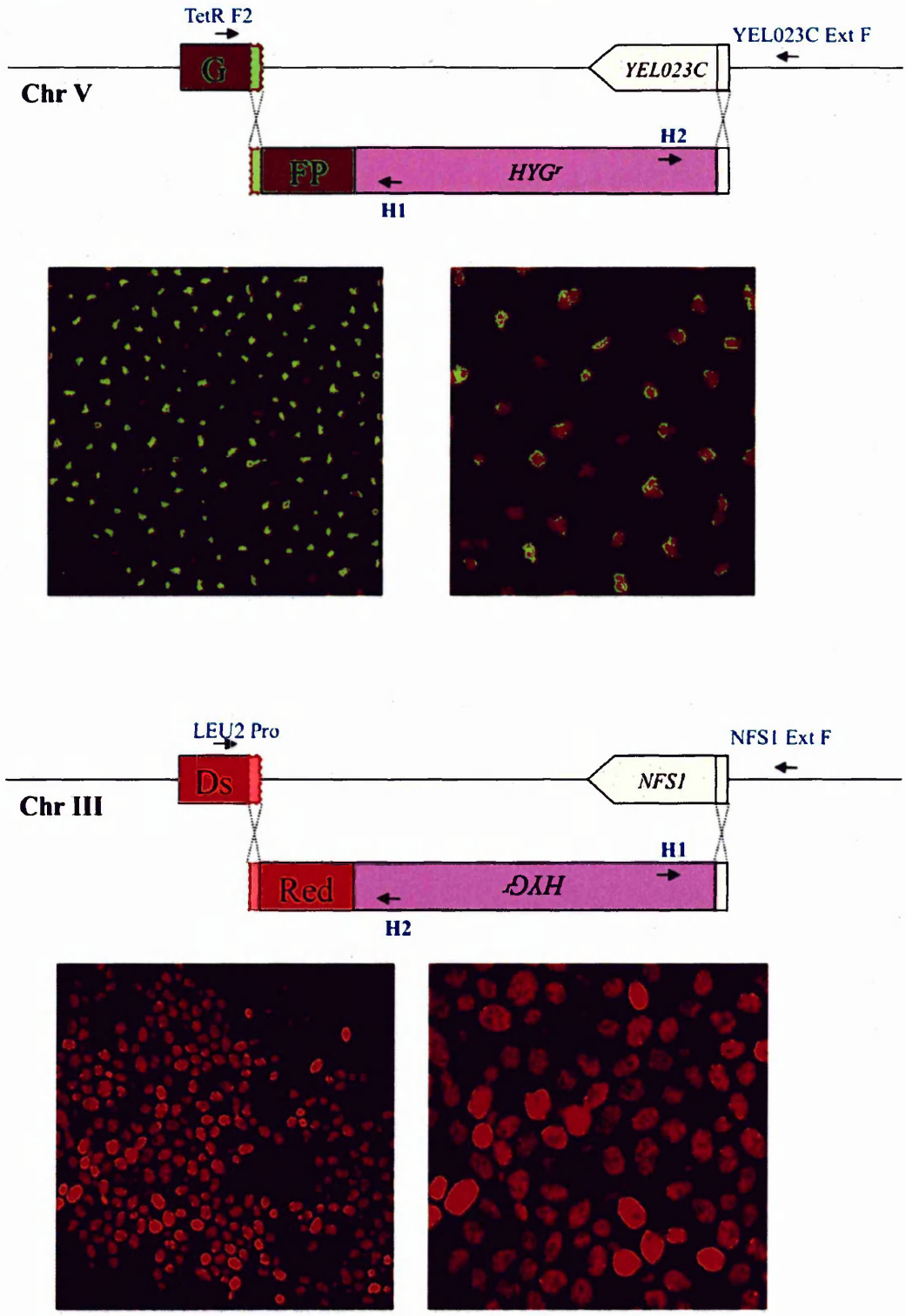

Figure 3.6 Reconstitution of NLS tagged GFP and DsRed on chromosomes V and III visible in the cell nuclei and cytoplasm, respectively.

One translocant strain named TRAP1, was the only transformant positive for correct integration of the RGBIT cassette on both chromosomes V and III, with subsequent reconstitution of GFP and DsRed respectively. This was evident from fluorescent imaging of this strain (**Figure 3.7**) and later confirmed by PCR analysis and southern hybridization, and no loss of sequence information was seen at the level of the translocation breakpoints.

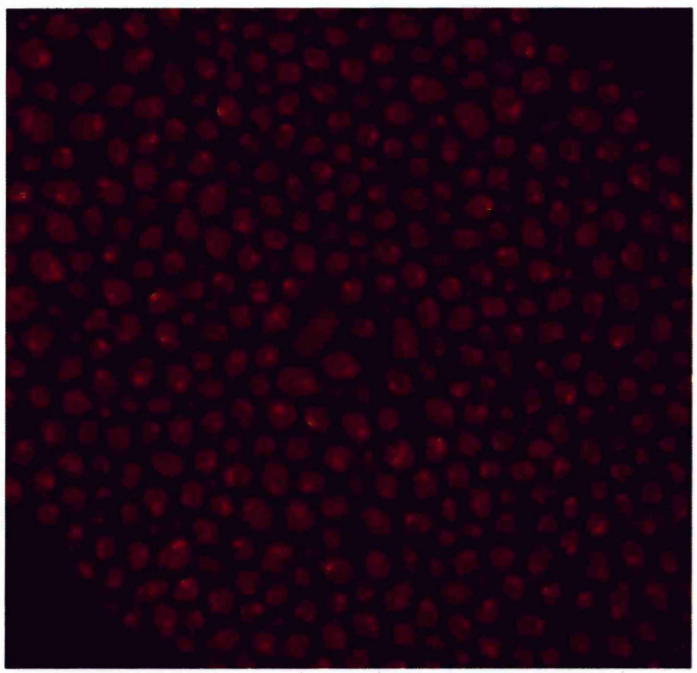

Figure 3.7 Translocant strain TRAP1 visualized with fluorescence microscopy showing NLS tagged GFP in the cell nuclei, and DsRed in the cytoplasm.

3.4 Timing of targeted RG-BIT construct integration in PAW1:

With an experimentally feasible genetic system in hand, an attempt to elucidate the timing of linear DNA integration into targeted loci on yeast chromosomes was carried out. Firstly, we asked, at what stage of the yeast transformation process is the exogenous RG-BIT DNA being assimilated and integrated into targeted loci in the genome? This

was essentially a prerequisite to define a timeframe, following which; the integration events would be monitored by fluorescence detection. Additionally, we were challenged by the inherent low induction frequency of BIT events, targeted for reconstruction of fluorescent signals. In other words, based on the total number of cells treated in each yeast transformation experiment, which on an average was 7.5 to 8×10^8 cells, we obtained just one translocant TRAP1, after several such transformations. Bearing in mind this extremely low rate of the induction of BIT events, a distinct window of time for fluorescence detection had to be established in the experimental setup. Moreover, it was previously reported that PEG-3350 treatment followed by its removal from the transformation reaction is essential for DNA uptake by yeast cells (BRUSCHI *et al.* 1987).

In our experimental setup, based on the standard EUROFAN protocol for yeast transformation, PEG removal was carried out just after the heat shock treatment at 42 °C, before incubating cells in rich media for recovery. Thus, a PCR based approach using junction specific primers was employed for the detection of integration signals from samples taken at temporal intervals after PEG removal. To do this, cultured PAW1 cells were harvested in the mid-log phase of growth (~$1.8\text{-}2\times10^7$ cells/ml) and transformed with purified linear RG-BIT cassette, previously PCR amplified from plasmid pNP001. After PEG removal, the cell pellet was resuspended in "n" ml of YPD, where "n" represented the number of samples to be taken. All 1ml samples were blocked and fixed instantly in 1% sodium azide (110μl of 10% stock for a 1ml sample) solution and water slush. Genomic DNA was extracted from samples by standard phenol chloroform method and the presence of DNA integration events was monitored by PCR using specific primers amplifying GFP and DsRed junctions (see **Figure 3.8**). Initially, we collected

three samples at a time interval of ten minutes after PEG removal. Interestingly, PCR signals for integration on both truncated GFP (Chr V) and truncated DsRed (Chr III) were noticed in samples taken even just 10 minutes after PEG removal. Remarkably, when we reduced the time frame of PCR analysis within these initial ten minutes, we were still able to detect PCR signals of integration in samples taken instantly after PEG removal (**Figure 3.8**).

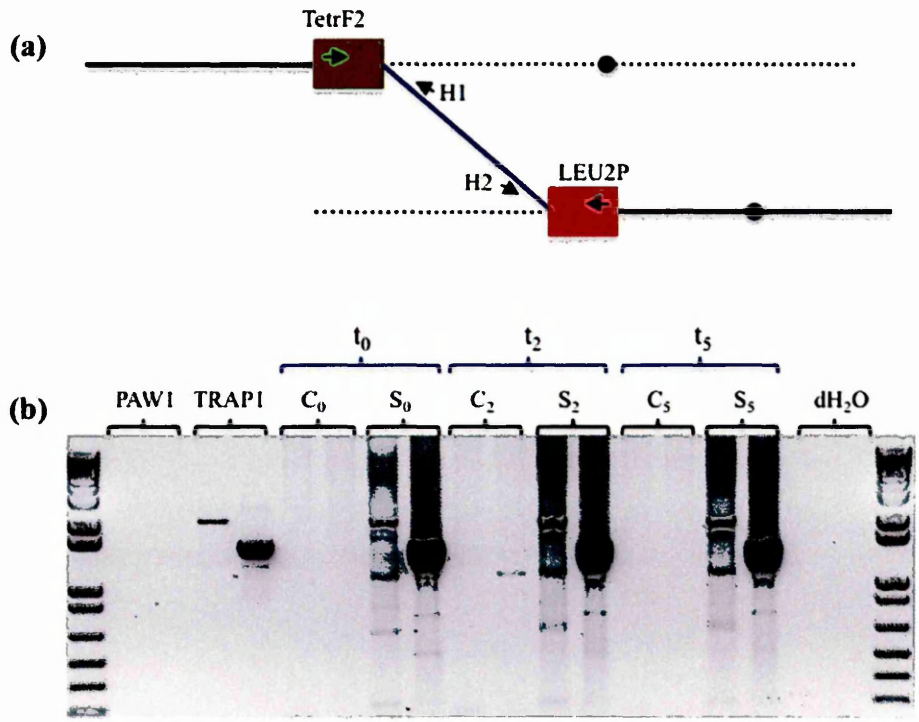

Figure 3.8 (a) Schematic depiction of position of PCR primers used for detection of PCR signals for integration on GFP and DsRed loci. **(b)** PCR signals for integration detected in samples taken at times: zero, 2 and 5 minutes (t_0, t_2 and t_5, respectively) after PEG removal. C: control untreated sample; S: treated sample. Subscripts depict time in minutes at which sample was collected. For each sample: Lane1 is PCR with TetrF2 and H1, lane 2 is PCR with LEU2P and H2.

The detection of integration signals in t_0 samples led us to investigate if any DNA was picked up prior to PEG removal, challenging published data (BRUSCHI *et al.* 1987) contrary to our observations. We wondered if assimilation of exogenously added DNA

was so rapid as to generate PCR signals for integration in such a short time frame. Were we looking at genuine integration events, or mere PCR artifacts in these experiments? To this end, samples were rescued at different stages of the transformation process until PEG removal and PCR analyzed. Samples were collected at 20 minute temporal intervals (i) after incubation in LiAC; (ii) after incubation in carrier DNA and RG-BIT DNA; (iii) after incubation in PEG/LiAc solution; and (iv) after heat shock at 42 °C and PEG removal. Astonishingly, similar PCR signals for integration were detected even from samples taken much before addition of PEG itself (**Figure 3.9**).

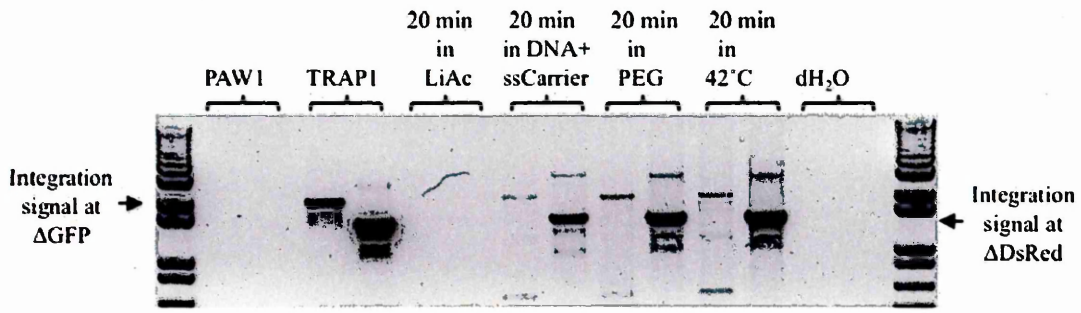

Figure 3.9 PCR generated integration signals of RG-BIT construct, targeted onto chromosomes V (ΔGFP) and III (ΔDsRed) sequences in samples derived prior to PEG removal. Only the LiAc treated cells were negative for such signals as they lacked the transforming DNA at this stage.

Following this, when a sample of lithium acetate treated competent yeast cells incubated with just single stranded carrier DNA and RG-BIT DNA was tested PCR positive for integration bands, we hypothesized the generation of PCR artifacts due to the presence of the carrier DNA. However, when we excluded the use of carrier DNA in further experiments, PCR was still positive for integration signals. This left the transforming RG-BIT DNA as the only other reaction component that could be responsible in generation of such PCR products. This might happen due to the formation

of a transient template between single stranded genomic DNA from PAW1 and the RG-BIT cassette after initial denaturation followed by subsequent primer annealing and amplification during PCR. Finally, we tested and confirmed that integration signals could be reproduced when a mixture of RG-BIT DNA and genomic DNA from PAW1 were together utilized as a PCR template (**Figure 3.10**). At the same time, using just genomic DNA or just the RG-BIT construct as templates for PCR with same primer pairs did not produce signals, supporting our previous observations and confirming the generation of PCR artifacts while detecting for integration signals.

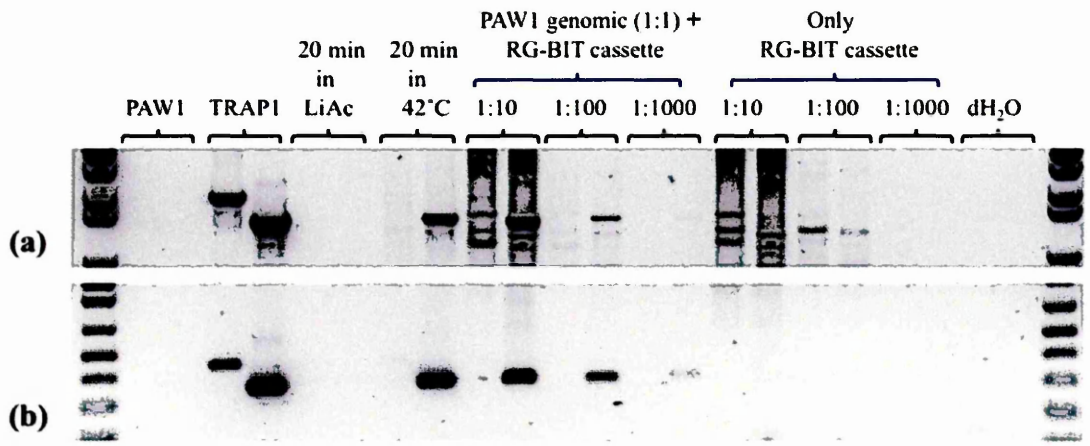

Figure 3.10 (a) PCR generation of integration signals reproduced for integration on chromosome III only in the presence of both genomic DNA and varying concentrations of RG-BIT DNA together, but not when either one was used separately. PCR was performed using primers complementary to ΔGFP on chromosome III and hygromycin on RG-BIT construct. For each sample **(b)** Similar PCR reproduction as in (a) using another set of primer pairs that did not produce other aspecific amplicons.

In our experiments, we have used approximately 5 to 10 μg of RG-BIT DNA in each transformation reaction. During DNA extraction from temporal samples, a significant amount of this transforming DNA is precipitated along with genomic DNA. When such a preparation is used as template for PCR, we have demonstrated that it can

reproduce similar bands as produced in TRAP1 control. We have further confirmed this by treating samples with DNaseI prior to genomic extraction from samples for PCR analysis. DNAseI treated samples did not produce PCR integration signal suggesting that the interference of the transforming DNA in our samples was responsible for the generation of PCR artifacts. Perhaps, such artefactual signals could be avoided by using a reduced amount of transforming DNA that can be washed away from the cell surface prior to genomic extraction for PCR analysis. However, based on our experience low concentrations of linear DNA used for transformation have not yielded transformants to be analysed.

Based on the above observations, an alternative approach was employed to differentiate between genuine *in vivo* integration events and experimental artifacts that might arise. So, we carried out restriction digestion of DNA derived from temporal samples taken during the transformation process, followed by southern hybridization approach using probes complementary to ΔGFP and ΔDsRed sequences. DNA produced from samples was restricted with *BglII* and *SpeI* enzymes, which produced distinct fragments of ~ 6650 bp and ~ 4727 bp on PAW1 native chromosomes V and III, respectively. Similarly, the same enzymes would produce ~ 2900 bp and ~ 1962 bp fragments, corresponding to integration on either chromosome (using TRAP1 as control). Using this approach we have been able to demonstrate that there is no DNA integration into targeted loci in the yeast genome until the heat shock stage of transformation process **(Figure 3.11)**.

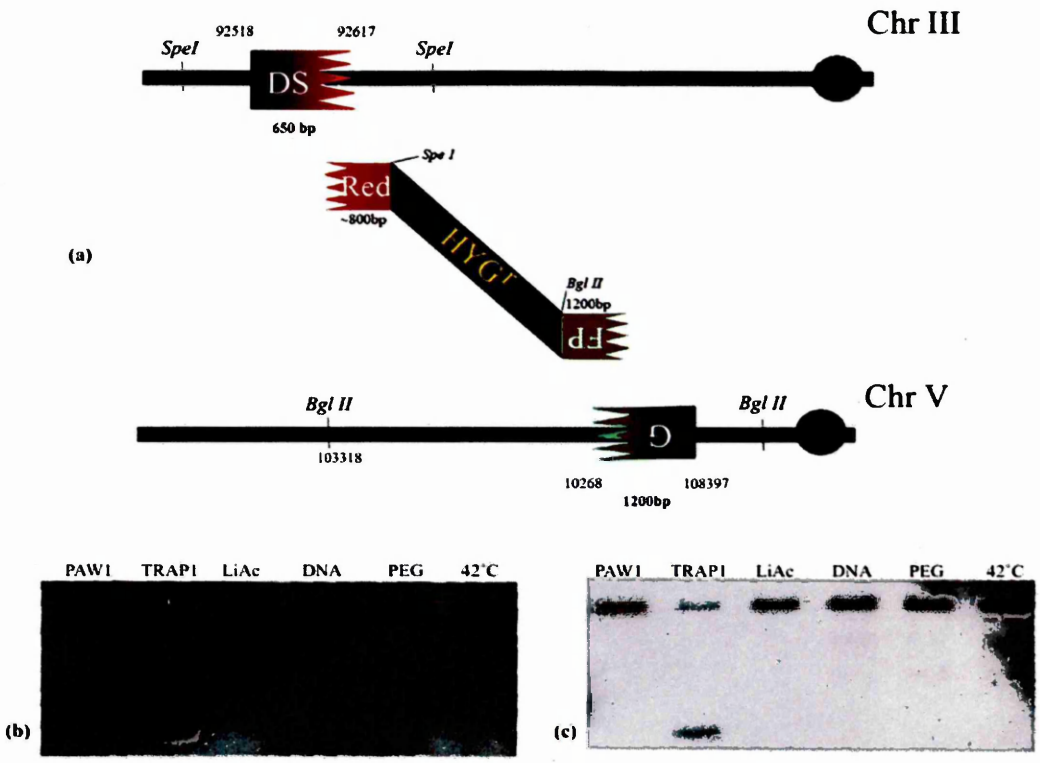

Figure 3.11 **(a)** Chromosome coordinates within which ΔDsRed and ΔGFP were introduced on chromosomes III and V. Also shown are chromosome coordinates for *BglII* and *SpeI* restriction sites and on the RG-BIT construct utilized for southern hybridization with specific probes. **(b)** *BglII* generated fragments hybridized with DIG-labeled probe complementary to ΔGFP; wild type signal seen in PAW1 and all other samples; integration signal only in control TRAP1. **(c)** *SpeI* generated fragments hybridized with DIG-labeled probe complementary to ΔDsRed.

Based on our observations, we eliminated the use of PCR based approach for the establishment of linear DNA integration timing and dynamics *in vivo*. Additionally, high repression of BIT events poses experimental limitation to screen for real time events by fluorescence.

We have recently started to exploit this in hand genetic system to shed light on DNA targeting at endogenous yeast sequences in comparison to those that are not native, but have been engineered at specific loci. This would involve establishing recombination rates for GFP reconstruction in comparison to that for an adjacent endogenous yeast

sequences. We are also attempting experiments that will use an *msh2* mutant PAW1strain to target only GFP reconstruction on chromosome V. To this end, variants of targeting constructs that carry point mutations at specific locations on the homologous sequence required for GFP reconstruction will be utilized. We presume that in a mismatch repair deficient strain, gene targeting will be favored by homeologous recombination, as it is known that *MSH2* is involved in the suppression of the same (SPELL and JINKS-ROBERTSON 2003). In such a MMR deficient background, mismatches introduced on the homologous sequence should not be repaired, but recombination mediated integration should be feasible. PCR positive transformants for integration at ΔGFP will be subjected to DNA sequencing of the GFP-reconstruction targeting junction. Depending on which originally introduced mismatches are detected along the length of the homologous sequence after DNA sequencing, we will be able to predict how much of the total homologous sequence was utilized and is necessary for gene targeting. This will allow detection of the extent to which linear molecules are nibbled at the ends during gene targeting.

Results (Part 2) – Chromosomal deletions in yeast cells carrying translocation between chromosomes XV and IX

4.1 Generation of SAD translocant strains:

4.1.1 *In wild type parental strains PAW1 and SAN1:*

The previously described BIT system was employed to obtain a series of ten translocant strains, collectively referred to as the SAD translocants, however, each one is referred to by its own strain number/name in this study. This name comes from the chromosomal loci, which were targeted to induce a translocation between the promoter regions of genes *SUC2* and *ADH1* on chromosomes IX and XV, respectively, and hence, the name SAD (*SUC2-ADH1*). We have specifically chosen these genetic loci for targeting BIT, to favorize increased recombination at both ends of the linear targeting DNA. This choice and experimental design stems from observations by others in our group, where each of the chosen loci individually exhibited increased rates of targeted recombination in separate experiments. All SAD translocants described in this work are derivatives arising from translocation induction in two wild-type strains PAW1 and SAN1. Three SAD translocants numbered 3, 33 and 801 were obtained in the BY4743 genetic background of PAW1, whereas the others numbered 1, 16, 17, 18, 31, 59 and 802 were generated in the SAN1 strain, a cross between haploid strains, FAS20a and YPH250α (refer to MATERIALS AND METHODS for genotype details). A PCR-amplified linear DNA construct, bearing the KAN^R selectable marker flanked with 65 base pairs of homologous sequences, to promoter regions of genes *ADH1* and *SUC2*, was employed in translocation induction in both reference strains. Upon correct integration on both the targeted loci, chromosomes XV and IX were bridged together, leading to the generation

of an aberrant chromosome bearing centromere of chromosome IX and two distinct chromosomal fragments, a centromeric fragment containing the centromere of chromosome XV and an acentric telomeric fragment of chromosome IX (**Figure 4.1**). The theoretically calculated dimension of the resulting translocated chromosome upon successful integration on both targeted loci was expected to be ~ 565.5 Kbps. Two discrete free-ended fragments, one ~ 36 Kbps acentric fragment of chromosome IX and an ~ 931 Kbps fragment containing the centromere of chromosome XV, were also expected to be generated upon the occurrence of this translocation event.

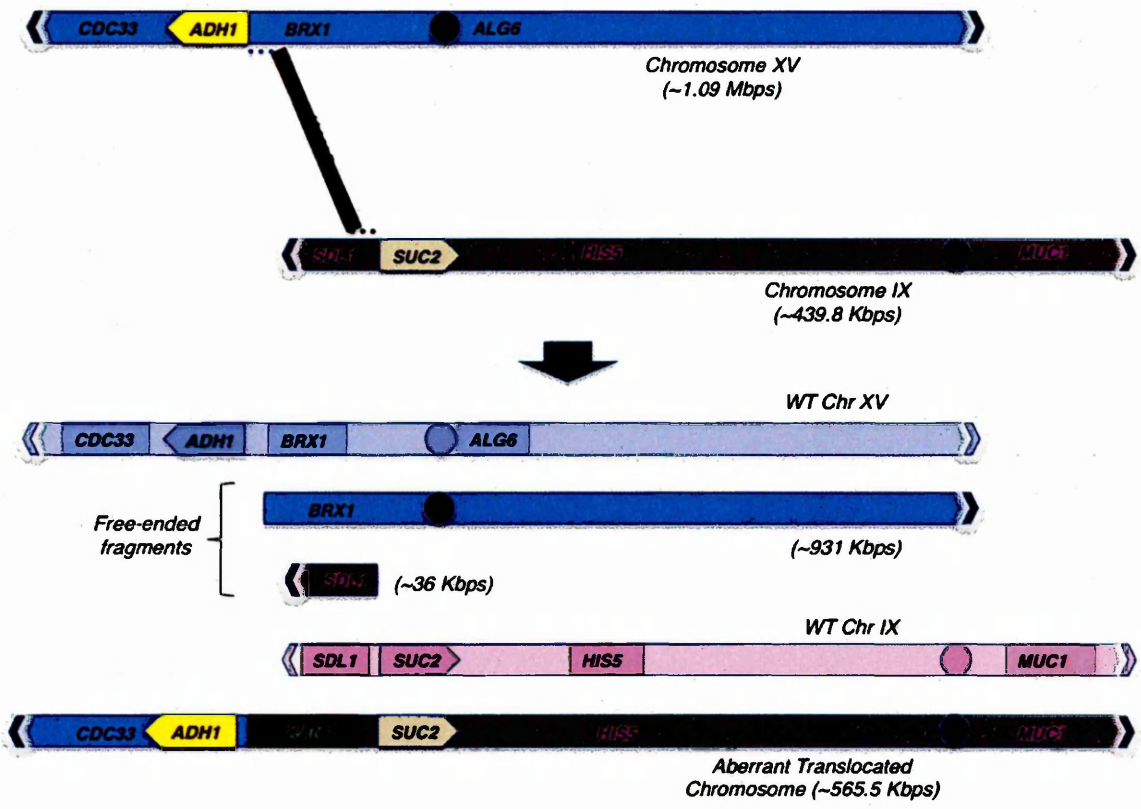

Figure 4.1 Graphical representation of BIT induction between chromosomes XV and IX leading to the generation of a bridged translocated chromosome and the resulting chromosomal fragments. Gene names mark the relative location of various probes used to determine the nature of these rearrangements. Shadowed chromosomes represent native wild type chromosomes. Approximate sizes of resulting fragments and chromosomes involved in BIT are mentioned in brackets.

All G418 resistant transformants obtained upon transformation of the two reference strains with such a linear construct were carefully streaked onto fresh YPD plates containing 200 μg/ml G418, to eliminate all false positives. Those that exhibited stable resistance to G418 were subjected to analysis by colony PCR in order to screen for clones carrying integration of the externally introduced BIT construct at targeted loci. This was carried out using a set of locus specific primers, which amplify the breakpoint junctions of the translocation and amplicons on either native chromosome.

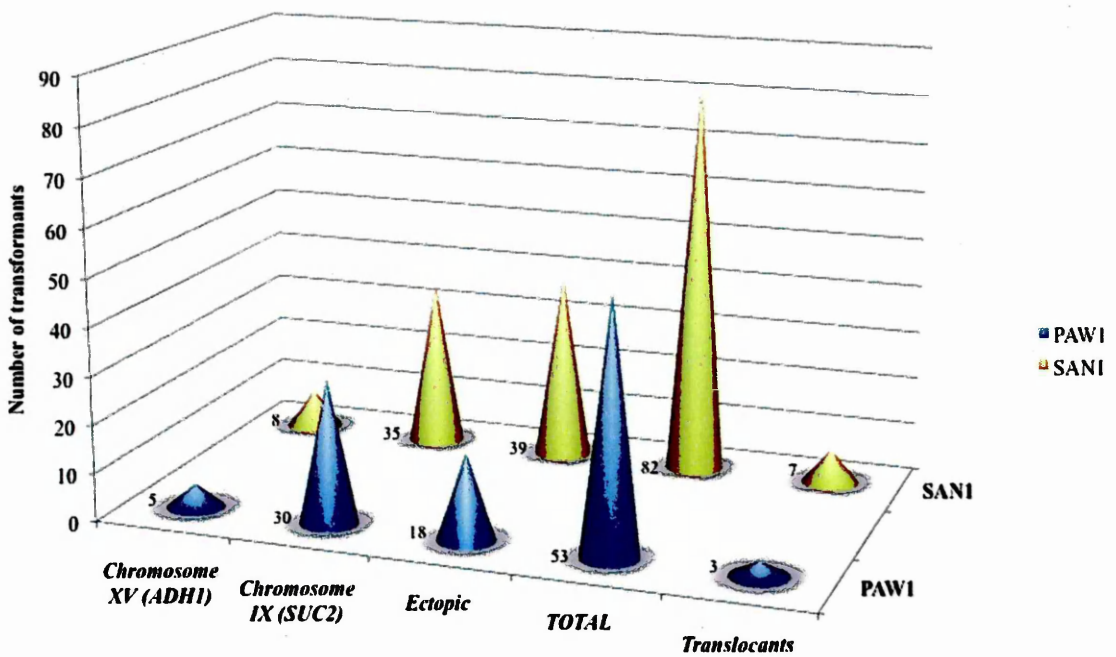

Figure 4.2 Data derived from PCR analysis of G418 resistant transformants obtained in PAW1 and SAN1 strains, showing one sided integration events on either *ADH1* or *SUC2* loci, two sided events leading to the generation of translocants and those that were ectopically integrated elsewhere in the genome.

A total of 135 kanamycin resistant transformants (53 from the PAW1 strain and 82 from the SAN1 strain) were obtained after several transformation reactions performed

as described in Materials and Methods. Each clone was first analysed by colony PCR to detect any signals of targeted integration at loci located on either chromosome XV or IX. The detection of PCR signals for integration on both loci in any given clone was scored as a translocation, which was then further confirmed by PCR performed on genomic DNA of these clones. Furthermore, we also confirmed the physical connection of the two chromosomes involved in the translocation by PCR analysis employing specific primers for each chromosome. A total of ten translocants, 3 in the PAW1 strain and 7 in SAN1, were obtained which are referred to as the SAD translocants in this study.

4.1.2 *In mre11Δ, tel1Δ, ku70Δ, sgs1Δ, elg1Δ, esc2Δ, mrc1Δ and tel1Δsgs1Δ mutants:*

In *Saccharomyces cerevisiae*, redundant and extensive pathways have been implicated in the suppression of GCR formation. A large number of genes including those that function in intra S-phase and replication checkpoints, recombination pathways and telomere maintenance have clear roles in the maintenance of genome integrity mediated by suppressing GCR rates (CHEN and KOLODNER 1999; KOLODNER *et al.* 2002; PUTNAM *et al.* 2009) In an attempt to investigate the molecular regulation of induced BIT events, we selected a few candidate genes that have clear and well-established roles in some of the genome maintenance pathways mentioned above.

For instance, Mre11 a member of the MRX complex in *S. cerevisiae* has roles in several processes like HR, NHEJ, intra-S checkpoint activation and telomere maintenance, implicated in the suppression of GCRs. In these processes, Mre11 plays diverse functions that have been attributed to three major activities it possesses. Its 5′-3′ endonuclease activity, the activity to form the MRX (Mre11-Rad50-Xrs2) complex and

another activity related to its telomere maintenance function are thought to mediate suppression of GCRs, which are often translocations (SMITH *et al.* 2005).

The role of Tel1 in DNA damage checkpoint control has been described earlier on in this report. Apart from its roles in telomere maintenance and checkpoint functions, it has been reported to efficiently suppress interchromosomal end joining (LEE *et al.* 2008). It does so, by mediating Sae2-dependent intrachromosomal tethering at DSBs to promote 5′-3′ degradation, in concert with the MRX complex. This prevents error prone NHEJ and interchromosomal end joining, thereby preserving genome integrity upon DNA damage.

On the other hand, the Ku70-Ku80 heterodimer contributes to genome stability by mediating the NHEJ pathway of DNA repair. Besides this it plays roles in diverse processes such as transcription, apoptosis and telomere maintenance which have been reviewed in (DOWNS and JACKSON 2004). Ku binds to a variety of DNA ends in a sequence non-specific manner. At chromosomal termini, it functions by protectively capping them to prevent end-to-end fusions, thus repressing GCR formation. More recently, the role of Ku70-Ku80 heterodimer in suppression of GCRs has been associated to occur via its crosstalk with DNA damage checkpoints (BANERJEE *et al.* 2006).

Another GCR repressor gene, *ELG1*, encodes for a component of an alternative replication factor complex. Among its various roles in different DNA metabolism processes, its importance in DNA replication and genome stability is highlighted by its physical interaction with PCNA and Rad27 (BELLAOUI *et al.* 2003; BEN-AROYA *et al.* 2003; KANELLIS *et al.* 2003). Elg1, which is redundant with Rad24 in the DNA damage response, contributes to Rad53 activation in the absence of the latter (BELLAOUI *et al.*

2003). Strains deficient for Elg1 exhibit delayed cell cycle, enhanced spontaneous DNA damage, increased telomere size, activation of intra-S checkpoint and elevated rates of GCR formation (BANERJEE and MYUNG 2004).

Among the RecQ-like 3′-5′ DNA helicases, which are conserved from bacteria to humans, Sgs1 in *S. cerevisiae* is required for genome stability (BACHRATI and HICKSON 2008; CHU and HICKSON 2009; COBB *et al.* 2002; HICKSON 2003; KAROW *et al.* 2000; WATT *et al.* 1996). Human homologs of *SGS1* like *BLM*, *WRN* and *RECQL4* are mutated in premature aging and cancer predisposition syndromes like Bloom's, Werner and Rothmund-Thomson syndromes, respectively. During homologous recombination repair (HRR), RecQ helicases can resolve various types of recombination intermediates such as single and double Holliday junctions, D-loops and Rad51-dependent cruciform DNA structures, which can accumulate at damaged replication forks (LIBERI *et al.* 2005). Very recently, full length Sgs1 has been reported to preferentially unwind Holliday junctions (CEJKA and KOWALCZYKOWSKI 2010). In the budding yeast, Sgs1 has been implicated to play diverse and extensive roles such as: in the regulation of HR and suppression of crossovers during DSBR and faithful segregation of chromosomes (IRA *et al.* 2003; ONODA *et al.* 2000; VERSINI *et al.* 2003; WATT *et al.* 1995), coordination of DNA replication and recombination (CHEN and KOLODNER 1999; VERSINI *et al.* 2003), suppression of homeologous recombination (MYUNG *et al.* 2001a), intra-S checkpoint activation (COBB *et al.* 2003; FREI and GASSER 2000; KOLODNER *et al.* 2002) and in transcriptional regulation (LEE *et al.* 1999). Cells deficient for Sgs1 exhibit a hyper-recombination phenotype (YAMAGATA *et al.* 1998) and a higher incidence of GCR formation. Elevated rates of HR-mediated chromosomal translocations (PUTNAM *et al.*

2009; SCHMIDT *et al.* 2006) and an increased incidence of aneuploidy leading to LOH (AJIMA *et al.* 2002) have also been reported in *sgs1* mutant cells. In addition to its genome stability functions, Sgs1 and Ku70 also have also been reported to regulate homologous DNA integration into yeast chromosomes (YAMANA *et al.* 2005).

Finally, DNA replication-stress checkpoint functions like Esc2 and Mrc1 have recently been implicated in strong suppression of duplication mediated GCR formation in *S. cerevisiae* (PUTNAM *et al.* 2009). Mrc1 is a mediator of the replication checkpoint and required for leading-strand replication, where it stabilizes Pol2, the catalytic subunit of DNA polymerase ε (LOU *et al.* 2008). At stalled replication forks and under replication stress conditions, Mrc1 has also been reported to be phosphorylated by Mec1 and transduce the checkpoint signal to activate Rad53 (ALCASABAS *et al.* 2001; OSBORN and ELLEDGE 2003). Esc2 on the other hand is also recruited to stalled replication forks and has implications in gene silencing. Recently, the role of Esc2 in preventing the accumulation of Rad51-dependent HRR intermediates and in mediating intra-S phase DNA damage checkpoint signaling has been reported (MANKOURI *et al.* 2009). These roles of Esc2 are similar to those of Sgs1. However, unlike Sgs1, these Esc2 functions are dependent on Mph1 and mediated via a functionally distinct branch of the HRR pathway.

Because BIT events were infrequently observed in wild type cells and rely on HR for interchromosomal bridging, we hypothesized that similar pathways that carry out genome maintenance functions might also influence and account for the low frequency of translocation induction. Thus, it was necessary to investigate the molecular regulation of BIT events and to elucidate pathways responsible for their suppression. To this end, we carried out the construction of homozygous deletion mutants for a few candidate genes

involved in various genome maintenance pathways mentioned above. Deletion mutants were then subjected to BIT induction in various mutant genetic backgrounds. In this study we have generated strains deficient for each of the genes: *MRE11 (YMR224C), TEL1 (YBL088C), KU70 (YMR284W), SGS1 (YMR190C), ELG1 (YOR144C), ESC2 (YDR363W)* and *MRC1 (YCL061C)*. A double mutant strain deficient in both *TEL1* and *SGS1* was also constructed. All gene knockout mutants were constructed in the reference strain PAW1. Gene deletion by marker recycling to obtain double deletion mutants in diploid yeast cells is described in MATERIALS AND METHODS. Translocation induction and screening for the selection of integrants on one or both targeted loci in all double deletion mutants was performed in the same way as that described above (section 4.1.1). A list of all the translocants generated and characterized in this study is available in *Appendix 1* for reference to further reading.

4.2 PCR analysis of SAD translocants:

4.2.1 *SAD translocants derived from diploid wild type parental strains:*

A total of 135 transformants, stably resistant to G418, were obtained and analysed for the presence or absence of PCR signals for integration using specific primer pairs for each event to be detected. Among the analysed transformants were clones in which integration signals were detected for just one out of the two loci under investigation, either on chromosome XV or on chromosome IX (**Figure 4.2**). In these cases we have not investigated the site of integration of the second end of the BIT construct, as it is beyond the scope of the present study. However, similar preliminary investigation by other members to this end has revealed that the second free end may randomly integrate

elsewhere in the genome. This might possibly occur by illegitimate recombination leading to large deletions on the same chromosome, or ectopically into other chromosomal sequences. Additionally, clones that conferred stable resistance to kanamycin despite no detection of PCR signals for targeted integration at both loci in question were scored as ectopic integrants. The frequency of targeted integration at the *ADH1* promoter locus on chromosome XV was noted to be very similar in both PAW1 and SAN1 strains. This accounts to approximately 14% of the total integration events on either or both loci, detected by PCR analysis in both strains. On the other hand, the same at the *SUC2* promoter region on chromosome IX was slightly higher in PAW1 than in SAN1 cells. Based on these measurements the frequency of targeted integration at this genomic locus accounts to 53.5% in PAW1 and 39.3% in SAN1 genetic backgrounds. However, on the contrary, the rate of ectopic DNA integration elsewhere in the genome was slightly elevated in SAN1 cells in comparison to PAW1 cells, which was noted to be about 47.6% and 34% respectively. These findings and other data from our laboratory introduce a novel aspect of preferential integration (that we call "integration bias") of linear DNA towards one of the two genomic loci targeted on separate chromosomes, during BIT events. In the present study we provide evidence that in wild type cells, this integration bias is clearly favored towards the *SUC2* promoter locus in comparison to the *ADH1* promoter locus. Moreover, in wild type strains the frequency of inducing translocations was ~ 7.5% of total events, which is relatively higher than that noticed by others in our group targeting loci on other chromosomes. Potential factors that might affect the rate of inducing translocations are discussed later, although findings within our

group suggest that locus specific effects might majorly regulate targeting frequency in BIT experiments.

4.2.2 *PCR analysis of SAD translocants in mre11Δ, tel1Δ, ku70Δ, sgs1Δ, elg1Δ, esc2Δ, mrc1Δ and tel1Δsgs1Δ mutants:*

The number of transformants screened in each deletion strain varied with the transformation efficiency of each mutant strain. Strains bearing deletions in *tel1*, *mrc1* or the *tel1 sgs1* double mutant exhibited poor transformation efficiencies, although the minimum number of transformants obtained in any strain was not less than 12.

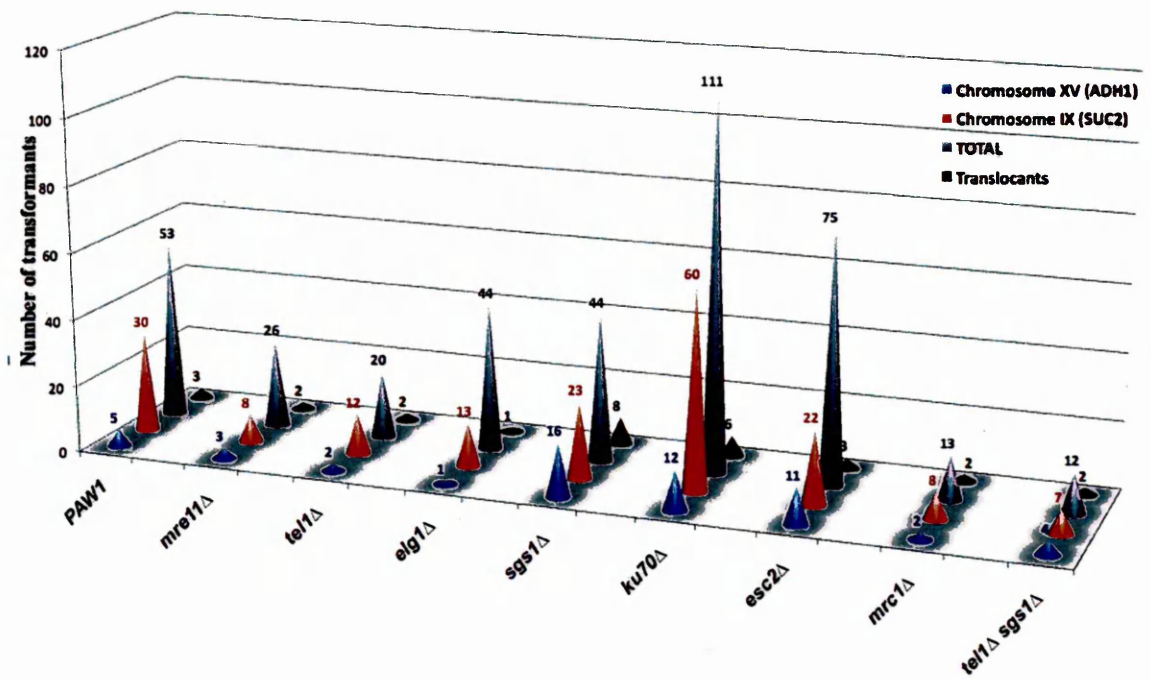

Figure 4.3 Graphical representation of data obtained from PCR analysis of transformants obtained in wild type and mutant strains. For each strain are denoted by conical bars: total number of G418-resistant clones analysed (purple); events targeted on either *ADH1* locus (blue) or *SUC2* (red); and translocants (green) generated, as detected by PCR using specific primers. Numbers along each bar represent the exact count of measured events.

On the other hand strains with deletions in *ku70, sgs1, elg1* or *esc2* transformed with higher efficiency. PCR screening of all true transformants was carried out as

described in the above section using specific primer pairs for each event to be detected (**Figure 4.3**). Based on the number of integration events detected on each locus under investigation we calculated the *ADH1* versus *SUC2* integration bias for each mutant strain. Interestingly, we noticed that this "integration bias" is significantly elevated in translocant strains obtained in *sgs1Δ*; *mre11Δ*, *esc2Δ* single mutants and *tel1Δsgs1Δ* double mutant background strain (**Figure 4.4**). In other words, preferential integration of the translocation-inducing construct towards *SUC2* was compromised/weakened with concomitant rise in the number of events targeted towards *ADH1* in these mutant backgrounds. We did not notice pronounced variations for transformants analysed in *tel1Δ* and *ku70Δ* single mutant backgrounds. In *mrc1Δ* cells integration bias was slightly elevated and the same was halved in an *elg1* null strain in comparison to wild type levels.

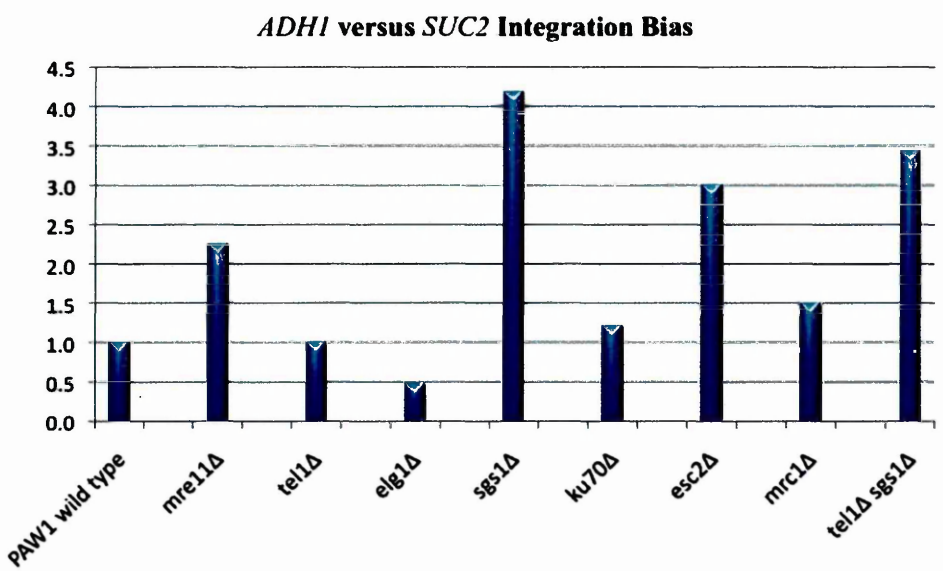

Figure 4.4 Fold increase in integration bias calculated for BIT between *ADH1* and *SUC2* loci in various genetic backgrounds. Wild type integration bias was calculated as the ratio of *ADH1* versus *SUC2* targeted events out of total number of events and considered as unit. Increased bias for integration towards *ADH1* as opposed to *SUC2* is evident in strains lacking *sgs1* or *mre11* or *esc2*.

Our results provide clear evidence that preferential integration of the BIT construct to integrate at chromosome IX locus is pronounced in wild type cells, and compromised in cells lacking either the nuclear helicase *SGS1*; or cells deficient for an intra-S checkpoint member *ESC2*, which is also involved in the establishment of silent chromatin; or in cells lacking both *SGS1* and the human ATM checkpoint kinase homologue, *TEL1*. The same was true for cells lacking Mre11, a component of the MRX/MRN complexes that function in HR-mediated pathways for DSB repair. Variations in integration bias noticed in these mutants might reflect their functions in modulating the structural context on each side of the translocation breakpoint, possibly by influencing local chromatin relaxation, DNA end-resection, and even DNA invasion followed by synthesis and D-loop migration on separate chromosomes in response to BIT DNA integration, in a similar manner alternatively modeled in (JAIN *et al.* 2009)

Moreover, we noticed that the frequency of translocation induction increased more than 3 fold in *sgs1Δ* cells and about the same in *mrc1Δ* and *tel1Δ sgs1Δ* double mutant background strains. The rate if inducing BIT slightly increased in *tel1Δ* and *mre11Δ* strains, was unaffected in *ku70Δ* strain and was reduced in the *esc2Δ* and *elg1Δ* strains (**Figure 4.5**).

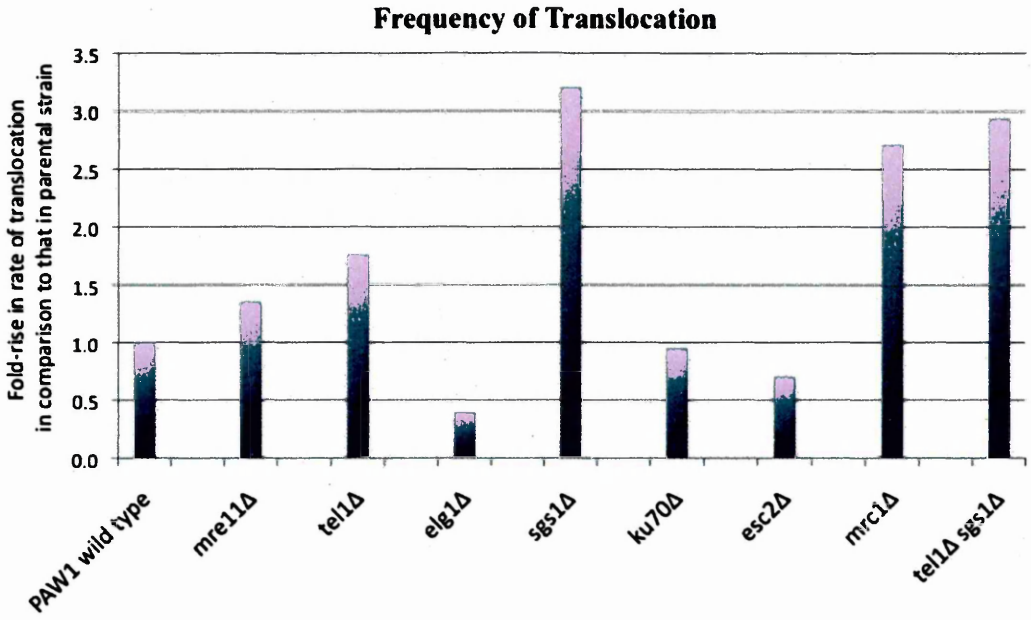

Figure 4.5 The frequency of translocation induction targeted at promoter regions of *ADH1* and *SUC2* genes in wild type and mutant backgrounds. Values are represented as fold rise with respect to BIT rates in wild type (5.9%), normalized as unit for making comparisons with values derived for those in mutants.

In cells lacking only *TEL1*, integration bias was unaffected, although the frequency of translocation induction showed about a two-fold increase. In *ESC2* deficient cells, integration bias was elevated 3 fold corresponding with a higher incidence of integration at the *ADH1* promoter locus, although the rate of translocation induction was lower than that in wild type cells. On the other hand, in a *MRC1* null strain compromised for replication checkpoint function, we noticed a subtle increase in integration bias accompanied with around a 3-fold elevated rate of translocation. A concomitant increase in both integration bias and rate of translocation induction was noticed only in cells lacking just *SGS1* and in cells deficient for both *SGS1* and *TEL1*.

4.3 CHEF and Southern hybridization analyses of SAD translocants:

Figure 4.1 shows a graphical representation of a chromosomal translocation targeted at promoter regions of *ADH1* and *SUC2* loci on chromosomes XV and IX, respectively. In addition to the formation of the aberrant chromosome, our experimental methodology to generate translocant strains inherently involves the generation of chromosomal fragments arising from translocation participant chromosomes. These so called, "free-ended DNA fragments" represent potential elements capable of advancing and leading into further genomic rearrangements. Thus it was necessary to monitor and determine the fate of the generated fragments and to elucidate the role of the selected candidate genes in this context.

To this end, we carried out the investigation of the fate of these fragments using pulsed-field gel electrophoresis to separate chromosomal fragments. This was followed by subsequent detection using various probes located on the two chromosomes involved in the translocation event. To do this, translocant cells from each SAD strain were harvested and subjected to contour-clamped homogeneous electric field (CHEF) gel electrophoresis to separate individual chromosomes and/or chromosomal fragments. Total chromosomal DNA was then transferred onto positively charged nylon membranes, followed by their detection upon hybridization using various labeled probes. Digoxigenin labeled probes for *CDC33* and *BRX1* were used to investigate the fate of the fragments of chromosome XV, while *SDL1* and *HIS5* probes were used to investigate the fate of the different chromosomal fragments of chromosome IX. More precisely, *CDC33* lies ~61Kbp distal from telomere XV-L and *BRX1* about 186Kbp from the same. The latter however lies ~27Kbp from the translocation breakpoint on chromosome XV-L at the

promoter region of *ADH1*. In the same way, *SDL1* lies about 24Kbp from telomere IX-L and is ~12Kbp upstream of the translocation breakpoint on IX-L at the promoter region of *SUC2*. The *HIS5* locus lies about 143Kbp from telomere IX-L, or nearly 106Kbp from *SUC2* (refer to **Figure 4.1** for relative chromosomal locations of loci in question).

4.3.1 *Chromosomal analysis of translocants obtained in wild type strains SAN1 and PAW1:*

Firstly, we employed the KANMX4^{DIG} probe to detect the presence of the aberrant translocated chromosome ensuing BIT induction. An aberrant chromosome of expected size was detected in all the ten SAD strains. As expected no detection with KANMX4^{DIG} was noticed in samples derived form parental strains. Ethidium bromide stained CHEF gels did however represent subtle abnormal patterns of chromosomal separation in some of the SAD mutants (**Figure 4.6**). For instance, in SAD1 derived from SAN1 and in SAD33 and SAD801 derived from the PAW1 yeast strains, we did not detect the presence of the wild-type copy of chromosome IX. This observation is supported by the lack of wild-type chromosome IX detection using HIS5^{DIG} and SDL1^{DIG} probes, both of which would otherwise hybridize to the left arm of chromosome IX flanking the translocation breakpoint on the same. Moreover, as expected HIS5^{DIG} also hybridized to the aberrant translocated chromosome in all the 10 SAD mutants.

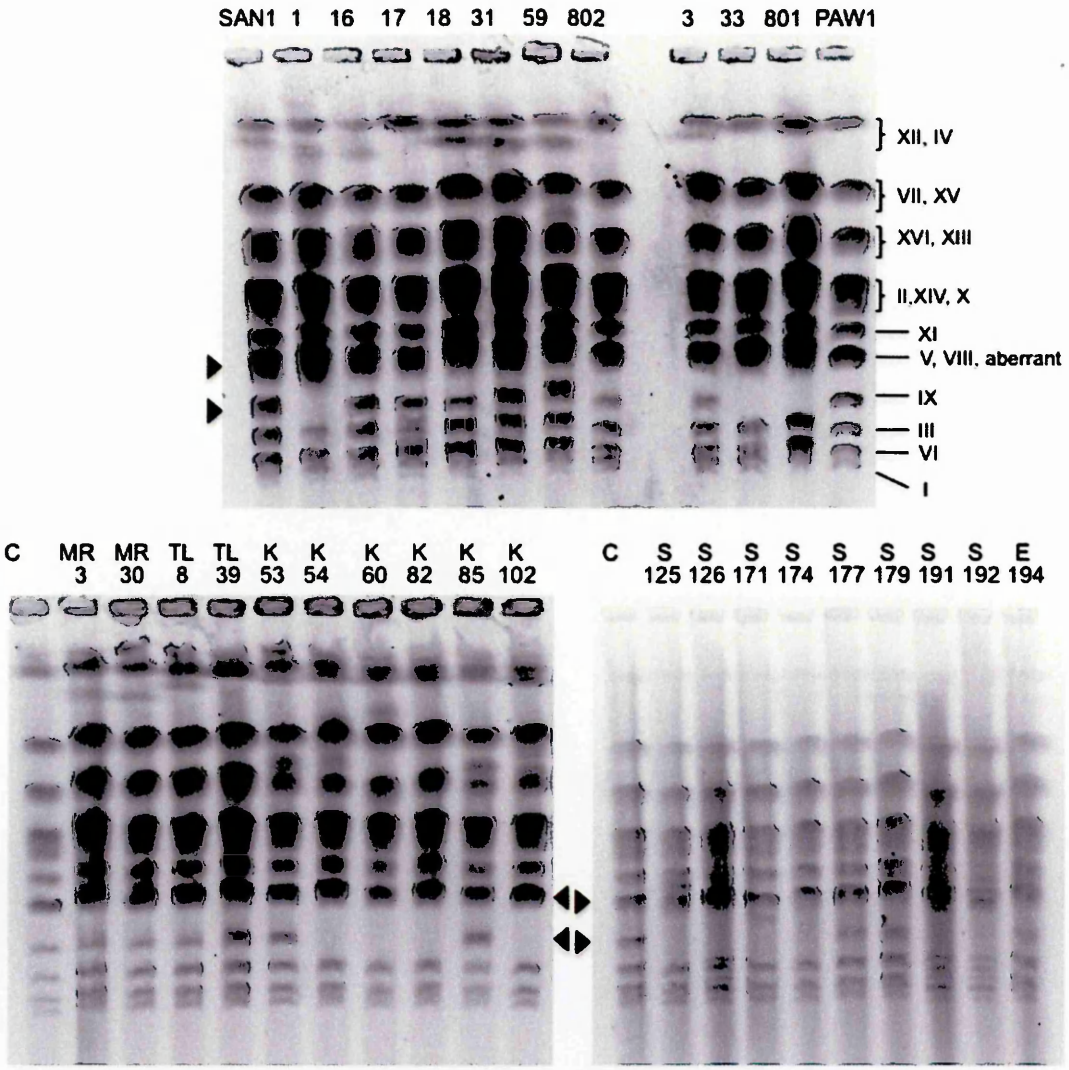

Figure 4.6 Representative ethidium bromide stained CHEF gels showing the separation of individual or groups of chromosomes derived from translocant cells generated in wild type and mutant strains. Several lanes corresponding to distinct translocants generated in various genetic backgrounds clearly depict the absence of native chromosome IX band. Black arrow: chromosome IX; Green arrow: aberrant translocated chromosome.

Additionally, $SDL1^{DIG}$ hybridized only to wild-type chromosome IX in all samples except in SAD1, SAD33 and SAD801 as mentioned above. We did not detect any ectopic hybridization of $SDL1^{DIG}$ in any of the analysed samples. This suggests that the telomeric fragment carrying the *SDL1* sequence is putatively degraded by nucleases

and eventually lost without undergoing any further rearrangements to be rescued/captured by another chromosome. Interestingly, in the case of SAD16, we discovered rearrangement of the centromere-containing fragment of chromosome XV generated after BIT following hybridization with $BRX1^{DIG}$ or $ALG6^{DIG}$ (ALG6 data not shown), both of which bind to XV-L downstream the translocation breakpoint. The higher molecular weight of the rearranged molecule seen in **Figure 4.7** suggests that the free end of the initial fragment putatively captured a sequence *in trans*, possibly mediated by micro-homology to acquire a telomere and attain stability. However, there could be other possibilities involving rescue of this centromeric fragment, possibly by illegitimate recombination into other instability prone fragile sites throughout the genome. NHEJ mediated joining to another broken chromosome, or capture at spontaneously arising DSBs could well be responsible in the generation of such a configuration. A possible effect of template switching leading to extensive lengthening via BIR or even during DNA synthesis could account for the same. The only possibility we exclude, that could not be involved in the generation of a higher molecular weight configuration, is *de novo* telomere additions. If this would happen, we would expect a lower molecular weight form in comparison to the wild type chromosome, after having lost a huge bulk of the left arm of chromosome XV.

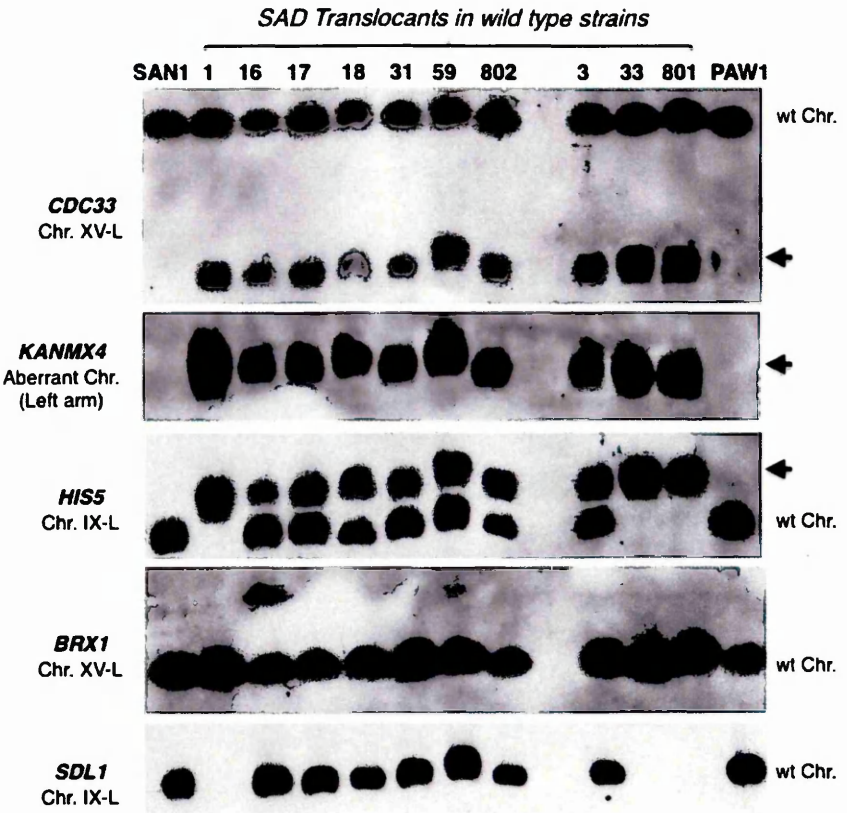

Figure 4.7 Southern hybridization of CHEF-separated chromosomal-DNA, derived from SAD translocants generated in wild-type strains. Chromosomes XV and IX were hybridized using digoxigenin labeled probes to monitor various chromosomal regions. Translocated chromosome was monitored using KANMX4^{DIG}, chromosome XV using CDC33^{DIG} and BRX1^{DIG} and chromosome IX using SDL1^{DIG} and HIS5^{DIG} probes. Refer to Figure 4.1 for relative locations of these chromosomal loci. Black arrow: aberrant chromosome.

4.3.2 *Chromosomal analysis of translocants obtained in mutant backgrounds:*

A total of 26 translocants were generated and analysed in eight different mutant backgrounds. Translocants MR3 and MR30 were obtained in an *mre11Δ* strain; TL8 and TL39 in a *tel1Δ* strain; K53, K54, K60, K82, K85 and K102 in *ku70* deficient strain; and S125, S126, S171, S174, S177, S179, S191 and S192 in a *sgs1Δ* strain. Similarly, E194 was obtained in an *elg1Δ* background; EC18, EC57 and EC70 were generated in an *esc2* deficient strain, whereas, MC7 and MC55 were obtained in an *mrc1* null strain.

Translocants named TS2-13 and TS2-14 were obtained in a double mutant strain carrying deletion in both *sgs1* and *tel1*. Chromosomal preparation and separation for each sample was carried out (described in MATERIALS AND METHODS section 2.9). Detection of various chromosomes and chromosomal fragments was carried out using DIG-labeled probes similarly as described above in section 4.3.1. The aberrant translocated chromosome was monitored using KANMX4^{DIG}. Free-ended fragments of participant chromosomes XV and IX arising after BIT formation, on the other hand were monitored using BRX1^{DIG} and SDL1^{DIG} probes, respectively. CDC33^{DIG} was employed to detect native chromosome XV in addition to the left arm on the translocated chromosome. Similarly, HIS5^{DIG} was used to monitor both the native chromosome IX as well as the translocated chromosome. In some cases we have used MUC1^{DIG} to monitor the right arm of native chromosome IX and that of the translocated chromosome.

Firstly, most translocant samples showed expected size of the translocated chromosome upon hybridization with the KANMX4^{DIG} probe expect for K70, S192 and MC55 (**Figure 4.8**). In the case of K70 and MC55, we noticed that the KANMX4^{DIG} probe hybridized to DNA with a higher molecular weight than that expected, like in other samples. On the other hand in S192, the KANMX4^{DIG} probe hybridized to reveal two distinct bands. One of these corresponded to the expected size of the translocated chromosome, while the other lower band appears to be the size of native chromosome IX (see figure ahead).

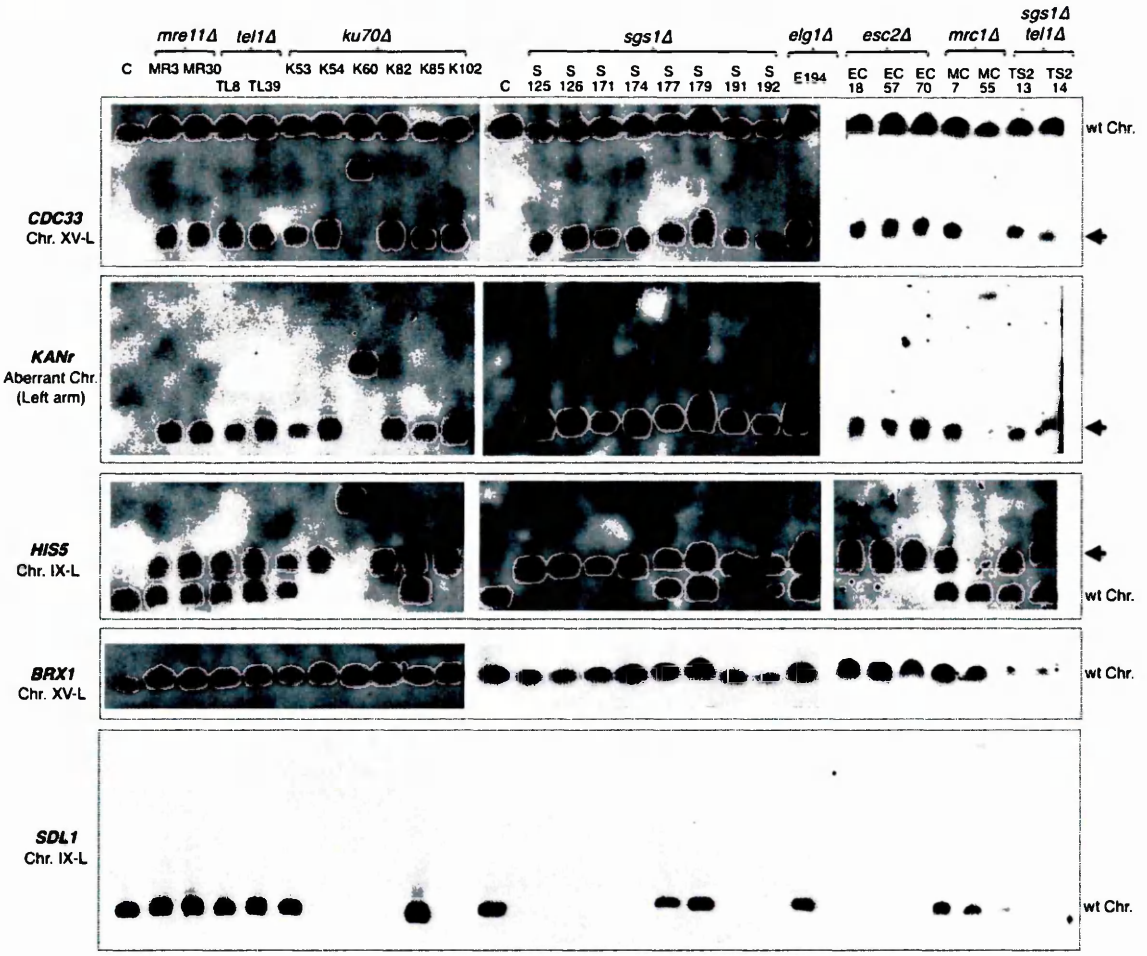

Figure 4.8 Southern hybridization of CHEF-separated chromosomal-DNA, derived from SAD translocants generated in various deletion-mutant strains. Each outlined panel shows hybridization with a specific probe mentioned on the right. Certain mutant translocants such as K60, S192 and MC7 reveal unexpected patterns of chromosome rearrangements. In certain others, more apparent is the lack of hybridization with $HIS5^{DIG}$ representing rearrangement of native chromosome IX. More evidently those same samples also show lack of hybridization with the $SDL1^{DIG}$ probe representing complete loss of this locus in the representative translocants. Black arrow: aberrant chromosome, wt: wild type.

In all 4 translocants derived in *mre11Δ* and *tel1Δ* strains, we got normal expected patterns of hybridization with all five tested probes. The same was true for the one translocant, E194 obtained in the *elg1Δ* mutant strain and the two translocants TS2-13 and TS2-14 generated in double mutant *sgs1Δ tel1Δ* strain. Among the others, secondary rearrangements were noticed in K60, S192 and MC55 as described above. Apart from

this, the most striking observation was lack of hybridization with $SDL1^{DIG}$ and $HIS5^{DIG}$ probes (see **Figure 4.8**) located on chromosome IX-L in many translocant strains. In these samples $HIS5^{DIG}$ hybridized only to the translocated chromosome also positive for $KANMX4^{DIG}$ hybridization. For some of these, we have also probed with $MUC1^{DIG}$ (**Figure 4.10**), which should otherwise hybridize IX-R, thus suggesting lack of native chromosome IX configuration in these translocants. Interestingly, the prevalence of this loss/rearrangement was much pronounced in *sgs1Δ*, *ku70Δ* and *ecs2Δ* background translocants. In other words, upon probing sequences along chromosome IX, native chromosome IX was not detected in five out of eight translocants in an *sgs1Δ* background, and in four out of six translocants in a *ku70Δ* background. Similarly, all three *esc2Δ* background translocants were negative for chromosome IX detection. So we asked whether this lack of hybridization along chromosome IX represented complete loss of the native copy, or its rearrangement into another form? Does native chromosome IX acquire the translocant chromosome configuration, or is it rearranged in another manner? To shed light on this, we have quantified gene dosage along chromosomes IX for the same genes probed with DIG labeled probes. This was done to estimate exact aneuploidy arising from this particular translocation, more of which in context of other targeted loci is described in the next chapter.

4.4 QPCR determination of gene dosage along translocated chromosome:

In the present context, we have utilized hydrolysis-probe (dual labeled fluorescent probe / TaqMan® probe) based QPCR analysis to quantify gene dosage of ORF sequences representing distinct parts of the chromosomes involved in the translocation. Gene quantization using QPCR is described in MATERIALS AND METHODS (section 2.8).

We chose *ACT1* as the endogenous control for all gene copy number experiments as a two-copy gene. Our results provide clear evidence of the presence of aneuploidy in all tested strains carrying the translocation. A particularly interesting observation was the lack of any PCR detection using probes to quantify *SDL1*, a gene located on IX-L. This location of *SDL1* on chromosome IX also corresponds to the same on the telomeric fragment generated after the BIT event (**Figure 4.1**). In our CHEF and southern hybridization experiments, all samples that were negative for SDL^{DIG} hybridization were also negative for QPCR detection with SDL1 specific probes. Additionally, $HIS5^{DIG}$ that was negative for hybridization on native chromosome IX but positive for the translocated chromosome (**Figures 4.7** and **4.8**), was also positive for detection with specific QPCR probes (**Figure 4.9** ahead). This suggested that only the part of chromosome IX-L containing the *SDL1* sequence was lost in these representative translocant cells. This also suggests that the terminal 36 Kbp fragments arising translocant participant chromosome IX upon BIT, was not rescued/captured elsewhere in the genome. Interestingly, we have noticed greater than two copies for some probes in several translocants. This suggests segmental aneuploidy for these regions, which were complementary to which the analysed probes that were quantified. Whether such data represents higher copy number of whole chromosomes seems unlikely, as not all probes along the entire length of a chromosome showed equally increased amplification by QPCR. Such abnormally elevated copy number of certain regions might represent tandem duplications or even represent potential instability prone genomic loci. However, at the genome wide scale, this must be precisely clarified in the future using comparative genome hybridization and similar methods, to precisely measure the nature of such aberrations.

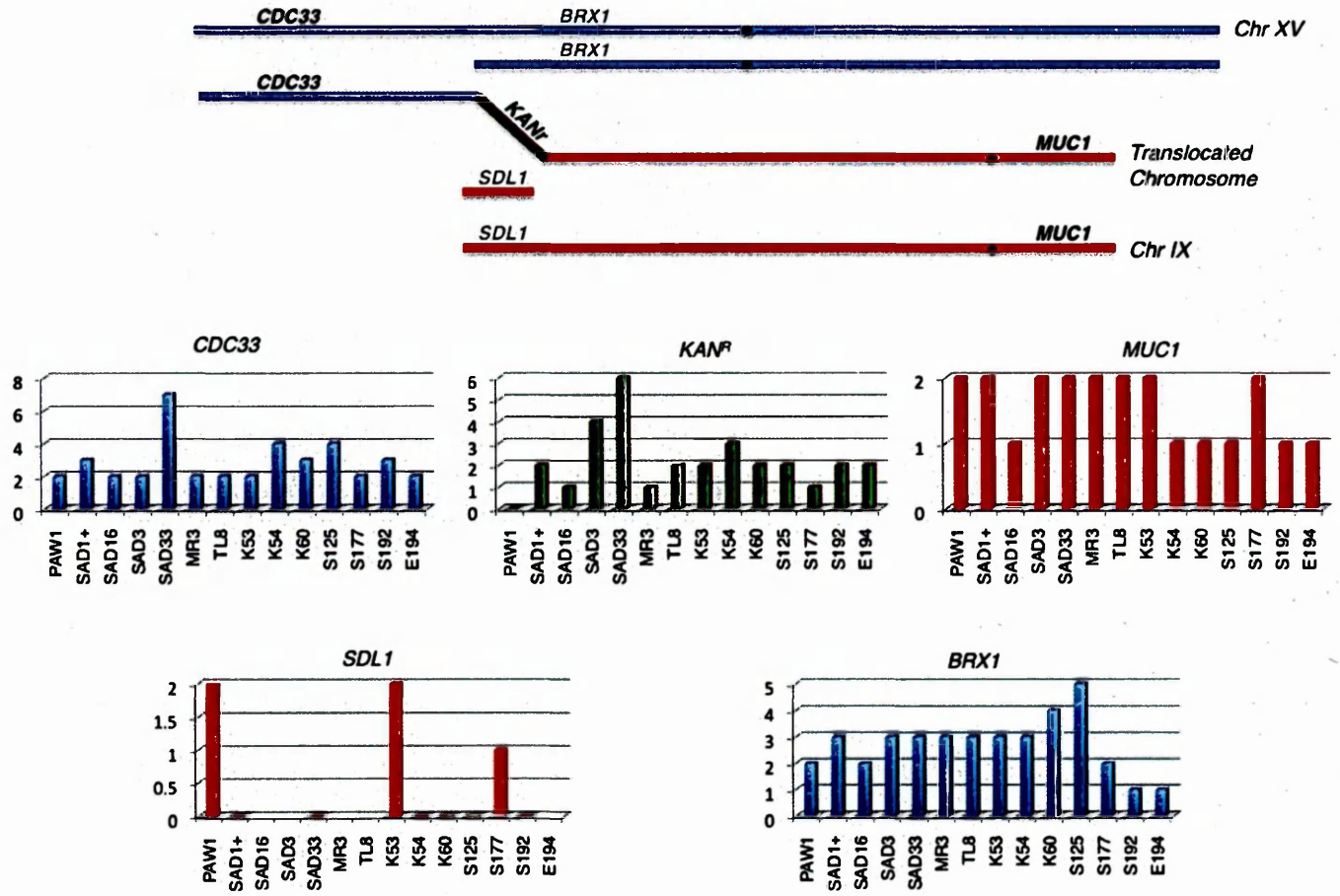

Figure 4.9 Gene dosage of various genes obtained by QPCR analysis. Gene names are mentioned in italics above, with their relative positions on chromosomes XV and IX. In certain samples *SDL1* was undetectable suggesting complete loss of this sequence. Certain probes with abnormally higher copy numbers might reflect tandem duplications of regions prone to elevated instability.

We propose that a similar analysis, for sequences that lie adjacent to the ones showing unexpectedly higher copy number changes, must be carried out before any definitive conclusions can be drawn based solely on the current data. Alternatively, ChIP on CHIP based strategies followed by QPCR could be employed to specifically rescue the sequence in question in order to precisely quantify DNA content of loci involved. Nevertheless, despite our limitations in understanding the causes of such abberations, it is clear the BIT events are associated with variable aneuploidy and gross chromosomal rearrangements ensuing the primary chromosomal bridging event.

4.5 Stability of secondary chromosome rearrangements observed in SAD strains:

Chromosome rearrangements are often unstable and lead to the generation of secondary and tertiary abberations. When we first detected abnormal chromosomal abberations in some of our translocant cells (apart from the formation of expected translocated chromosome), we asked whether these were stably maintained in those translocants or not? Thus, we analysed 4 different translocants namely SAD16, SAD33, K60 and S192, which carried secondary rearrangements evident on hybridized CHEF gels (see **Figures 4.7** and **4.8**). To this end, a single isolated colony (SIC) of each translocant strain was cultured for 1 day to harvest cells for CHEF analysis. The same culture was re-inoculated into fresh rich media after every 24 hours for 15 consecutive days, to maintain a continuously growing chronological culture of translocant cells. At the end of this period cells were harvested for CHEF analysis.

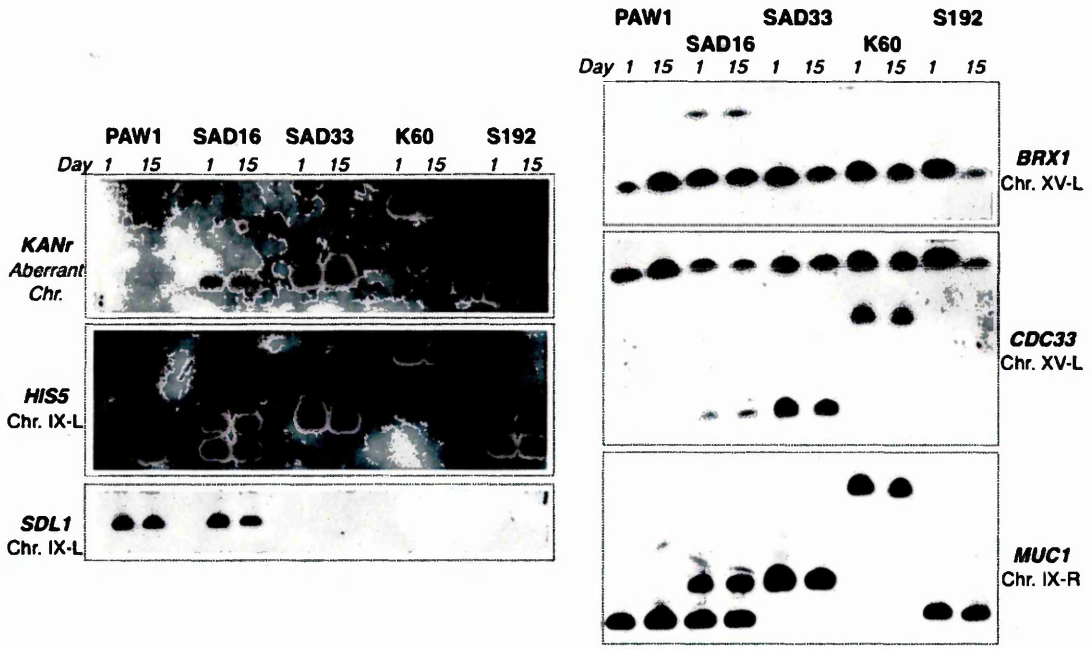

Figure 4.10 Southern hybridized CHEF-separated DNA derived from translocant cells bearing secondary rearrangements. Strains were cultured for either 1 day or 15 days to prepare DNA and chromosomal patterns were analysed using various probes mentioned on side panels.

We tested whether the unusual/novel secondary rearrangements persisted stably over several generations or lead to tertiary and further rearrangements. In our analysis we compared the pattern of chromosomal rearrangements seen in translocant cells cultured for 1 day or upon continuous growth for 15 days. Within this time scale aneuploid yeast cells usually lose control of ploidy and we could expect that the tested mutants possibly foster additional rearrangements. However, we did not detect any differences in the nature of detected secondary rearrangements in all 4 analysed translocants cells, which were cultured for 1 day or for 15 days (**Figure 4.10**). This suggests that rearrangements ensuing BIT events in translocant cells are stably maintained over successive generations without fostering additional rearrangements. Although, this stable maintenance of any

aberrant fragments or chromosomes in the analysed translocants does not mean that instability didn't occur early in the process.

The most interesting observation from this analysis was the detection of variation in S192 chromosomal patterns in comparison to those previously obtained for the same translocant (refer to **Figures 4.8** and **4.10**). Hybridization of S192 DNA with $KANMX4^{DIG}$ and $HIS5^{DIG}$ probes as seen in figures mentioned above, clearly reveals differences in these two independent analyses. Both probes in the first analysis (**Figure 4.8**) hybridize to two specific DNA sequences of different molecular weights. Contrary to this, in the current analysis (**Figure 4.10**), the same probes hybridized S192 DNA to reveal only to one of the two bands. After careful consideration we were able to pinpoint the apparent cause of these differences. We discovered that in these two independent experiments, chromosomal DNA for analysis was derived from two separate S192 single isolated colonies, picked from the same growth plate. Could SICs arising from an individual translocation-carrying strain have varied karyotypes? To test this, we randomly selected 12 SICs from the same culture plate on which S192 was streaked to SICs. This was the same plate from which S192 SICs were used in the above two analyses described. Chromosomal DNA derived from each clone was hybridized with appropriate DIG labeled probes to clarify the nature of variability in karyotypes among clones (**Figure 4.11** below).

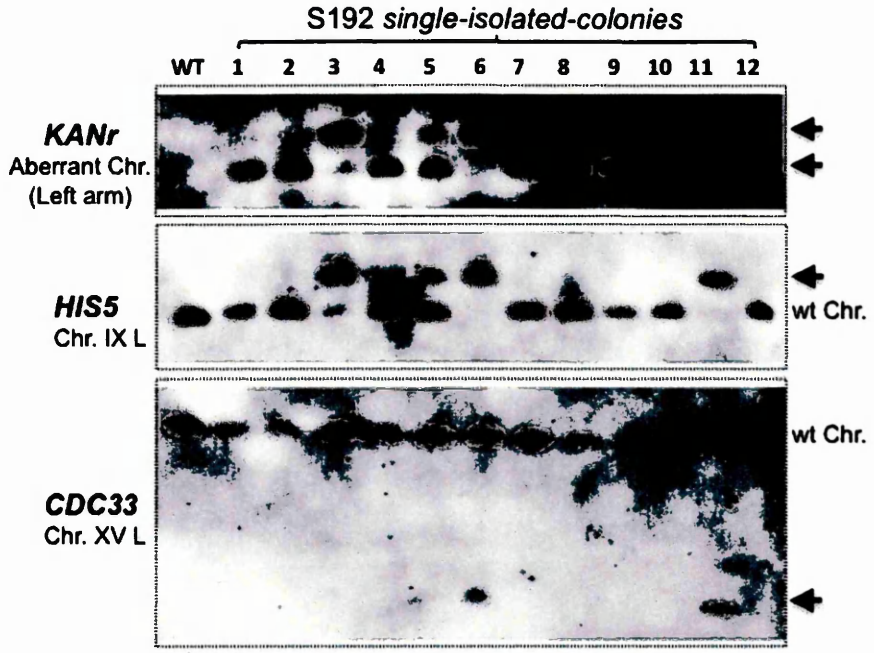

Figure 4.11 Southern hybridized chromosomal DNA derived from 12 randomly selected single isolated colonies arising from S192 translocant strain. Each lane from 1 to 12 represents an individual clone arising from S192. Among these clones show varied patterns when hybridized with probes specific for sequences on the translocated chromosome (KANr) and those on chromosome IX (HIS5) and XV (CDC33). Black arrow: aberrant chromosome, wt: wild type.

Among the twelve S192 SICs analysed, we noticed at least 3 different patterns of hybridization using probes binding to similar regions on chromosomal DNA. For instance in **Figure 4.11**, clones 2 to 6 represent altered chromosomal patterns for the translocated chromosome. Putatively, the same upon probing with KANr (same as KANMX4^{DIG}) should otherwise hybridize to reveal just one upper band in southern blots. This notion is supported by HIS5^{DIG} hybridization of wild type DNA, which binds only to the lower band corresponding to native chromosome IX. Additionally, KANMX4^{DIG} and HIS5^{DIG} hybridization patterns were the same in all samples. This suggests that in most samples (1-5, 7-10 and 12) KANMX4^{DIG} was located on native chromosome without bridging together with chromosome XV. Moreover, very interestingly in samples 3 and 5 we

detected the presence of the aberrant translocated chromosome in addition to KANr hybridization to native chromosome IX. On the other hand, samples 6 and 9 were positive for hybridization to just the translocated chromosome. Interestingly, unlike samples 6 and 9, which were positive for $CDC33^{DIG}$ hybridization, sample 3 was not. However, the latter was positive for hybridization to translocated chromosome with $KANMX4^{DIG}$ and $HIS5^{DIG}$. Overall, our findings about BIT associated secondary rearrangements in *S. cerevisiae* cells reveal both stable and varied patterns. The detection of varied patterns especially among S192 clones poses novel queries on mechanisms that might be involved in generation of such abberations.

4.6 Native chromosome IX stability in translocant strains:

Analyses of translocation carrying yeast strains described in sections 4.3 and 4.4 The stability of wild type chromosome IX was monitored in translocant strains originating from wild type PAW1 cells and those bearing deletions in genes like *MRE11, TEL1, KU70, SGS1* and *ELG1*. This investigation stems from the observation in S192 translocant cells, in which we have noticed the presence and absence of the native copy of chromosome IX in individual colonies growing on the same media plate (**Figure 4.11**). S192 as described above bears a translocation between *ADH1* and *SUC2* promoter loci, and was a translocant strain obtained in an *sgs1Δ* genetic background. Other mutant translocants like SAD1, SAD33 and K60 clones were tested negative for the presence of wild type chromosome IX in our PCR and CHEF/Southern blotting approaches of investigating the fate of chromosomal fragments proceeding BIT events targeting chromosomes XV and IX. In other words, translocant strains generated and collected in this study fall into two major categories. One, in which the wild type copy of

chromosome IX is retained and stably maintained after BIT and the second in which it is not. The mechanism by which this chromosome was destabilized and eventually undetectable in our assays forms the crux of our current investigation. In order to test our hypothesis, we cultured translocant strains in which wild-type chromosome IX was detectable after the *ADH1-SUC2* translocation. All translocant strains chosen to perform this test were derived from wild-type PAW1 cells, and from the same in which double deletions were made for genes *MRE11, TEL1, SGS1, KU70* and *ELG1*. Strains were cultured as a continuous culture in rich YPD media, which was replenished and re-inoculated with a small volume of the pre-existing culture after every 24 hours of growth. Each day cultures were diluted to 10^3 cells/ml and plated on YPD plates at a density of approximately 100 cells per plate for each strain. However, every alternate day 10 single isolated colonies derived from each plated strain were randomly selected, picked and analysed using colony PCR to monitor the retention/loss (stability) of chromosome IX in these clones. In other words, colony PCR analysis was performed on clones derived from plates plated on days 1, 3, 5, 7, 9, and 10 of all cultures.

We observed from our above-described analysis that none of the strains tested for the instability of chromosome IX revealed the loss of the wild type chromosome. These observations of growing cells analysed periodically during the 10 days of growth time suggests, that the instability of chromosome IX observed in other translocant strains cannot be correlated to the gradual loss of the entire chromosome with increasing growth time. However, it might either be completely lost or alternatively rearranged by other repair mechanisms during the very early rounds of cell duplication following the induction of the translocation event.

Results (Part 3) – Multiple aneuploidies from the same BIT event

5.1 A new series of SUSU translocants between chromosomes XVI and IX:

The previously described BIT system (TOSATO *et al.* 2005) was used to generate a collection of 10 translocants carrying translocation between chromosomes XVI and IX of *S. cerevisiae*. Translocation was induced using a BIT construct harboring the *KANMX4* selectable marker flanked by two 65-bp sequences, one homologous to the terminator region of *SSU1* (that is also the promoter region for *GLR1*) and the other to the promoter region of *SUC2*, located on chromosomes XVI and IX, respectively (**Figure 5.1**). Both these loci harbor metabolic genes that are not involved in genome regulatory processes (AVRAM and BAKALINSKY 1997; FLEMING and PENNINGS 2007; LUTFIYYA and JOHNSTON 1996; PEREZ-ORTIN *et al.* 2002; PERLMAN *et al.* 1982; TAUSSIG and CARLSON 1983). The aberrant chromosome generated by translocation between these two loci contains 374 Kbp of chromosome XVI-L and a 403 Kbp centromeric fragment of chromosome IX bridged together by the selectable marker *KANMX4*.

A PCR-amplified linear DNA cassette was used to transform the diploid yeast strain San1, following the selection of kanamycin resistant transformants on G418 containing plates. We have used two different transformation techniques to induce BIT in San1 cells. A total of 104 transformants were obtained using the standard LiAc transformation and a collection of 138 transformants using sphaeroplast transformation. All G418 resistant transformants were analyzed by colony PCR to check the integration of the BIT construct, at both target loci in the genome, using specific primers (see **Figure 5.1**). All colony PCR-positive clones were further confirmed by performing PCR using

genomic DNA of the same. When the transformants showed integration at both loci, the presence of the translocation was confirmed performing a bridge-PCR from genomic DNA and further validated by sequence analysis. Clones bearing the sSU1-SUc2 (SUSU) translocation were named SUSU1 through to SUSU10 and will be referred to as such throughout the following text.

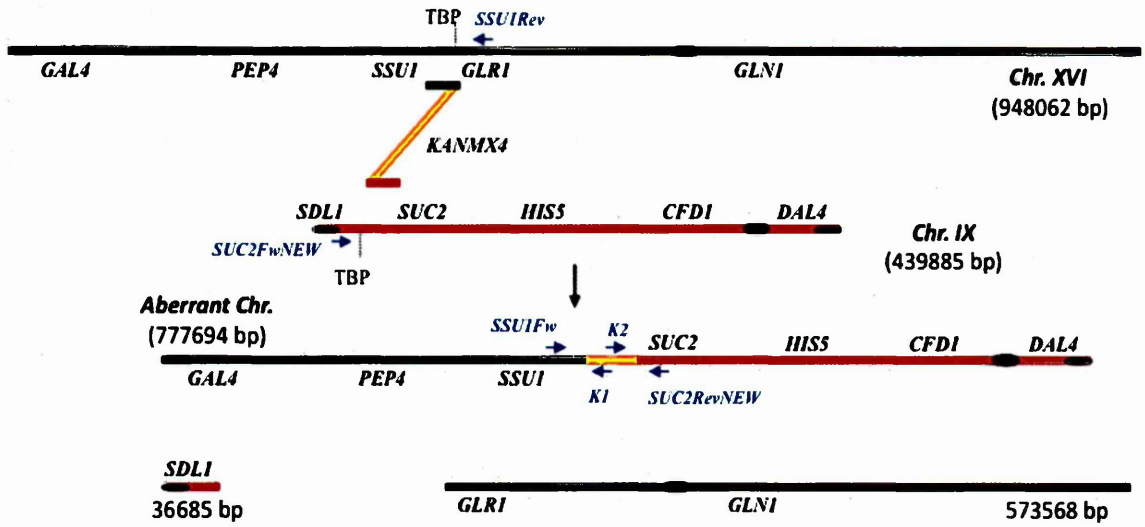

Figure 5.1 Schematic representation of BIT between chromosomes XVI and IX. The 777694bp-aberrant chromosome along with the two hypothetic fragments that originate after a non-reciprocal BIT translocation are shown. The key genes analyzed by Southern hybridization are reported along the chromosomes together with the primers used to test the integration of the BIT construct at the level of the two targeted loci. SSU1Fw and SUC2RevNEW primers were used to perform the bridge-PCR to validate the presence of the translocant chromosome. TBP: translocation breakpoint.

Among a collection of 10 translocants obtained, nine translocants were obtained using the LiAc transformation technique and one translocant (SUSU10) using sphaeroplast transformation. Furthermore, sequence analysis of the translocation breakpoints revealed no mismatches or mutations in all 10 mutant strains.

5.2 Chromosomal pattern of the SUSU translocants:

The chromosomal pattern of all the SUSU translocants was analyzed using pulsed field gel electrophoresis (PFGE/CHEF) followed by Southern blot analysis. These experiments confirmed that all translocations induced by transformation with a BIT cassette, between two non-homologous chromosomes, are non-reciprocal (**Figure 5.2** on page 112).

Digoxygenin labeled probes for *GAL4, PEP4, GLR1* and *GLN1* were used to investigate the fate of the various parts of chromosome XVI; *SDL1, HIS5* and *CFD1* probes were used to investigate the fate of the different chromosomal fragments of chromosome IX. A KANMX4^{DIG} probe was use to monitor the formation and occurrence of the aberrant chromosome. The SDL1 panel in **Figure 5.2** shows that the small acentric fragment of 36685bp, supposedly originating after the translocation, was lost or degraded. On the other hand, the 573Kbp-centromeric fragment of chromosome XVI was not detected in all the ten translocants. Probes used against chromosome XVI revealed that SUSU2, SUSU7 and SUSU9 harbor complex rearrangements of this chromosome (see **Figure 5.2**). In SUSU2, a fragment of chromosome XVI containing the *PEP4* and *GLR1* genes was rearranged elsewhere in the genome leading to the formation a new chromosome (**Figures 5.2**). Using a polynomial equation to calculate chromosome size, this aberrant chromosome containing *PEP4* and *GLR1* was estimated to be about ~1067 Kbp. In SUSU7, a large fragment of chromosome XVI encompassing the centromere, was fused to an other chromosomal fragment giving rise to a bigger chromosome of about ~1307 Kb. Southern blot analyses revealed that in SUSU9 the aberrant chromosome containing the kanamycin resistance gene and the sequenced BIT junction

between chromosome XVI and IX was larger than expected. This chromosome of about ~1042 Kbp size did not contain *GLR1, CFD1* and *DAL4* (not shown) but harbored *GLN1*, as detected using specific probes. Additionally, it did not contain the centromere of chromosome IX but that of chromosome XVI.

Moreover, it seems that a portion of chromosome XVI close to the translocation break point was lost in this translocant. We propose that this novel aberrant chromosome of higher molecular weight that the expected size, may have originated either by a complex fork-stalling template switching-like (FosTeS) mechanism during synthesis (see DISCUSSIONS 6.3 and *Appendix 2*).

Hybridization with the KANMX4^{DIG} probe revealed the presence of the expected 778 Kbp-sized translocant chromosome in all the other SUSU mutant strains. Based on the fact that the parental strain San1 is diploid, at least one copy of both wild-type chromosomes XVI and IX are also present in all mutant strains, with the exception of SUSU1, in which the wild type copy of chromosome IX was not detected. Furthermore, we noticed an additional polymorphism in SUSU5, which is clearly visible as an extra-band between the native chromosome III (370 Kb) and chromosome IX (440 Kb) (**Figure 5.2A**). Probes located along chromosome IX and XVI used in our experiments failed to hybridize to DNA corresponding to this band. Others in our group have noticed a similar higher molecular weight band in other translocants being studied (TOSATO, personal communication). We speculate that the formation of such polymorphism is not specifically correlated with the SUSU-BIT translocation events, but could still be correlated with BIT events happening, generally.

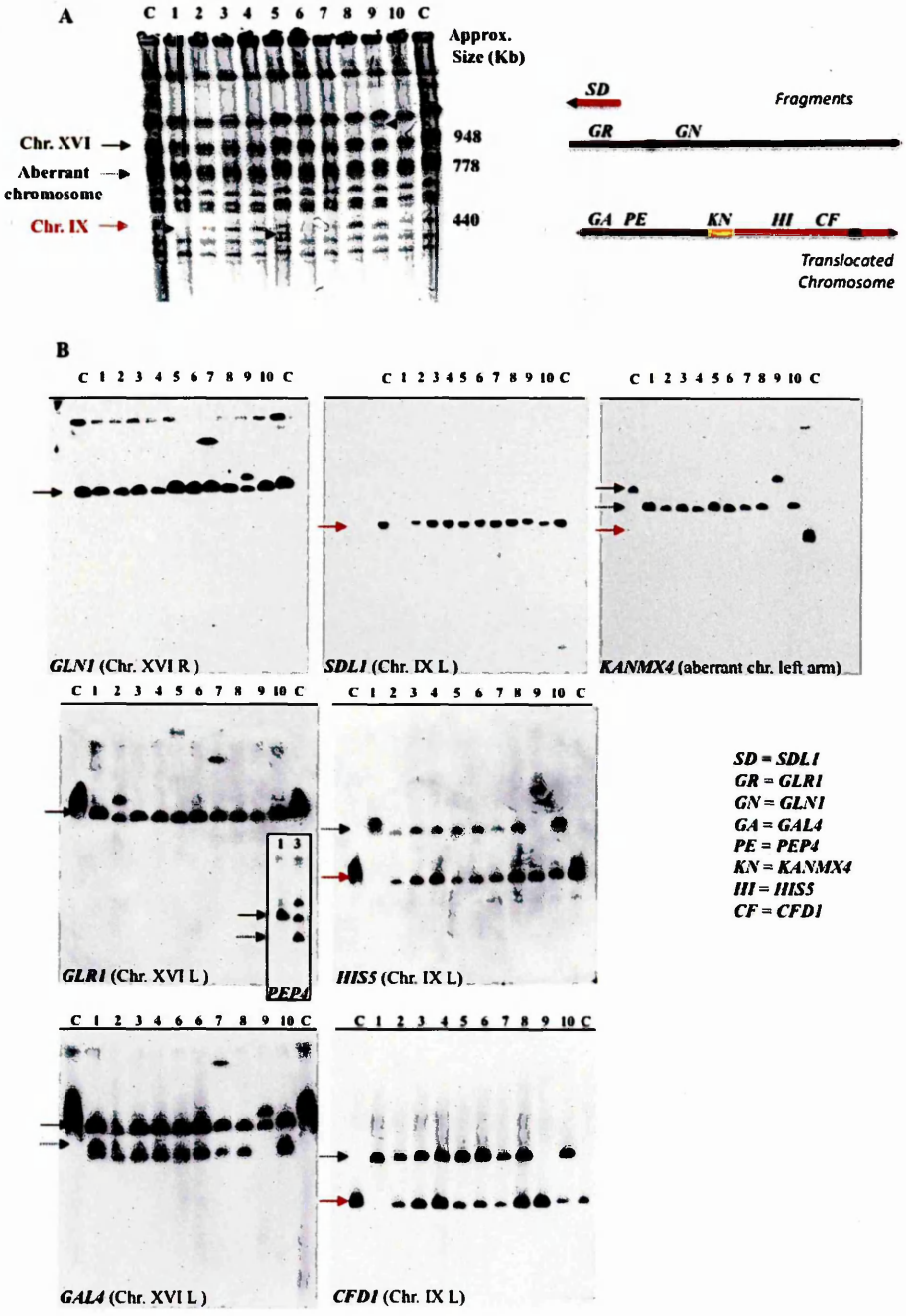

Figure 5.2. Chromosomal analysis of SUSU translocants (**A**) Chromosome separation by CHEF. Black arrows point out visible chromosomal polymorphisms in the SUSU1, SUSU5 and SUSU9 translocants. (**B**) Southern blot analyses: Blots were hybridized to the DIG-labeled GAL4, PEP4, GLR1 and GLN1 probes on chromosome XVI; SDL1, HIS5 and CFD1 probes are on chromosome IX; KANMX4 probe was use to detect the aberrant chromosome. In all pictures, with the exception of that hybridized with KANMX4, lanes C contain San1 diploid control strain DNA. In the membrane hybridized with KANMX4 the lanes C (left) contains San1-(*DBP1/dbp1::KAN*^{R}) DNA; lane C (right), San1-(*GUT2/gut2::KAN*^{R}) DNA. The adjoining PEP4-probed membrane on the GLR1 panel shows the SUSU2 chromosomal pattern in comparison to the control strain San1. All the other translocants have the same pattern as in the GAL4 panel. Red arrow: Ch. IX; dashed arrow: translocant chromosome; green arrow: Ch. XVI.

5.3 Gene copy number determination:

To better understand the nature of chromosomal aberrations in the SUSU translocants and to investigate whether aneuploidy might arise from the induction of the BIT translocation, we determined the copy number of some genes located along chromosome XVI and IX. This was done by quantitative PCR using limiting number of cycles (see MATERIALS AND METHODS). The gene dosage of *VMR1*, located on chromosome VIII (not involved in translocation) was also determined as control for the accuracy of our experiments. The histograms in **Figures 5.3** and **5.4** show copy number of the analyzed genes in the control strain and in the translocants.

Gene dosage experiments suggest that integration of a linear BIT construct into targeted loci in the yeast genome might also lead to the generation of aneuploidy, as seen in all analyzed SUSU translocants. For instance, copy number determination for genes located along chromosome XVI like *GAL4*, *GLR1* and *GLN1* show that all the analyzed mutants have at least two copies of the native chromosome XVI. Trisomy of chromosome XVI was detected in SUSU5, SUSU6 and SUSU10. Triploid and tetraploid status of various parts of chromosome XVI was also detected in SUSU2, SUSU7 and SUSU9. Moreover, the same translocants harbored complex rearrangements of that chromosome. PCR data on *SUC2* promoter, *SUC2* ORF and *DAL4* located on chromosome IX pointed out that in five translocant strains, a single copy of native chromosome IX was present; whereas in SUSU3 and SUSU9 two copies were detected. Three copies were detected in SUSU4 and four copies in SUSU8. In SUSU1 the absence of the wild type copy of chromosome IX was confirmed together with the duplication of the aberrant chromosome. With the exception of SUSU1 the presence of only one copy of the aberrant

chromosome was noticed for all the other translocants by the amplification of *KANMX4* together with *ACT1* using San1-*GUT2*/*gut2::KANMX4* as reference strain containing one copy of the kanamycin resistance gene.

Our observations suggest that all SUSU translocants exhibit whole or partial aneuploidy of either entire chromosomes or chromosomal segments, measured as copy number variation of certain regions. Such secondary events emanating from the initial BIT event could also induce further loss or rearrangement possibly by template switching like mechanisms, which can partly explain some of the observations described above and discussed in further detail in Chapter 6 Part 6.3.

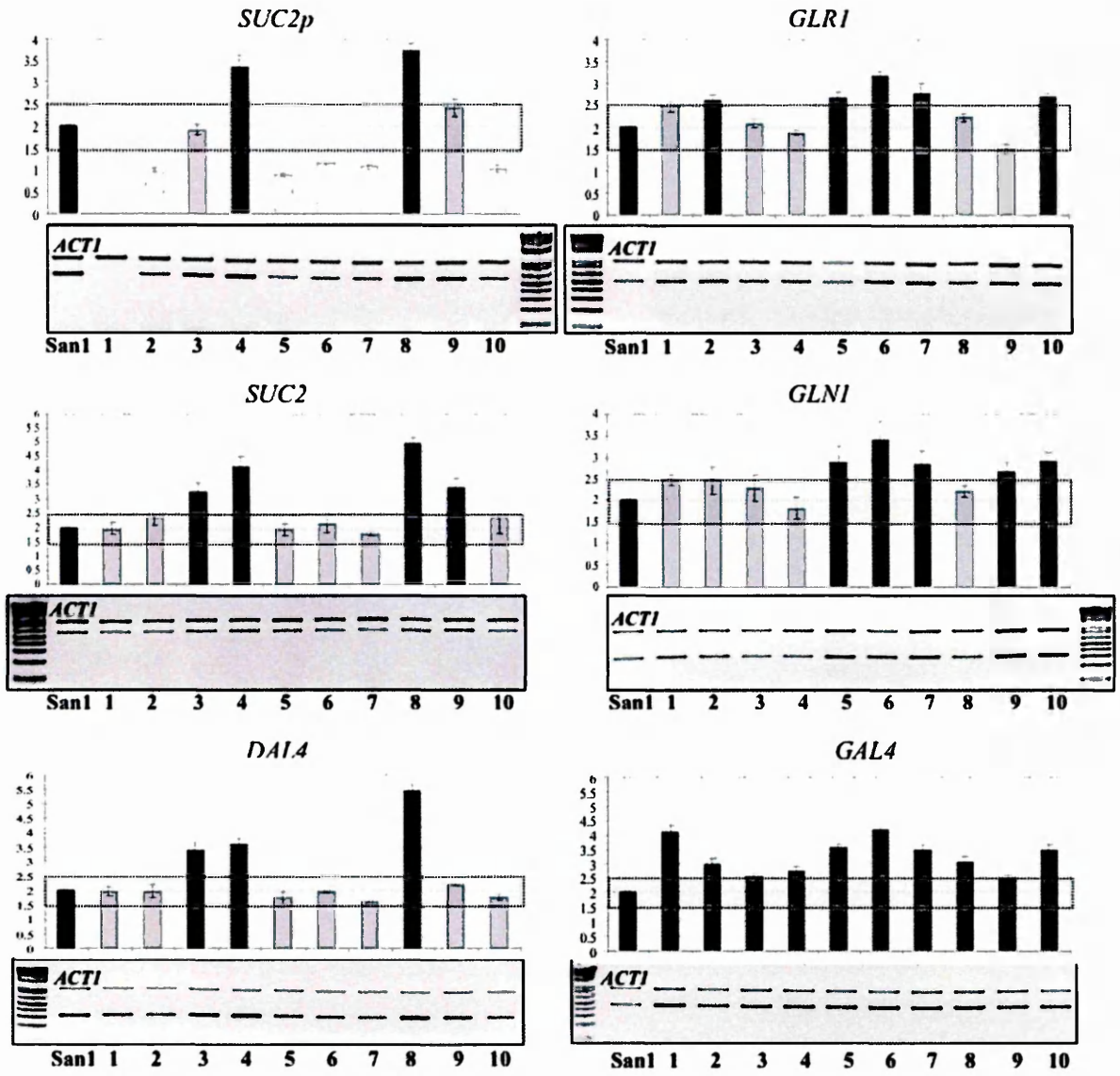

Figure 5.3 Quantitative PCR copy number analysis of genes located on chromosomes XVI and IX. In each gel picture the higher band corresponds to that of chromosome VI *ACT1* control gene amplicon, whereas the lower band corresponds to the amplicon of the analyzed gene involved in the translocation. The gene dosage of *VMR1* (see **Figure 5.4**), located on chromosome VIII, but not involved in translocation, was also determined as control for the accuracy of our experiments. Each analyzed gene and *ACT1* were co-amplified in the same reaction and loaded on the gel. Values presented on the graph above the gel pictures show the gene dosage expressed as an average of at least three independent-densitometric determinations from four gels. Data normalized with respect to *ACT1* considered as a constant two-copy number gene were then compared with the normalized values in the San1 control strain containing two copies of the gene. San1, control strain; From1 to 10: the 10 SUSU translocants. The grey rectangle highlights a ± 0.5 variation in gene copy number. Variations within this interval were considered as insignificant variation in gene copy number with respect to the wt situation. Black bar: San1 control strain; white bars: gene copy number lower than the control strain; light grey bars: gene copy number equal to that of the control strain; dark grey bars: gene copy number higher than the control strain.

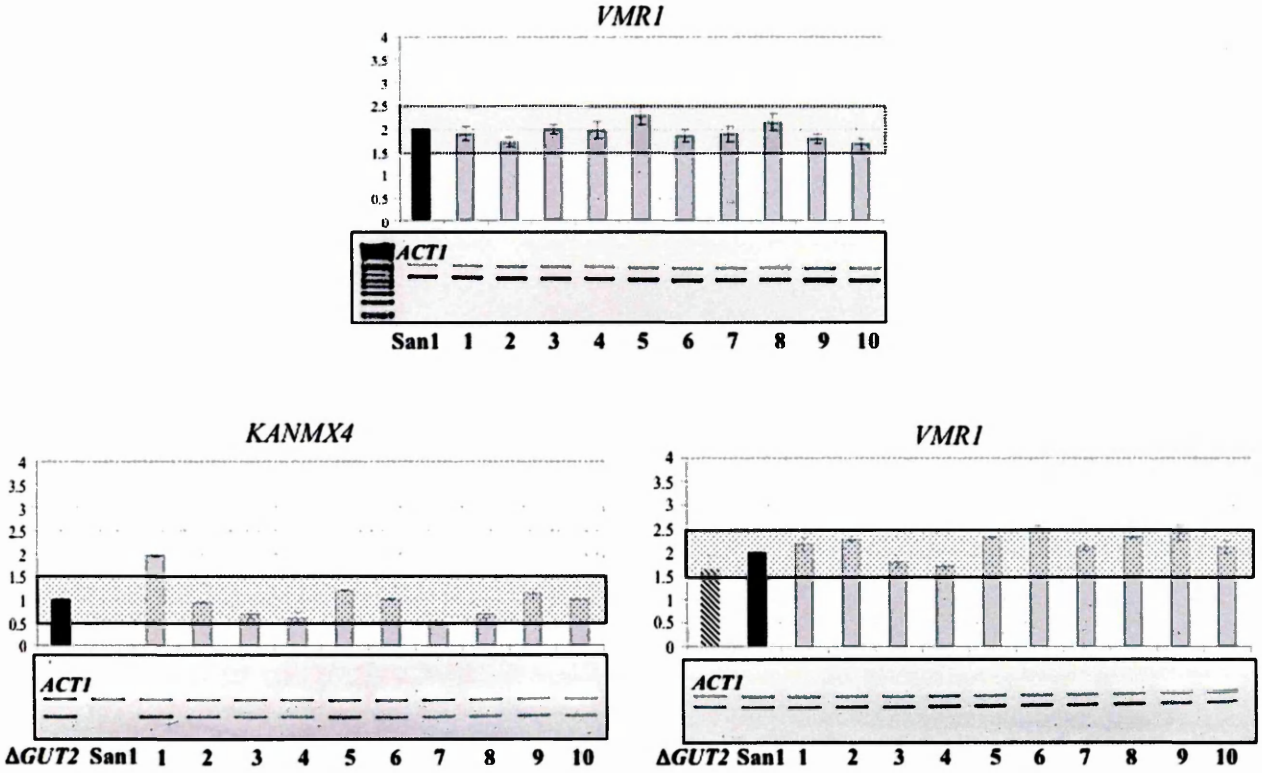

Figure 5.4 Quantitative PCR copy number analysis of KANMX4. In the two gel pictures the higher band corresponds to the band of the *ACT1* control gene amplicon on chromosome VI, whereas the lower band corresponds to the amplicon of *KANMX4* or *VMR1*. The gene dosage of *VMR1*, located on chromosome VIII (not involved in translocation) was determined as control of the accuracy of our experiments. The analyzed gene and *ACT1* were co-amplified in the same reaction. Values presented on the graphs above the gel pictures show the gene copy number expressed as average of at least three independent densitometric determinations of four gels normalized with respect to *ACT1* considered as a constant two-copy number gene and then compared with the normalized value in the San1-*GUT2/gut2::KANMX4* containing one copy of the KANMX4 gene or with the value in San1 containing 2 copies of *VMR1*. *ΔGUT2*, San1-*GUT2/gut2::KANMX4* control strain; San1: original parental strain; From1 to 10: the 10 SUSU translocants. The grey rectangle highlights on the graphs a ± 0.5 variation in gene copy number. Variations within this interval were not considered as a significant gene copy number change with respect to the wilt type values. Black bar: San1 control strain; light grey: gene copy number equal to that of the control strain; dark grey: gene copy number higher than the control strain.

5.4 Gene Expression analyses in SUSU translocants:

A genome wide expression profiling of translocants using microarray analysis has been recently described for strains bearing a bridge induced translocation between *ADH1* and *DUR3* genes on chromosomes XV and VIII, respectively (NIKITIN *et al.* 2008). In these translocant called D10 cell, the authors have reported a general upregulation of gene expression around a 50Kbp region flanking the translocation breakpoint. At the same time, it was demonstrated by others in our group that a near-reciprocal translocation between homologous chromosomes generally does not affect gene expression at these genomic loci (TOSATO *et al.* 2009). In this study, we have used a semi-quantitative RT-PCR based approach to study the effect of the SUSU translocation on the expression of the selected genes located at the translocation breakpoints, and also along the two chromosomes involved in the translocation. This was done to better understand SUSU translocation-specific affect on the expression of genes located on the aberrant chromosome. Additionally, we also analyzed the expression pattern of a set of genes involved in diverse cellular processes like cell-cycle regulation, oxidative stress response, apoptosis and multi-drug resistance. The expression patterns various analyzed genes in all 10 SUSU translocants are reported in **Figure 5.5**. As in previous expression analyses of BIT translocants, *HSC82* was chosen as a constitutive control gene (NIKITIN *et al.* 2008; TOSATO *et al.* 2009). For all analyzed genes, an expression level higher than twice the expression level of the control strain was considered as a significant up-regulation of gene expression; whereas, we considered a significant down-regulation of transcription when the expression level was equal to or lower than half the expression level of San1 control strain.

Figure 5.5 clearly shows that the effect of the same BIT translocation between chromosome XVI and IX differentially altered transcription in the various SUSU translocants. Only the cell cycle related gene *CLB1* and the arginase gene *CAR1* exhibited an expression level similar to that of the control strain in all the 10 SUSU translocants.

Furthermore, the increased gene expression at the translocation breakpoint and along the translocated chromosome observed in the BIT translocants previously described (NIKITIN *et al.* 2008), was not a common observation noticed in all the SUSU mutant strains. In fact, SUSU2 and SUSU3 did not show any significant alteration in the transcription level of the analyzed genes. The only alteration observed was the previously described down-regulation of *SSU1* and *RRD1* in SUSU3.

On the other hand, SUSU1, SUSU4 and especially SUSU6 showed strong de-regulation in the expression of many analyzed genes, suggesting a larger alteration of their physiology and metabolism. In SUSU1, a 2.1 fold increase in the mRNA level of *GAL4* located on chromosome XVI and a 3.5 fold increase of the multidrug-resistant gene *VMR1* transcript were observed. In the same strain we also found the over-expression of the caspase *YCA1* gene and of *GSH1*, which is also involved in apoptosis and cellular response to oxidative stress. Interestingly, previous works (TOSATO *et al.* 2009); (NIKITIN personal communication) have revealed that *VMR1* up-regulation was also present in other translocants obtained with the BIT system between both homologous and heterologous yeast chromosomes. Nevertheless, so far, the transcriptional up-regulation of *YCA1* and *GSH1* was only observed in some of the SUSU translocants described in this study (**Figure 5.5**).

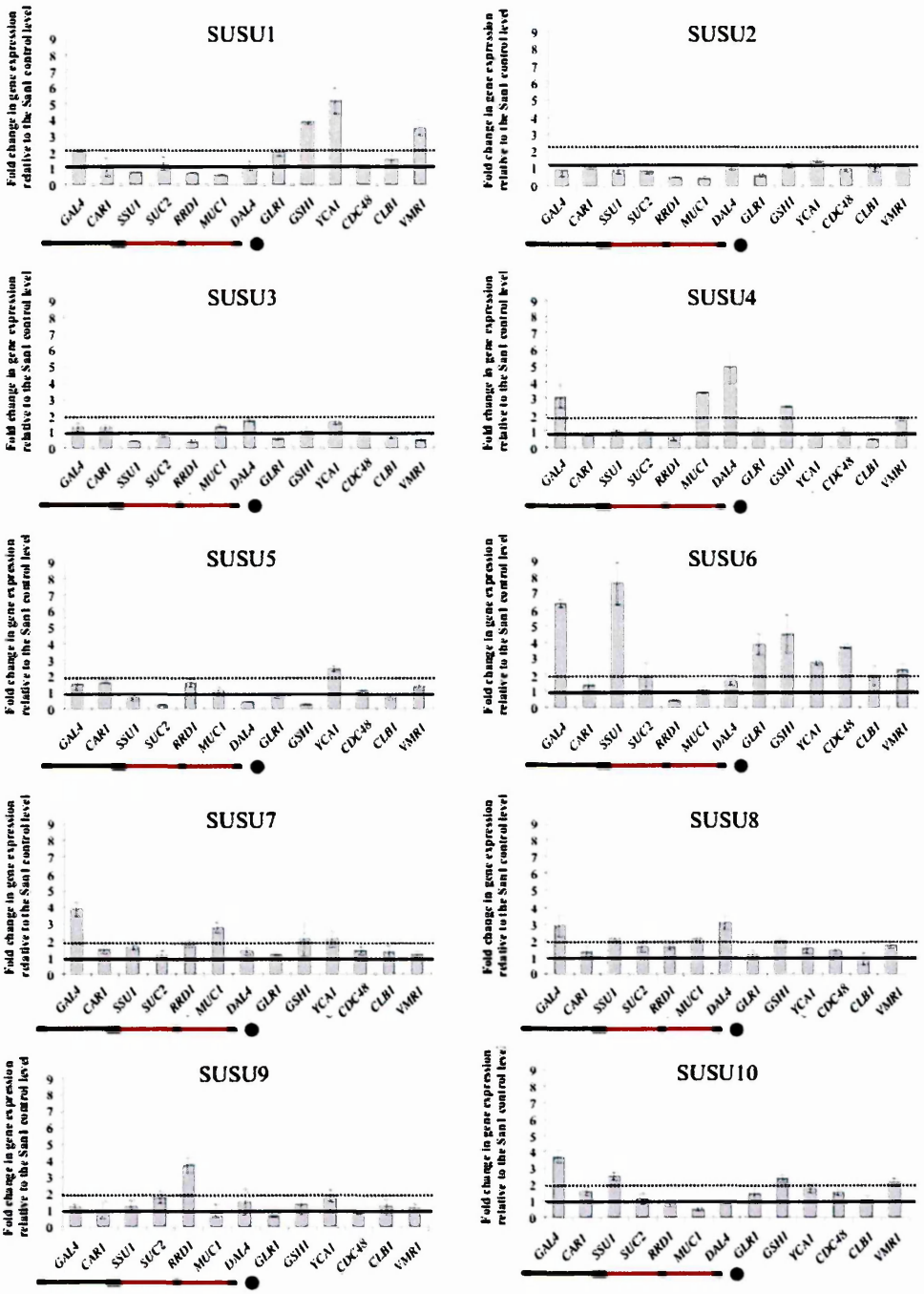

Figure 5.5 Semi-quantitative RT-PCR analysis of gene expression in the SUSU translocants. Expression level of various genes located along the translocated chromosome or those involved in various cellular processes of *S. cerevisiae*. Values reported in the graphs represent the expression level of each gene normalized with the expression level of the control gene *HSC82* and then compared with the normalized expression of the analyzed gene in the San1 control strain considered as unit (horizontal black line). Dotted black line represents a two-fold increase in gene expression relative to the expression level in parental strain. The scheme of the translocated chromosome shown below each histogram indicates the relative position of the genes along this chromosome. The green circle below *GLR1* indicates its presence on chromosome XVI but not on the translocated chromosome.

The three genes mentioned above (*GSH1, YCA1* and *VMR1)* were also highly over-expressed in SUSU6, which is characterized by a strong de-regulation of transcription of almost all the analyzed genes with the exception of *CAR1, SUC2, MUC1* and *CLB1*. Besides this, the two genes located on both sides of the translocation break point on chromosome XVI, showed a pronounced increase in their steady mRNA levels (7.6 and 3.8 fold mRNA level increasing for *SSU1* and *GLR1,* respectively). The over-expression of *GLR1*, coding the cytosolic and mitochondrial glutathione oxidoreductase, can be correlated to the increased *GSH1* transcription and could suggest oxidative stress conditions generated within SUSU6 cells. Additionally, over-expression of *YCA1* suggests that an apoptotic response might be activated in this strain. The over-expression of the cell cycle-related gene *CDC48* in this strain is an indication of the presence of cell cycle defects. Among other genes been analyzed, only *RRD1* located on chromosome IX was down-regulated in SUSU6. In the SUSU5 strain, which exhibits a petite phenotype, two of the analyzed genes - *SUC2* and *GSH1* showed a reduced level of the mRNA in comparison to the control strain San1. The transcription of *GSH1* was decreased about 1/4 fold in comparison to the San1 strain. As proposed earlier here, this could be due the absence of respiratory oxidative stress in the SUSU5 translocant strain. As in SUSU1, SUSU6 and SUSU7 the up-regulation of *YCA1* caspase might refer to apoptotic activation, but further investigation in these lines is beyond the scope of the current study.

Finally, we noticed a heterogeneous situation of gene expression in several SUSU translocants. In general, certain translocants had expression patterns in which some genes were up-regulated, in others certain genes were down regulated and still others had similar expression levels like that of the control strain. In some cases, the over-expression

of a certain gene could be correlated with the presence of an increased gene copy number as for *GAL4* in strains SUSU4, SUSU7, SUSU9 and SUSU10. The same holds true for *DAL4* and *MUC1* in strains SUSU4 and SUSU8. In other cases, an increased gene copy number did not correspond to an increased gene expression as for *GAL4* in SUSU2, SUSU3 and SUSU5 or for *CAR1* in all the translocants.

5.5 Physiological and morphological variations within SUSU strains:

Variations among SUSU translocants were clearly and evidently demonstrated by analysis of chromosomal patterns, gene copy number determination and gene expression experiments. Observations along these lines suggest that SUSU translocants carry variable aneuploidy with simple and complex genomic rearrangements. Besides differences in karyotypes and gene expression patterns, others in our group (ROSSI *et al.* 2010) have elucidated that all 10 SUSU translocants are physiologically and morphologically distinct as well. Their observations suggest differences in growth rates of SUSU translocants on various carbon sources, differences in the ability to sporulate and a variety of altered cellular phenotypes in addition to the karyokinetic defects harbored in these cells.

Overall our results and observations by others in our group suggest that a single initial BIT event can lead to the generation of diverse phenotypes and genotypes, despite its common origin. We also suggest that this diversity is not solely a consequence of the formation of a translocated chromosome, but is rather augmented by differential rearrangement of chromosomal fragments ensuing BIT events. The end result of such genomic rearrangements seen in SUSU translocants is the generation of aneuploidy that can be whole chromosome aneuploidy or confined to specific chromosomal regions. In

short, despite carrying the same bridge-induced translocation breakpoints, all SUSU translocants exhibit phenotypic and genotypic variations among them.

Discussions

6.1 Defining the time-frame of BIT events *in vivo*:

Under natural conditions in the environment, cells and organisms are exposed to challenges that can have detrimental consequences. Many times, genomes are most vulnerable to such exogenous and endogenous assaults. This can often lead to cell death via apoptosis or adaptation into specialized cells as those found in various cancers. Despite the enormity of factors that can cause genomes to become unstable, a hallmark of such instability is the detection of GCRs in affected cells. The consequences of such instability have been briefly described earlier, although the molecular causes still remain obscure to date. To understand the molecular mechanisms underlying GCR formation, it is essential to understand fundamental processes that lead to the formation of such genomic lesions. Throughout this study, we have focused on shedding new light on understanding genomic aberrations, particularly, chromosomal translocations. Using the powerful homologous recombination system of *S. cerevisiae*, we have induced molecular bridging of chromosomes resulting into non-reciprocal translocations, using a simple linear DNA construct within the BIT system. In nature, molecules like viral DNA particles, transposons, retrotransposons, linearised plasmids, free-ended chromosomal fragments might behave in an analogous manner to the BIT-inducing cassette.

The HR-dependent BIT system offers a unique tool for GCR induction in unmodified diploid yeast cells (NIKITIN *et al.* 2008; TOSATO *et al.* 2009; TOSATO *et al.* 2005). Transformant cells conferring resistance to a selectable marker is the primary selection, usually followed by PCR analysis using specific primers to confirm correct bridging of chromosomes or loci involved. In Chapter 3, we have devised a system to

monitor correct integration of a linear DNA construct inducing translocation, by fluorescence detection. Notably, we have engineered exogenous, "non-yeast" sequences into specific yeast loci, followed by targeting recombination at these foreign DNA sequences. We have exploited HR dependent reconstruction of fluorescent markers to monitor the integration of BIT inducing DNA constructs into artificially introduced exogenous DNA sequences. Following this, we successfully screened representative clones for reconstruction of either or both fluorescent markers, GFP and DsRed, on chromosomes V and III, respectively.

Firstly, the choice of genomic loci at which foreign sequences were artificially introduced, was carried out carefully. Intergenic sequences favoring higher recombination frequencies (GJURACIC *et al.* 2004) were exploited as sites of truncated flourophore integration using the STIK methodology (WAGHMARE *et al.* 2003). We learnt that integration of truncated GFP construct within the *GEA2-URA3* intergenic sequence resulted in colony sectoring. However, the same within the intergenic sequence between *RIP1* and *YEL023C* genes on chromosome V-L gave rise to a normal round colony phenotype. Our observations suggest that the choice of chromosomal loci for integrating foreign DNA sequences on yeast chromosomes is critical in designing such experiments. This was essentially necessary to eliminate interference with normal cellular homeostasis, when exogenous non-yeast sequences were introduced on either chromosomes V and III. Experimental setup prior to translocation induction was expected to yield normal cellular phenotype and was a pre-requisite before translocation induction. In this manner it would be possible to detect any cellular phenotypes that might arise after translocation induction, as have been reported in previous studies on other translocants in our group

(NIKITIN *et al.* 2008). On the other hand, the introduction of truncated DsRed construct between *LEU2* and *NFS2* intergenic region on chromosome III-L gave rise to normal round colony phenotype, and provided us a with a model strain to be used for BIT targeting experiments. Introduction of linear DNA molecules carrying sequence for HR-mediated reconstruction of functional GFP and DsRed in this setup was expected to aid real time monitoring of BIT events *in vivo*. In order to monitor DNA integration at targeted loci, a successful signal first had to go through a complete HR event, followed by expression and then protein production for fluorescent detection. Based on the separation of these events that may cloud detection of any temporal signal, a specific time frame had to be established for fluorescence detection in our experiments. In this manner it would be possible to detect DNA integration on either or both chromosomes as distinct fluorescent signals. Single-sided DNA integration on either chromosomes would result in detection of a monochrome signal, whereas, concomitant integration at both chromosomes resulting in chromosomal bridging was expected to be positive for both GFP and DsRed fluorescence.

A major drawback of this tested system that we observed was, the extremely low frequency of targeting exogenously integrated sequences on yeast chromosomes. Notably, the GC base-composition for exogenous DNA sequences targeted on chromosomes V (ΔGFP) and III (ΔDsRed) was 38% and 68%, respectively. In correlation, targeting at the more GC-rich ΔDsRed sequence was lower than that at the more AT-rich ΔGFP sequence. A near 1% of total transformants obtained after several rounds of transformations, carried positive signals for both GFP and DsRed reconstruction represented by the only translocation-carrying clone. Thus, if one were to

look at real time BIT events by fluorescence microscopy using standard instruments, it would be practically and technically difficult to specifically locate cells that potentially develop into translocation carrying cells, in order to elucidate real time dynamics of the BIT cassette. In other words, to carry out visual detection of reconstruction events from among ~10^8 cells treated per transformation reaction, would be highly improbable using standard fluorescence microscopy. To deal with large number of cells to be screened for the presence of green and/or red signals; we have attempted to sort out transformed cells by fluorescence activated cell sorting (FACS). This was carried out on the basis of previous experience by (BRUSCHI and CHUBA 1988) to sort out single adenine mutants by flow cytometry. Our initial experiments suggest that it might be necessary to employ high-throughput cell imaging based techniques (ANTCZAK *et al.* 2009; PUIGVERT *et al.* 2010; VIZEACOUMAR *et al.* 2009) to detect such infrequent events that were undetectable by FACS analysis. It could well be that BIT-DNA integration happens at a later time point during rescue in rich media or upon selection on appropriate growth media, and not immediately after heat shock, during which we have attempted to monitor such events by flow cytometry. One must also consider the maturation times and optimum levels of florescent molecules that must accumulate in cells after DNA integration following expression to allow efficient detection.

Additionally in our experiments, the detection of DsRed was problematic in clones that were PCR positive for integration and reconstruction of DsRed on chromosome III. The weak signal could be correlated to the fact that the DsRed construct in our experimental setup was the wild type version of the fluorescent protein. Despite high quantum yield and photostability, the wild type version of DsRed has been reported

to have several problems for use as a fluorescent reporter. Firstly, tetramerization of DsRed can perturb the function of the protein to which it is tagged (LAUF *et al.* 2001). However, in our experiments this was not the case. Rather, we were confronted by the slow maturation of the DsRed chromophore, which has a half-life of more than 24 hours at room temperature (BAIRD *et al.* 2000). Additionally, newly formed DsRed emits dim green fluorescent and can interfere when used in combination with GFP. Furthermore, in rapidly growing cells like *S. cerevisiae*, the slow development of red fluorescence limits the intensity of DsRed that can be detected. Recently, variants of DsRed have been described that mature much faster and yield brighter fluorescence (BEVIS and GLICK 2002). Such variants can be readily used in combination with GFP for dual detection in rapidly growing cells like yeast. We suggest that the detection of DsRed reconstruction in the constructed "Red-Green BIT system" can be further resolved by introducing brighter and fast maturing variants of the same.

Based on the inherent technical difficulties in real-time and rapid fluorescence detection as discussed above, we attempted to monitor real time integration events using a PCR approach. This simple method employing locus specific primers for PCR (see **Figure 3.8a**) would allow us to screen integration of the BIT construct on either or both chromosomes V and III, for GFP or DsRed reconstruction, respectively. Here, we came across other challenges using the PCR approach, when we discovered the presence of PCR signals in samples containing yeast cells incubated with transforming RG-BIT DNA (**Figure 3.9**). After careful consideration and further experimentation, we clarified that such signals could be reproduced *in vitro* using a mixture of PAW1 genomic DNA and RG-BIT DNA as template for PCR reactions (**Figure 3.10 a & b**). This meant that a

considerable amount of RG-BIT DNA was being precipitated along with genomic DNA from samples. This was contaminating the PCR reaction and triggering a putative homology based transient template for primer annealing and extension during PCR cycling. To avoid such interaction and to support our observations, DNAse treatment of samples prior to genomic extraction eradicated the generation of PCR artifact signals. Following this, and to clearly distinguish between genuine *in vivo* targeting signals from those that could arise as PCR artifacts *in vitro*, we utilized a restriction digestion / southern blotting based approach. To this end, genomic DNA from samples was restricted using unique cutters to give rise to fragments of discrete sizes. Such a restriction fragment length polymorphism (RFLP) based approach generated fragments representing either "no integration" or "integration" at the respective loci, which were then easily detected by probing with appropriate sequences. Using such a strategy, we have shown that until the heat shock stage of the transformation process, there is no real integration of RG-BIT into targeted loci (**Figure 3.11**), as previously seen using the PCR approach (**Figure 3.9**). Based on this we speculate again that the integration of the BIT cassette occurs at a later time point, probably during replication when heat shock recovered cells undergo the early rounds of cell division.

Using a PCR-based approach to analyze transformants, our results indicate that BIT events occur by independent strand invasion events on separate chromosomes. This is in accordance with a higher incidence of single-sided events detected on single chromosomes in contrast to those involving both targeted chromosomes. Simultaneous HR at both ends of the targeting construct seems to be discouraged correlating with infrequency of BIT events. This could occur due to spatial-temporal constraints

governing relative positions of targeted loci, chromatin context or even real time microenvironment of accessible HR factors within the nucleus at any given stage of the cell cycle. Moreover, our results suggest that BIT construct assimilation at targeted loci is initiated with a single-end capture, as evident from reconstruction of single flourophores, which happens more often than simultaneous capture at both ends to reconstruct both flourophores.

We propose that in a similar manner, exogenous DNA sequences like the ones used here could be integrated at various genomic loci to study genome wide recombination rates for BIT inducing constructs. Additionally, more than one copy of the same sequence could be introduced on multiple chromosomes to elucidate chromosome and locus specific competition of these loci as donors for BIT construct recombination. Similar work using repeat sequence elements has recently been performed by (AGMON *et al.* 2009). However, the authors have used native yeast sequences for investigation. The herein constructed and described system of flourophore reconstitution by BIT, which requires recombination between exogenously introduced non-yeast sequences, can serve as a visual tool in analysis of targeted recombination. Another possibility would be to construct a strain carrying different truncated flourophores on various chromosomes or chromosomal loci. A series of targeting constructs carrying combinations of flanking homology for reconstruction of flourophores can then be utilized to screen by fluorescence, yeast cells that carry single or multiple translocations. We must affirm here, that such a system will only allow rapid selection of desired events, but any further analysis of mechanisms leading to such events will have to be elucidated independently.

Thus it could serve as a quick fluorescence based screening alternative as opposed to standard PCR screening.

Although the developed system provides a means to screen DNA integration and BIT events by fluorescence detection, further modulation is necessary to investigate the real time dynamics of linear DNA integration into targeted loci in yeast chromosomal loci. It would be very interesting to develop such a system with increased sensitivity to detect rapidly maturing chromophores from large sample sizes, within which similar events happen infrequently.

In general, we have demonstrated that the herein described genetic system is experimentally feasible not just for independent reconstruction but also for the simultaneous reconstruction of fluorescent markers and their subsequent detection. This is of utmost importance in rapid and visual screening of transformants obtained, which might carry one-sided integration of BIT constructs, or alternatively carry translocations in cells positive for the detection of dual signals. This strategy is useful for studying events where recombination at specific loci in question is to be investigated, screening out all ectopic non-targeted recombination events. Moreover, despite the low frequency of BIT events targeting fluorescent marker reconstruction, we have for the first time screened translocation events by fluorescence detection in *S. cerevisiae*. This system requires pre-engineering of the yeast strain with truncated versions of a wide range of flourophores available these days. We propose that by making a more stringently compatible choice of flourophores available today, simultaneous detection of dual or multiple flourophores can considerably aid in quick screening of specific chromosomal rearrangements to be studied.

6.2 Genetic Regulation of BIT events accompanying chromosome deletions:

Bearing in mind the inherent drawback feature of a low frequency of BIT induction in yeast, we wondered whether the frequency of inducing recombination at both ends could be successfully elevated by targeting highly recombinagenic genomic loci. Furthermore, we have also aimed at providing insights into the molecular regulation of BIT events using mutant yeast strains carrying deletions of various genes implicated in the maintenance of genome stability. In Chapter 4, while we attempted to elucidate this further, we came across other interesting findings, some of which have been described earlier and form the subject of this discussion.

6.2.1 Influence of sequence context and integration bias:

Since the introduction of the BIT system (TOSATO *et al.* 2005), genomic loci like promoter regions of *ADH1* and *ALD5* in combination with 3′ or 5′ termini of *DUR3* have been targeted by others in our laboratory. Intergenic regions as opposed to open reading frame (ORF) sequences have been employed for targeted recombination, based on the higher targeting capacity of the former as reported by others (GJURACIC *et al.* 2004). Interestingly, the frequency of recombinational targeting at these loci varies for the same locus, when present in different combinations. For example, upon targeting *ADH1* and *DUR3* loci, the former exhibited higher tendency to be targeted, with 41% of events being targeted, in comparison to 24% on *DUR3*. Similarly, in a combination of *ALD5* and *DUR3* loci, targeting frequencies were 15% and 46 % for either locus, respectively. The authors report that in contrast to the *ADH1* promoter sequence, the *ALD5* promoter behaved as a cold-spot for recombination, despite having similar base composition. This has been correlated with possible skew arising from sequence context, which can

modulate accessibility for recombination at various loci. Additionally, increasing the targeting homology from 40 nucleotides (nt) to 64-67 nt remarkably increased the rate of chromosomal translocation induction from 1.6% to 4.8%. This was also accompanied by a reduction in the frequency of ectopic DNA integration elsewhere in the genome from 87% with 40 nt to 25% with 64-67 nt homology. Recently, collaborative work performed with others in our group, partly described in Chapter 5, targeted promoter regions of *SSU1* and *SUC2* genes on chromosomes XVI and XV, respectively. In this case, the targeting frequencies at the respective loci have been noticed to be 1.6% and 67% of the total events measured. A high AT base content of 75% and 52% at *SSU1* and *SUC2* targeted sites, respectively, once again highlights the modulation of recombination by the sequence context rather than base composition *per se*. The rate of chromosomal bridging between these loci was noticed in 8.6 % of the total transformants analysed.

Based on this, we have utilized the more-recombinagenic *ADH1* and *SUC2* promoter sequences to be targeted for BIT induction between chromosomes XV and IX, respectively. Homologous sequences of 63 nt and 65 nt were utilized to target the respective promoter loci. Data derived from experiments in two different genetic backgrounds show that the overall rate of chromosomal bridging between these two loci was 7.4%. Interestingly, we noticed that despite behaving as a hotspot in previous work, the *ADH1* promoter sequence in combination with that of *SUC2* representing flanking homologous sequences of the BIT construct, showed a targeting frequency of 9.6% in comparison to 48% noticed for the latter. In other words, DNA integration at *SUC2* was much more pronounced than that at *ADH1* in our experiments. This suggests that site-directed BIT events are intrinsically skewed for preferential integration at one of the two

targeted loci, despite them behaving otherwise in combination with another locus. Thus, even if the *ADH1* locus behaved as a recombination hotspot in combination with *DUR3*, it showed remarkable decrease in targeting when used in combination with *SUC2* on the same BIT construct. Such "integration bias" for preferential integration towards the *SUC2* locus in contrast to the *ADH1* promoter locus seems surprising, as it is known that the *SUC2* promoter is repressed in the presence of glucose (LUTFIYYA and JOHNSTON 1996), as it was in our experimental setup. On the other hand, the constitutive *ADH1* promoter with an open sequence context seems to be disfavored for strand invasion and HR mediated integration of the BIT construct. This is consistent with observations by the Jinks-Robertson group showing that during TAR, DNA-invasion on a transcribed DNA strand may be reduced by transcription (DATTA and JINKS-ROBERTSON 1995; SAXE *et al.* 2000), which also renders the non-transcribed strand more vulnerable to mutations and recombination. Targeting at *SUC2* has been discussed in further detail in section 6.3 of the discussions in a slightly different context.

6.2.2 Regulation of BIT events by S-phase specific functions:

Our observations point out that despite choosing more recombinagenic sequences for targeting, the rate of BIT induction was only slightly increased in comparison to data obtained by others in our group, targeting other genomic loci. The recombinational tendency of genomic loci was noticed to vary among experiments in which they occurred on the BIT construct in different combinations. Thus, although locus specific effects might account for targeting differences based on physical constraints within the cell nucleus, we hypothesized a multiple pathway regulation of BIT events *in vivo* accounting for their infrequency. Thus we analysed the rate of translocation induction between

ADH1 and *SUC2* promoter loci in various mutant backgrounds in order to shed light on molecular regulation of BIT events.

Firstly, in wild type cells, we noticed that integration at the *SUC2* promoter locus was about 5 fold more than that at the *ADH1* locus (**Figure 4.3**). We have considered this bias as unit to make comparisons of the same in mutant strains (**Figure 4.4**). An increase in integration bias, which correlates to decrease in preferential integration at *SUC2*, was measured as a concomitant rise in the number of events targeted at the *ADH1* locus. Interestingly, we noticed pronounced variation of integration bias in certain mutants suggesting clear roles of those genetic factors in regulating DNA recombination of linear molecules targeting separate chromosomal loci. At least for some mutants such as *ku70*, *nre11*, *tel1* and *sgs1*, all of which are involved directly, or in mediating protein recruitment at DNA ends, such variations might arise perhaps due to the modulation of DNA resection, affecting strand invasion abilities and consequently BIR events, which presumably pay a role in generation of such events, as also discussed in section 6.3.

For instance, a four-fold increase of integration bias in *sgs1* deficient cells suggests that integration at *SUC2* probably requires Sgs1 to unwind DNA at this particular locus to facilitate HR. Sgs1 is known to perform multiple functions in cells, all of which in some way contribute to the maintenance of genome stability. In yeast cells, Sgs1 functions as a central component of the S-phase (FREI and GASSER 2000) and intra-S (MANKOURI *et al.* 2009) checkpoint responses to allow cell cycle arrest upon DNA damage or blocked fork progression during replication. We speculate that in the absence of Sgs1, such an arrest is abolished in response to recombination intermediates and structures formed at replication forks during BIT construct integration, thereby favoring

higher incidence of recombination at the *SUC2* locus. On the other hand, lack of Sgs1 only elevates the probability of the BIT construct to integrate more often at the less favored *ADH1* site. This seems unlikely, as HR at the constitutive *ADH1* promoter locus probably does not require unwinding of this already open configuration locus. Consistent with this, its difficult to imagine how a hyper-recombinagenic *sgs1* mutant (WATT *et al.* 1996) can account for reduced recombination at *SUC2* in contrast to increased recombination at *ADH1*. These apparent differences in recombination rates at targeted loci in *sgs1* cells might be related to an alternative function rather than just its helicase activity.

A similar scenario holds true for our observations in strains deficient for *mre11* or *esc2*, in which integration bias was elevated by 2.3-fold and three-fold, respectively (**Figure 4.4**). The lack of Mre11 or Esc2 in *S. cerevisiae* has been associated with increased mitotic recombination and both genes, or at least the complexes in which they function, are also implicated in mediating the intra-S phase checkpoint response to DNA damage (D'AMOURS and JACKSON 2001; MANKOURI *et al.* 2009). The lack of Mre11 however, is exclusively known to result in decreased recombination of IR-induced sister-chromatid and inter-homologue recombination, which is independent of its nuclease function in DNA-DSB repair (BRESSAN *et al.* 1999). A reduction in recombination at *SUC2* might be correlated to such a function, however it doesn't hold the same at the *ADH1* site. Esc2, on the other hand, apart from its role in gene silencing via its interaction with Sir proteins, functions in a distinct branch of HRR to mediate intra-S checkpoint response, independently of Sgs1 (MANKOURI *et al.* 2009). To ascertain an S-phase specific role in regulation of BIT events, translocation induction in strains that carry

impairment of more than one GCR suppression branch/pathway functioning during S-phase must be performed to further elucidate synergistic interactions between independently acting GCR control mechanisms. For example, BIT induction in strains carrying combinations of *sgs1*, *mre11*, *mrc1* and *esc2* mutations or deletions would be essential in establishing the possibly overlapping roles of S-phase pathways for GCR suppression in which they function. A similar approach using dual and multiple deletion mutants elucidates redundant S-phase GCR suppression pathways in methyl methane sulfonate (MMS) challenged *S. cerevisiae* cells (MYUNG and KOLODNER 2002). Similarly, BIT induction in hydroxyurea arrested S-phase mutants of the above highlighted genes could further validate their S-phase specific functions in regulating chromosomal bridging by BIT. To this end, *SGS1* separation-of-function mutants that are proficient for recombinational repair but defective in the repair of DNA replication intermediates (BERNSTEIN *et al.* 2009) can be exploited to pin point its S-phase specific role in the regulating BIT events.

The rate of translocation induction resulting in chromosome bridging between *ADH1* and *SUC2* was more pronounced only in cells lacking *sgs1*, *mrc1* or both *sgs1* and *tel1*. Thus, even though *mre11 and esc2* cells showed altered bias during integration of BIT-DNA, they had a subtle effect on the overall rate of chromosomal bridging. In fact, *esc2* cells exhibited an even lower frequency of translocation induction in comparison to that in wild type cells. Despite its role in suppressing HR mediated GCRs via chromatin modifying pathways, *ESC2* does not seem to control HR mediated chromosomal bridging, although we noticed its effect on integration bias. This suggests that during BIT events, the checkpoint function of Esc2 in S-phase might modulate recombination at

either locus, but is not involved in the actual bridging of the two chromosomes. On the other hand, only a slight increase in translocation incidence in *mre11* cells was surprising despite its role in GCR suppression (SMITH *et al.* 2005) via multiple pathways.

Mutants deficient for both *SGS1* and *TEL1* exhibited similar levels of chromosome translocations to those in the *sgs1* deletion mutant, suggesting that they belong to the same pathway of suppressing chromosome translocations of the BIT nature. Furthermore, Sgs1 in concert with Tel1 is known to suppress translocations between highly diverged genes in *S. cerevisiae* (SCHMIDT *et al.* 2006), and cells lacking Sgs1 are also known to display elevated rates of interchromosomal HR between homologous sequences and heteroalleles (WATT *et al.* 1996; YAMAGATA *et al.* 1998). Our observations of an increased incidence of BIT events in a *sgs1* single mutant and in *sgs1 tel1* double mutant cells are in agreement with this, and we suggest that HR-mediated BIT events might be regulated by redundant pathways, in one of which Sgs1 and Tel1 function together. In support of our observations of elevated chromosomal bridging in *sgs1*Δ cells, others also report increased incidence of translocations and chromosome losses leading to LOH in *sgs1* deficient *S. cerevisiae* cells (AJIMA *et al.* 2002).

Deletion of *MRC1*, which has roles a replication stress checkpoint signaling and DNA replication, resulted in elevated rate of translocation, similar to that observed in *sgs1* cells. This once again points out to S-phase specific redundant checkpoint functions that seem to regulate chromosomal bridging via BIT in *S. cerevisiae* cells. It would be interesting to see if there is any synergistic effect of *MRC1* and *SGS1* on the overall rate of BIT induction.

Based on the common role of Sgs1, Mre11, Mrc1 and Esc2 in S-phase, we speculate that in replicating mutant cells challenged with recombinagenic BIT construct, targeting differences might be a combinatorial effect of non-simultaneous replication of targeted loci, in addition to lack of arrest in response to any HR intermediates that may arise at the loci in question. During chromosomal replication, these functions might influence the processing of HR intermediates and might also be involved in preventing recombinational repair in BIT challenged cells. We hypothesize that BIT constructs are assimilated at targeted loci, most probably when an open DNA context exists during replication. The observation of a significant increase in the frequency of BIT noticed in hydroxyurea-arrested S-phase yeast cells by others in our group, is in support of such speculation. The probability of integration at any given locus would thus be modulated by S-phase specific functions of genome maintenance factors that act at the chromosomal region under investigation. Further insights could be gained using strains in which replication or even transcription can be induced to favor an open DNA context at specific loci, which would also be substrates for BIT construct recombination. We speculate that BIT targeting autonomously replicating sequences (ARS) located on separate chromosomes might dramatically influence targeting frequencies and provide further insights into the replication connection of chromosomal bridging in yeast.

In general, in this study we have attempted to shed light on the role of a chosen set of genes on the regulation of BIT events. Despite the diversity of their functions and in the manner of suppressing GCRs, our results suggest that processes, which function during S-phase of the cell cycle, specifically suppress BIT events. Although, we must also consider that there could be other processes, beyond our choice of analysed

functions, which might directly or indirectly mediate their effects in governing control of chromosomal bridging in yeast.

6.2.3 Partial chromosome IX deletions in certain XV-IX translocants:

Our studies on the chromosomal analysis of translocants obtained in wild type and mutant backgrounds yielded some interesting observations. Firstly, the lack of genome wide hybridization with a *SDL1* specific probe suggests that the telomeric fragment (chromosome IX-L) carrying the *SDL1* sequence is putatively degraded by nucleases and eventually lost without undergoing any further rearrangements to be rescued/captured by another chromosome. Secondary rearrangements noticed in SAD16 and K60 (**Figures 4.7** and **4.8**) resulting in acquisition of altered forms of different chromosomes indicate the involvement of a BIR-like process in the generation of such aberrations. This mechanism has previously been proposed to be responsible for the generation of other translocants obtained with the BIT system between chromosomes V and VIII, XV and VIII (TOSATO *et al.* 2005) and between chromosomes XVI and IX (ROSSI *et al.* 2010).

The most striking observation was the loss of native chromosome IX detection in certain translocants. This was confirmed upon probing chromosomal sequences located on both arms of chromosome IX. Interestingly, although we noticed this loss in wild type derived translocants (**Figure 4.7**), it was more frequently observed in translocants obtained in *esc2*, *sgs1* and *ku70* mutant backgrounds (**Figure 4.8**), highlighting the role of these genes in maintaining genome stability. To investigate whether such loss of detection represented complete loss of chromosome IX or its rearrangement elsewhere, we used probe based QPCR to quantify gene dosage on various loci on chromosomes IX and XV, involved in the translocation. This was necessary to determine the ploidy of each

representative chromosome region. In case these observations represented entire chromosome IX loss events, we hypothesized that the short telomeric fragment ensuing the BIT process putatively undergoes recombination with its homologous sequence available on the native chromosome. This might possibly destabilize telomere IX-L, eventually leading to the loss of the entire chromosome. A single telomere lost in such a manner may eventually lead to the loss of the entire chromosome as described by others (SANDELL and ZAKIAN 1993). Contrary to this, QPCR data on gene dosage, points to the loss of only a terminal 36 Kbp fragment carrying the *SDL1* sequence. This together with the above observations suggests that in certain cases following chromosomal bridging, native chromosome IX possibly acquires the configuration of the aberrant translocated chromosome, and in the process looses the terminal 36 Kbp, which encodes no known essential functions. This interpretation is based on the fact that at least two copies of *KANMX4* and *MUC1* representing the aberrant chromosome and chromosome IX-R, respectively, whereas three copies of *CDC33* that lies on chromosome XV-L were detected in wild type derived translocants, SAD1 and SAD33, which were QPCR-negative for *SDL1* (**Figure 4.9**). On the other hand, a more complex chromosomal pattern was detected in *ku70* mutant translocants K54 and K60, in addition to *sgs1* mutant translocants S125 and S192, all of which were negative for *SDL1* detection by QPCR and also by hybridization. Based on this puzzling QPCR data, we suggest that complex rearrangements are triggered by BIT leading to the generation of varied aneuploidy, probably involving diverse DNA repair and damage adaptation mechanisms, in translocant cells. This aspect has been discussed in further detail in another chromosomal context in the following part of this chapter.

Moreover, unlike telomere loss associated genome wide instability noticed in human cancer cell lines (SABATIER *et al.* 2005), the secondary rearrangements detected in certain translocants in which the *SDL1* carrying telomeric fragment was lost, seem to be stably maintained in the translocants harboring them. However, among clones arising from one such *sgs1* mutant translocant S192 (**Figure 4.11**), varying and probably interchanging patterns/forms of the aberrant translocated chromosome suggest that not all rearrangements seem to be stable. An ongoing process of change in karyotype seen as heterogeneous karyotypes is a direct reflection of increased mutability displayed as a chromosome instability phenotype in S192 cells. Further investigation in these lines should allow us to know the time scale during which such forms might or not eventually attain stability in translocant cells. We presume the slow growth phenotype of *sgs1* mutant cells, might serve as good model in allowing us to investigate these events in "slow-motion" and to elucidate the function of Sgs1 in modulating BIT events.

It would be very interesting to clarify further, the nature of the detected aneuploidies in a more genome wide context by methods such as comparative genome hybridization (CGH) or even deep sequencing. In brief, this initial study on SAD translocants opens very interesting questions that can be pursued in future and marks the first such study in which the role of important genome maintenance factors has been assessed in terms of the genomic analysis of BIT carrying yeast strains. Our results point to S-phase specific functions of Sgs1, Mre11, Mrc1 and Esc2 in possible and redundant regulation of DNA recombination and chromosomal bridging during BIT events. The heterogeneity in chromosomal patterns and partial deletions of chromosome termini noticed in certain mutants must be further elucidated to ascribe clear roles to functions in

which they were described. From a mechanistic point of view, it would be necessary to provide biochemical evidence of the true function of some of the genes seen to modulate BIT events in *S. cerevisiae* cells.

6.3 Multiple aneuploidies can arise from the same BIT event in yeast cells:

Translocation events are not just gross chromosomal rearrangements that can be associated with cancer development in mammalian cells and acquisition of deleterious phenotypes in eukaryotic microorganisms, but are also a powerful evolutionary force capable of strongly reshaping the genome. For example, translocation events have been associated with the acquisition of advantageous antifungal drug resistance in the yeast *Candida glabrata* (POLAKOVA *et al.* 2009). Another view suggests that chromosomal rearrangements are not necessarily required for speciation in yeast, although reciprocal translocations might be responsible for mis-segregation during meiosis and act as a post mating isolating mechanism (FISCHER *et al.* 2000). Despite their importance for the maintenance and evolution of genome organization, little is still known about the molecular mechanisms and pathways involved in the formation and regulation of a translocation event.

In Chapter 5 we have described the molecular characterization of a series of SUSU translocants generated between *SSU1* and *SUC2* promoter loci located on chromosomes XVI and IX respectively. Chromosomal analyses and gene copy number determination revealed that the integration of the SUSU linear DNA cassette can not only induce the formation of a non reciprocal translocation, but also other complex rearrangements generating different types of aneuploidy in all the mutant strains analyzed. This complex abnormal karyotype bearing monosomy, disomy and trisomy for different segments of the translocation participants, strongly reminds what is described in leukemia patients carrying unbalanced translocations (PEDERSEN *et al.* 2000).

Even though *Saccharomyces cerevisiae* well tolerates aneuploidy, it is common knowledge that aneuploidy has severe effects on growth and development, as reported in

the baker's yeast (TORRES *et al.* 2007). Maintenance of euploidy is essential for survival of a species, and correlations between cancer and aneuploidy have been reported since 1890 by Hansemann and in 1902 by Boveri (BIGNOLD *et al.* 2006). Recently, aneuploidy was proposed to be the major pre-neoplastic condition leading to chromosome instability and promoting transformation of the normal cells (DUESBERG *et al.* 2005). Variations in chromosome numbers and aneuploidy formation are often strongly inhibited by checkpoint mechanisms. Such control in SUSU mutant strains and in other analyzed translocants seem to be bypassed, thereby favoring formation of GCRs involving different mechanisms.

BIR has been implicated as a possible mechanism for recombination associated generation of aneuploidy (JAIN *et al.* 2009; MORROW *et al.* 1997). This process can well explain the partial trisomy of chromosome XVI detected in SUSU3, SUSU4 and SUSU8 strains. According to the two-step integration model of the BIT construct proposed for other translocants previously described (TOSATO *et al.* 2005), we speculate that in these mutants, the BIT construct initially integrates at the *SUC2* locus via HR, and then in a second step, completes the integration at the *SSU1* locus by strand invasion and synthesis towards the telomere. This model is also supported by the fact that the integration of the BIT cassette might mimic the condition in which a single homologous end of the DSB is present, a condition that strongly favors DSB repair via BIR (JAIN *et al.* 2009; MALKOVA *et al.* 2005; VANHULLE *et al.* 2007). However, it is difficult to explain the partial trisomy of chromosome IX observed in SUSU3 strain by a BIR-like event, as it is known that the BIR replication apparatus is blocked at the centromere (MORROW *et al.* 1997). A possible explanation leading to a complete and functional chromosome might involve an alternative replication apparatus capable of passing through the centromeric region during

the integration of the BIT construct. A striking observation of about a 10-fold increase in the occurrence of a translocation event, upon transforming S-phase blocked yeast cells with the BIT construct has recently been noticed in our laboratory (TOSATO, personal communication). Indeed, recent research reveals that a non-reciprocal translocation, leading to duplication of chromosomal regions, can also arise from unconventional Pol32-independent BIR-like mechanism (PUTNAM *et al.* 2009) This suggests that formation of complex rearrangements might occur by different mechanisms capable of repair by DNA synthesis. Furthermore, in support of this view, recent observations in our group show that deletion of *POL32* does not affect the rate of translocation induction (TOSATO *et al.*, unpublished data). However, this hypothesis does not provide an exhaustive explanation of all the rearrangements noticed in SUSU cells. In particular, an explanation of the multiplication of chromosome IX in SUSU4 and SUSU8 strains, or its triploidy in SUSU5, SUSU6 and SUSU10 strains cannot be based on such speculation. Another explanation for these phenomena could be that, in adapted cells, able to bypass cell cycle arrest, the recombination of the BIT cassette interferes with chromosome segregation during mitosis giving rise to the aneuploidy noticed for both chromosomes XVI and IX. Missegregation due to inter-chromosomal association as described (KAYE *et al.* 2004) was also proposed to be linked to the generation of disomy following the integration of a DNA construct with short heterologous termini in *S. cerevisiae* (SVETEC *et al.* 2007). A defect in chromosome segregation, possibly due to the size differences between chromosome IX and the aberrant chromosome, might account for the duplication or triplication of chromosome IX observed in the SUSU4 and SUSU8 strains. Indeed, the cells, perhaps unable to identify the remaining portion of chromosome IX, could behave as monosomic for that chromosome, restoring a euploid situation by endo-re-duplication,

with a mechanism similar to that already described (WAGHMARE and BRUSCHI 2005). Defects in chromosome IX segregation that lead to the loss of the native chromosome IX copy followed by the duplication of the translocant chromosome can also explain the karyotype of SUSU1, although a double translocation event leading to such a karyotype cannot be ruled out. It is noteworthy that in SUSU1 there is a loss of genetic material. In fact, it lacks all the genes contained on the 36 Kbp fragment located on the sub-telomeric region upstream the *SUC2* locus. All genes located on this fragment are non-essential. This is a similar situation to that discussed in Chapter 4 (Part 2) earlier.

Complex rearrangements involving chromosome XVI have been described in SUSU2, SUSU7 and SUSU9 (**Figure 5.2**). For further reference, *Appendix 2* at the end of this report contains a schematic representation of the rearrangements extrapolated from gene copy number and CHEF/Southern hybridization analyses of SUSU translocants. In particular, the SUSU9 strain does not posses the expected translocant chromosome but a different aberrant chromosome in which only a small part of chromosome IX was rearranged together with chromosome XVI. The configuration of this chromosome strongly suggests that a template switching-like mechanism, similar to the FoSTeS described in mammalian cells (LEE *et al.* 2007), might account for this rearrangement. We hypothesize that in this mutant the cassette first integrates at the *SSU1* locus via HR and then completes the integration at the *SUC2* locus by strand invasion and synthesis or by BIR. After this starting event, we suppose a stalling of the replication fork before the centromere of chromosome IX is followed by template dissociation and re-invasion of chromosome XVI and new DNA synthesis to the end of chromosome XVI.

Overall, our data also indicates that the integration of the linear DNA fragment into the yeast genome can be a great force for evolution. In fact, in our experiments, the integration of the same cassette at the two target loci was processed in eight different ways generating strains different in karyotype and consequently in phenotype and physiology. Such variation in morphology, phenotype and in the expression level of various genes among the different translocants were not observed in strains carrying Kan^R integration on individual chromosomes at level of the translocation break point. This observation suggests that the mere integration of *KANMX4* by itself does not destabilize and deregulate gene expression or other physiological aspects (not shown) such as sporulation, flocculation or growth rate.

Some of the mutant phenotypes described in this work, such as the presence of slow growth rate, morphological aberrations and defects in nuclear segregation, are similar to those recently illustrated for the D10*big* and *small* mutants carrying a translocation between chromosomes VIII and XV (NIKITIN *et al.* 2008). However, the over-expression of the genes located at the translocation breakpoints typical of the D10 mutant is not observed in most of the SUSU translocants. This suggests that the effect of a translocation on gene expression might be locus-specific, depending on the genomic loci and chromosomes involved in BIT. Moreover, the presence of aneuploidy in SUSU translocants, previously undetected in D10*big* and *small* mutants, might also influence global gene expression. Torres and colleagues (TORRES *et al.* 2007) recently demonstrated that aneuploidy causes a transcriptional response with the doubling of gene expression along the entire length of a disomic chromosome. However, upregulation of genes present in a higher copy number were observed in only certain SUSU mutants

(**Figure 5.5**). Perhaps in these mutants, a combinatorial effect of chromosomal translocation and aneuploidy is established at later time point after the initial BIT event.

Interestingly, some of the SUSU translocants exhibited an over expression of the *YCA1* caspase, suggesting the activation of apoptotic pathways. In addition to *GSH1* and *GLR1* involved in oxidative stress response, the multi-drug resistance gene *VMR1*, homologous to the ABCC-type multi-drug transport proteins, was also over-expressed in some of the translocant strains. Upregulation of *VMR1* has also been reported in other BIT translocants between both heterologous and homologous chromosomes (TOSATO *et al.* 2009); (NIKITIN personal communication). The common over-expression of *VMR1* in SUSU translocants and its human homologue Mrp4p in some aggressive primary neuroblastoma characterized by unbalanced chromosomal translocations, has been previously reported (JANOUEIX-LEROSEY *et al.* 2005; NORRIS *et al.* 2005). This suggests that *VMR1* over-expression might be considered as a general effect of such aberrations. In this view, the detection of generally shared mutant phenotypes among translocants will have to be analyzed to clarify their dependency or not from the specific breakpoints. We think that the BIT system provides a valuable tool for obtaining a statistically significant numbers of different translocation mutants, without prior genomic engineering of cells. Results presented in this work also suggest that BIT could be considered as an experimentally reliable system to mimic the spontaneous mitotic translocation of higher eukaryotic cells. In fact, as observed by others in mammalian cells, our findings strongly support that aneuploidy arising from an initial translocation event may generate a heterogeneous population of mutant cells, that are phenotypically and genotypically diverse.

Future Perspectives

In this work, the BIT system has been exploited to provide insights into various aspects of DNA integration based generation of chromosomal rearrangements and the associated aneuploidies. Work done on mutants indicates possible regulatory pathways that keep inter chromosomal bridging to a minimum in wild type yeast cells, and those that might be involved in the generation of BIT associated aneuploidy.

Firstly, the Red-Green BIT system developed for defining the timing of linear DNA integration into targeted loci on yeast chromosomes indicates that DNA integration ensuing BIT occurs in a two step manner, and, might occur during the initial rounds of replication after heat shocked cells undergo stress recovery. However, to pinpoint the exact timing and to enable visualization of BIT events *in vivo*, further work is required to resolve limitations posed by detection of slow maturing flourophores. Thus, as discussed earlier, the introduction of rapidly maturing variants of flourophores in a compatible choice, and employing high-throughput methods to allow detection of infrequent signals from large cell samples is essential to proficiently implement these experimental approaches.

Secondly, BIT experiments carried out in mutant backgrounds have elucidated genetic data on putative and redundant pathways that might regulate the incidence of such chromosomal bridging events. Our initial work, done in a few selected mutants, points to an S-phase role in the control of BIT induced chromosomal bridging. However, future work must involve high-throughput genome wide screening to test potential disparate candidate functions, which might directly or indirectly play roles in regulating BIT

events. This would not only help unravel control mechanisms just for BIT events, but also those that are involved in the rearrangement of the ensuing fragments and generation of secondary rearrangements. Aneuploidy analysis employing methods like array CGH and deep sequencing to precisely measure BIT associated genome wide aberrations in translocant cells, will greatly aid in pinpointing putative aberration-prone genomic locations, as well as the implicated mechanisms leading to genome instability. Following this, it will also be important to elucidate novel and known implicated mechanisms, from a biochemical perspective, to ascribe roles at the molecular level. Based on our observations of increased BIT rates in S-phase cells and in mutants in which certain S-phase functions were inactivated, it will be interesting to elucidate the molecular intricacies for such a preponderance of BIT events in the replicative phase of the cell cycle. Additional experiments must be performed to understand the causes of unstable forms of aneuploidy observed in certain translocant backgrounds as discussed earlier. In this context, the *sgs1* deficient S192 translocant cell line can be used as a model to investigate ongoing instability after BIT induction in *S. cerevisiae.*

Lastly, future work must also be focused upon ways in which BIT can be modeled in higher eukaryotic cells and model organisms, despite inefficient HR in such cells. The great value of the BIT system in providing the user a choice of genomic loci for chromosomal bridging opens many fields to explore, and to provide fundamental and interesting insights of chromosomal translocations in yeast, which can then be modified and extrapolated to mammalian models to understand in further detail the connection between GCRs, aneuploidy and cancer.

References

ABRAHAM, R. T., 2001 Cell cycle checkpoint signaling through the ATM and ATR kinases. Genes Dev **15:** 2177-2196.

AGMON, N., S. PUR, B. LIEFSHITZ and M. KUPIEC, 2009 Analysis of repair mechanism choice during homologous recombination. Nucleic Acids Res **37:** 5081-5092.

AGUILERA, A., 2002 The connection between transcription and genomic instability. EMBO J **21:** 195-201.

AGUILERA, A., and B. GOMEZ-GONZALEZ, 2008 Genome instability: a mechanistic view of its causes and consequences. Nat Rev Genet **9:** 204-217.

AJIMA, J., K. UMEZU and H. MAKI, 2002 Elevated incidence of loss of heterozygosity (LOH) in an sgs1 mutant of Saccharomyces cerevisiae: roles of yeast RecQ helicase in suppression of aneuploidy, interchromosomal rearrangement, and the simultaneous incidence of both events during mitotic growth. Mutat Res **504:** 157-172.

ALCASABAS, A. A., A. J. OSBORN, J. BACHANT, F. HU, P. J. WERLER *et al.*, 2001 Mrc1 transduces signals of DNA replication stress to activate Rad53. Nat Cell Biol **3:** 958-965.

ANTCZAK, C., T. TAKAGI, C. N. RAMIREZ, C. RADU and H. DJABALLAH, 2009 Live-cell imaging of caspase activation for high-content screening. J Biomol Screen **14:** 956-969.

ARGUESO, J. L., J. WESTMORELAND, P. A. MIECZKOWSKI, M. GAWEL, T. D. PETES *et al.*, 2008 Double-strand breaks associated with repetitive DNA can reshape the genome. Proc Natl Acad Sci U S A **105:** 11845-11850.

AVRAM, D., and A. T. BAKALINSKY, 1997 SSU1 encodes a plasma membrane protein with a central role in a network of proteins conferring sulfite tolerance in Saccharomyces cerevisiae. J Bacteriol **179:** 5971-5974.

BACHRATI, C. Z., and I. D. HICKSON, 2008 RecQ helicases: guardian angels of the DNA replication fork. Chromosoma **117:** 219-233.

BAILEY, S. M., and J. P. MURNANE, 2006 Telomeres, chromosome instability and cancer. Nucleic Acids Res **34:** 2408-2417.

BAIRD, G. S., D. A. ZACHARIAS and R. Y. TSIEN, 2000 Biochemistry, mutagenesis, and oligomerization of DsRed, a red fluorescent protein from coral. Proc Natl Acad Sci U S A **97:** 11984-11989.

BANERJEE, S., and K. MYUNG, 2004 Increased genome instability and telomere length in the elg1-deficient Saccharomyces cerevisiae mutant are regulated by S-phase checkpoints. Eukaryot Cell **3:** 1557-1566.

BANERJEE, S., S. SMITH and K. MYUNG, 2006 Suppression of gross chromosomal rearrangements by yKu70-yKu80 heterodimer through DNA damage checkpoints. Proc Natl Acad Sci U S A **103:** 1816-1821.

BARR, F. G., 1998 Translocations, cancer and the puzzle of specificity. Nat Genet **19:** 121-124.

BATZER, M. A., and P. L. DEININGER, 2002 Alu repeats and human genomic diversity. Nat Rev Genet **3:** 370-379.

BELLAOUI, M., M. CHANG, J. OU, H. XU, C. BOONE *et al.*, 2003 Elg1 forms an alternative RFC complex important for DNA replication and genome integrity. EMBO J **22:** 4304-4313.

BEN-AROYA, S., A. KOREN, B. LIEFSHITZ, R. STEINLAUF and M. KUPIEC, 2003 ELG1, a yeast gene required for genome stability, forms a complex related to replication factor C. Proc Natl Acad Sci U S A **100:** 9906-9911.

BERNSTEIN, K. A., E. SHOR, I. SUNJEVARIC, M. FUMASONI, R. C. BURGESS *et al.*, 2009 Sgs1 function in the repair of DNA replication intermediates is separable from its role in homologous recombinational repair. EMBO J **28:** 915-925.

BEVIS, B. J., and B. S. GLICK, 2002 Rapidly maturing variants of the Discosoma red fluorescent protein (DsRed). Nat Biotechnol **20:** 83-87.

BIGNOLD, L. P., B. L. COGHLAN and H. P. JERSMANN, 2006 Hansemann, Boveri, chromosomes and the gametogenesis-related theories of tumours. Cell Biol Int **30:** 640-644.

BOSCO, G., and J. E. HABER, 1998 Chromosome break-induced DNA replication leads to nonreciprocal translocations and telomere capture. Genetics **150:** 1037-1047.

BRACHMANN, C. B., A. DAVIES, G. J. COST, E. CAPUTO, J. LI *et al.*, 1998 Designer deletion strains derived from Saccharomyces cerevisiae S288C: a useful set of strains and plasmids for PCR-mediated gene disruption and other applications. Yeast **14:** 115-132.

BRADBURY, J. M., and S. P. JACKSON, 2003 The complex matter of DNA double-strand break detection. Biochem Soc Trans **31:** 40-44.

BRESSAN, D. A., B. K. BAXTER and J. H. PETRINI, 1999 The Mre11-Rad50-Xrs2 protein complex facilitates homologous recombination-based double-strand break repair in Saccharomyces cerevisiae. Mol Cell Biol **19:** 7681-7687.

BRUSCHI, C. V., and P. J. CHUBA, 1988 Nonselective enrichment for yeast adenine mutants by flow cytometry. Cytometry **9:** 60-67.

BRUSCHI, C. V., A. R. COMER and G. A. HOWE, 1987 Specificity of DNA uptake during whole cell transformation of S. cerevisiae. Yeast **3:** 131-137.

BRUSCHI, C. V., and G. A. HOWE, 1988 High frequency FLP-independent homologous DNA recombination of 2 mu plasmid in the yeast Saccharomyces cerevisiae. Curr Genet **14:** 191-199.

CEJKA, P., and S. C. KOWALCZYKOWSKI, 2010 The full-length Saccharomyces cerevisiae Sgs1 protein is a vigorous DNA helicase that preferentially unwinds holliday junctions. J Biol Chem **285:** 8290-8301.

CHALEFF, D. T., and G. R. FINK, 1980 Genetic events associated with an insertion mutation in yeast. Cell **21:** 227-237.

CHEN, C., and R. D. KOLODNER, 1999 Gross chromosomal rearrangements in Saccharomyces cerevisiae replication and recombination defective mutants. Nat Genet **23:** 81-85.

CHI, P., S. VAN KOMEN, M. G. SEHORN, S. SIGURDSSON and P. SUNG, 2006 Roles of ATP binding and ATP hydrolysis in human Rad51 recombinase function. DNA Repair (Amst) **5:** 381-391.

CHU, W. K., and I. D. HICKSON, 2009 RecQ helicases: multifunctional genome caretakers. Nat Rev Cancer **9:** 644-654.

CIMINI, D., 2008 Merotelic kinetochore orientation, aneuploidy, and cancer. Biochim Biophys Acta **1786:** 32-40.

COBB, J. A., L. BJERGBAEK and S. M. GASSER, 2002 RecQ helicases: at the heart of genetic stability. FEBS Lett **529:** 43-48.

COBB, J. A., L. BJERGBAEK, K. SHIMADA, C. FREI and S. M. GASSER, 2003 DNA polymerase stabilization at stalled replication forks requires Mec1 and the RecQ helicase Sgs1. EMBO J **22:** 4325-4336.

COBB, J. A., T. SCHLEKER, V. ROJAS, L. BJERGBAEK, J. A. TERCERO *et al.*, 2005 Replisome instability, fork collapse, and gross chromosomal rearrangements arise synergistically from Mec1 kinase and RecQ helicase mutations. Genes Dev **19:** 3055-3069.

D'AMOURS, D., and S. P. JACKSON, 2001 The yeast Xrs2 complex functions in S phase checkpoint regulation. Genes Dev **15:** 2238-2249.

DALEY, J. M., P. L. PALMBOS, D. WU and T. E. WILSON, 2005 Nonhomologous end joining in yeast. Annu Rev Genet **39:** 431-451.

DATTA, A., and S. JINKS-ROBERTSON, 1995 Association of increased spontaneous mutation rates with high levels of transcription in yeast. Science **268:** 1616-1619.

DELLAIRE, G., J. YAN, K. C. LITTLE, R. DROUIN and P. CHARTRAND, 2002 Evidence that extrachromosomal double-strand break repair can be coupled to the repair of chromosomal double-strand breaks in mammalian cells. Chromosoma **111:** 304-312.

DELNERI, D., I. COLSON, S. GRAMMENOUDI, I. N. ROBERTS, E. J. LOUIS *et al.*, 2003 Engineering evolution to study speciation in yeasts. Nature **422:** 68-72.

DOWNS, J. A., and S. P. JACKSON, 2004 A means to a DNA end: the many roles of Ku. Nat Rev Mol Cell Biol **5:** 367-378.

DRESSER, M. E., D. J. EWING, S. N. HARWELL, D. COODY and M. N. CONRAD, 1994 Nonhomologous synapsis and reduced crossing over in a heterozygous paracentric inversion in Saccharomyces cerevisiae. Genetics **138:** 633-647.

DUESBERG, P., R. LI, A. FABARIUS and R. HEHLMANN, 2005 The chromosomal basis of cancer. Cell Oncol **27:** 293-318.

EGLI, D., E. HAFEN and W. SCHAFFNER, 2004 An efficient method to generate chromosomal rearrangements by targeted DNA double-strand breaks in Drosophila melanogaster. Genome Res **14:** 1382-1393.

FINKEL, T., and N. J. HOLBROOK, 2000 Oxidants, oxidative stress and the biology of ageing. Nature **408:** 239-247.

FISCHER, G., S. A. JAMES, I. N. ROBERTS, S. G. OLIVER and E. J. LOUIS, 2000 Chromosomal evolution in Saccharomyces. Nature **405:** 451-454.

FLEMING, A. B., and S. PENNINGS, 2007 Tup1-Ssn6 and Swi-Snf remodelling activities influence long-range chromatin organization upstream of the yeast SUC2 gene. Nucleic Acids Res **35:** 5520-5531.

FOIANI, M., A. PELLICIOLI, M. LOPES, C. LUCCA, M. FERRARI *et al.*, 2000 DNA damage checkpoints and DNA replication controls in Saccharomyces cerevisiae. Mutat Res **451:** 187-196.

FREI, C., and S. M. GASSER, 2000 The yeast Sgs1p helicase acts upstream of Rad53p in the DNA replication checkpoint and colocalizes with Rad53p in S-phase-specific foci. Genes Dev **14:** 81-96.

GASPARINI, P., G. SOZZI and M. A. PIEROTTI, 2007 The role of chromosomal alterations in human cancer development. J Cell Biochem **102:** 320-331.

GIETZ, D., A. ST JEAN, R. A. WOODS and R. H. SCHIESTL, 1992 Improved method for high efficiency transformation of intact yeast cells. Nucleic Acids Res **20:** 1425.

GJURACIC, K., E. PIVETTA and C. V. BRUSCHI, 2004 Targeted DNA integration within different functional gene domains in yeast reveals ORF sequences as recombinational cold-spots. Mol Genet Genomics **271:** 437-446.

GOFFEAU, A., B. G. BARRELL, H. BUSSEY, R. W. DAVIS, B. DUJON *et al.*, 1996 Life with 6000 genes. Science **274:** 546, 563-547.

GOLLIN, S. M., 2007 Mechanisms leading to nonrandom, nonhomologous chromosomal translocations in leukemia. Semin Cancer Biol **17:** 74-79.

GORDENIN, D. A., and M. A. RESNICK, 1998 Yeast ARMs (DNA at-risk motifs) can reveal sources of genome instability. Mutat Res **400:** 45-58.

HACKETT, J. A., D. M. FELDSER and C. W. GREIDER, 2001 Telomere dysfunction increases mutation rate and genomic instability. Cell **106:** 275-286.

HARRISON, J. C., and J. E. HABER, 2006 Surviving the breakup: the DNA damage checkpoint. Annu Rev Genet **40:** 209-235.

HAVIV-CHESNER, A., Y. KOBAYASHI, A. GABRIEL and M. KUPIEC, 2007 Capture of linear fragments at a double-strand break in yeast. Nucleic Acids Res **35:** 5192-5202.

HICKSON, I. D., 2003 RecQ helicases: caretakers of the genome. Nat Rev Cancer **3:** 169-178.

HINNEN, A., J. B. HICKS and G. R. FINK, 1978 Transformation of yeast. Proc Natl Acad Sci U S A **75:** 1929-1933.

HOEIJMAKERS, J. H., 2001 Genome maintenance mechanisms for preventing cancer. Nature **411:** 366-374.

HOLLAND, A. J., and D. W. CLEVELAND, 2009 Boveri revisited: chromosomal instability, aneuploidy and tumorigenesis. Nat Rev Mol Cell Biol **10:** 478-487.

IRA, G., A. MALKOVA, G. LIBERI, M. FOIANI and J. E. HABER, 2003 Srs2 and Sgs1-Top3 suppress crossovers during double-strand break repair in yeast. Cell **115:** 401-411.

JACKSON, J. A., and G. R. FINK, 1981 Gene conversion between duplicated genetic elements in yeast. Nature **292:** 306-311.

JAIN, S., N. SUGAWARA, J. LYDEARD, M. VAZE, N. TANGUY LE GAC *et al.*, 2009 A recombination execution checkpoint regulates the choice of homologous recombination pathway during DNA double-strand break repair. Genes Dev **23:** 291-303.

JANOUEIX-LEROSEY, I., P. HUPE, Z. MACIOROWSKI, P. LA ROSA, G. SCHLEIERMACHER *et al.*, 2005 Preferential occurrence of chromosome breakpoints within early replicating regions in neuroblastoma. Cell Cycle **4:** 1842-1846.

JINKS-ROBERTSON, S., and T. D. PETES, 1985 High-frequency meiotic gene conversion between repeated genes on nonhomologous chromosomes in yeast. Proc Natl Acad Sci U S A **82:** 3350-3354.

JINKS-ROBERTSON, S., and T. D. PETES, 1986 Chromosomal translocations generated by high-frequency meiotic recombination between repeated yeast genes. Genetics **114:** 731-752.

KAISER, C., S. MICHAELIS and A. MITCHELL, 1994 *Methods in Yeast Genetics*. Cold Spring Harbor Laboratory Press, New York.

KANELLIS, P., R. AGYEI and D. DUROCHER, 2003 Elg1 forms an alternative PCNA-interacting RFC complex required to maintain genome stability. Curr Biol **13:** 1583-1595.

KAROW, J. K., L. WU and I. D. HICKSON, 2000 RecQ family helicases: roles in cancer and aging. Curr Opin Genet Dev **10:** 32-38.

KAYE, J. A., J. A. MELO, S. K. CHEUNG, M. B. VAZE, J. E. HABER *et al.*, 2004 DNA breaks promote genomic instability by impeding proper chromosome segregation. Curr Biol **14:** 2096-2106.

KLEIN, H. L., 2001 Spontaneous chromosome loss in Saccharomyces cerevisiae is suppressed by DNA damage checkpoint functions. Genetics **159:** 1501-1509.

KLEIN, H. L., and T. D. PETES, 1981 Intrachromosomal gene conversion in yeast. Nature **289:** 144-148.

KOLODNER, R. D., C. D. PUTNAM and K. MYUNG, 2002 Maintenance of genome stability in Saccharomyces cerevisiae. Science **297:** 552-557.

KOPS, G. J., B. A. WEAVER and D. W. CLEVELAND, 2005 On the road to cancer: aneuploidy and the mitotic checkpoint. Nat Rev Cancer **5:** 773-785.

KURAHASHI, H., H. BOLOR, T. KATO, H. KOGO, M. TSUTSUMI *et al.*, 2009a Recent advance in our understanding of the molecular nature of chromosomal abnormalities. J Hum Genet **54:** 253-260.

KURAHASHI, H., H. INAGAKI, T. KATO, E. HOSOBA, H. KOGO *et al.*, 2009b Impaired DNA replication prompts deletions within palindromic sequences, but does not induce translocations in human cells. Hum Mol Genet **18:** 3397-3406.

LANGSTON, L. D., and L. S. SYMINGTON, 2004 Gene targeting in yeast is initiated by two independent strand invasions. Proc Natl Acad Sci U S A **101:** 15392-15397.

LAUF, U., P. LOPEZ and M. M. FALK, 2001 Expression of fluorescently tagged connexins: a novel approach to rescue function of oligomeric DsRed-tagged proteins. FEBS Lett **498:** 11-15.

LEE, J. A., C. M. CARVALHO and J. R. LUPSKI, 2007 A DNA replication mechanism for generating nonrecurrent rearrangements associated with genomic disorders. Cell **131:** 1235-1247.

LEE, K., Y. ZHANG and S. E. LEE, 2008 Saccharomyces cerevisiae ATM orthologue suppresses break-induced chromosome translocations. Nature **454:** 543-546.

LEE, S. K., R. E. JOHNSON, S. L. YU, L. PRAKASH and S. PRAKASH, 1999 Requirement of yeast SGS1 and SRS2 genes for replication and transcription. Science **286:** 2339-2342.

LEHMANN, A. R., 2001 The xeroderma pigmentosum group D (XPD) gene: one gene, two functions, three diseases. Genes Dev **15:** 15-23.

LEUNG, W., A. MALKOVA and J. E. HABER, 1997 Gene targeting by linear duplex DNA frequently occurs by assimilation of a single strand that is subject to preferential mismatch correction. Proc Natl Acad Sci U S A **94:** 6851-6856.

LIBERI, G., G. MAFFIOLETTI, C. LUCCA, I. CHIOLO, A. BARYSHNIKOVA *et al.*, 2005 Rad51-dependent DNA structures accumulate at damaged replication forks in sgs1 mutants defective in the yeast ortholog of BLM RecQ helicase. Genes Dev **19:** 339-350.

LICHTEN, M., R. H. BORTS and J. E. HABER, 1987 Meiotic gene conversion and crossing over between dispersed homologous sequences occurs frequently in Saccharomyces cerevisiae. Genetics **115:** 233-246.

LICHTEN, M., and J. E. HABER, 1989 Position effects in ectopic and allelic mitotic recombination in Saccharomyces cerevisiae. Genetics **123:** 261-268.

LIN, Y., and A. S. WALDMAN, 2001a Capture of DNA sequences at double-strand breaks in mammalian chromosomes. Genetics **158:** 1665-1674.

LIN, Y., and A. S. WALDMAN, 2001b Promiscuous patching of broken chromosomes in mammalian cells with extrachromosomal DNA. Nucleic Acids Res **29:** 3975-3981.

LINDAHL, T., 1993 Instability and decay of the primary structure of DNA. Nature **362:** 709-715.

LONGHESE, M. P., M. CLERICI and G. LUCCHINI, 2003 The S-phase checkpoint and its regulation in Saccharomyces cerevisiae. Mutat Res **532:** 41-58.

LONGHESE, M. P., M. FOIANI, M. MUZI-FALCONI, G. LUCCHINI and P. PLEVANI, 1998 DNA damage checkpoint in budding yeast. EMBO J **17:** 5525-5528.

LOU, H., M. KOMATA, Y. KATOU, Z. GUAN, C. C. REIS *et al.*, 2008 Mrc1 and DNA polymerase epsilon function together in linking DNA replication and the S phase checkpoint. Mol Cell **32:** 106-117.

LUTFIYYA, L. L., and M. JOHNSTON, 1996 Two zinc-finger-containing repressors are responsible for glucose repression of SUC2 expression. Mol Cell Biol **16:** 4790-4797.

LYDEARD, J. R., S. JAIN, M. YAMAGUCHI and J. E. HABER, 2007 Break-induced replication and telomerase-independent telomere maintenance require Pol32. Nature **448:** 820-823.

MA, J. L., S. J. LEE, J. K. DUONG and D. F. STERN, 2006 Activation of the checkpoint kinase Rad53 by the phosphatidyl inositol kinase-like kinase Mec1. J Biol Chem **281:** 3954-3963.

MAIZELS, N., 2005 Immunoglobulin gene diversification. Annu Rev Genet **39:** 23-46.

MALKOVA, A., M. L. NAYLOR, M. YAMAGUCHI, G. IRA and J. E. HABER, 2005 RAD51-dependent break-induced replication differs in kinetics and checkpoint responses from RAD51-mediated gene conversion. Mol Cell Biol **25:** 933-944.

MANKOURI, H. W., H. P. NGO and I. D. HICKSON, 2009 Esc2 and Sgs1 act in functionally distinct branches of the homologous recombination repair pathway in Saccharomyces cerevisiae. Mol Biol Cell **20:** 1683-1694.

MIECZKOWSKI, P. A., F. J. LEMOINE and T. D. PETES, 2006 Recombination between retrotransposons as a source of chromosome rearrangements in the yeast Saccharomyces cerevisiae. DNA Repair (Amst) **5:** 1010-1020.

MIKUS, M. D., and T. D. PETES, 1982 Recombination between genes located on nonhomologous chromosomes in Saccharomyces cerevisiae. Genetics **101:** 369-404.

MIMITOU, E. P., and L. S. SYMINGTON, 2008 Sae2, Exo1 and Sgs1 collaborate in DNA double-strand break processing. Nature **455:** 770-774.

MISTELI, T., and E. SOUTOGLOU, 2009 The emerging role of nuclear architecture in DNA repair and genome maintenance. Nat Rev Mol Cell Biol **10:** 243-254.

MITELMAN, F., B. JOHANSSON and F. MERTENS, 2004 Fusion genes and rearranged genes as a linear function of chromosome aberrations in cancer. Nat Genet **36:** 331-334.

MITELMAN, F., B. JOHANSSON and F. MERTENS, 2007 The impact of translocations and gene fusions on cancer causation. Nat Rev Cancer **7:** 233-245.

MORROW, D. M., C. CONNELLY and P. HIETER, 1997 "Break copy" duplication: a model for chromosome fragment formation in Saccharomyces cerevisiae. Genetics **147:** 371-382.

MURNANE, J. P., 2006 Telomeres and chromosome instability. DNA Repair (Amst) **5:** 1082-1092.

MYUNG, K., A. DATTA, C. CHEN and R. D. KOLODNER, 2001a SGS1, the Saccharomyces cerevisiae homologue of BLM and WRN, suppresses genome instability and homeologous recombination. Nat Genet **27:** 113-116.

MYUNG, K., A. DATTA and R. D. KOLODNER, 2001b Suppression of spontaneous chromosomal rearrangements by S phase checkpoint functions in Saccharomyces cerevisiae. Cell **104:** 397-408.

MYUNG, K., and R. D. KOLODNER, 2002 Suppression of genome instability by redundant S-phase checkpoint pathways in Saccharomyces cerevisiae. Proc Natl Acad Sci U S A **99:** 4500-4507.

NAMBIAR, M., V. KARI and S. C. RAGHAVAN, 2008 Chromosomal translocations in cancer. Biochim Biophys Acta **1786:** 139-152.

NIKITIN, D., V. TOSATO, A. B. ZAVEC and C. V. BRUSCHI, 2008 Cellular and molecular effects of nonreciprocal chromosome translocations in Saccharomyces cerevisiae. Proc Natl Acad Sci U S A **105:** 9703-9708.

NORRIS, M. D., J. SMITH, K. TANABE, P. TOBIN, C. FLEMMING *et al.*, 2005 Expression of multidrug transporter MRP4/ABCC4 is a marker of poor prognosis in neuroblastoma and confers resistance to irinotecan in vitro. Mol Cancer Ther **4:** 547-553.

OGAWA, T., X. YU, A. SHINOHARA and E. H. EGELMAN, 1993 Similarity of the yeast RAD51 filament to the bacterial RecA filament. Science **259:** 1896-1899.

OKA, A., H. SUGISAKI and M. TAKANAMI, 1981 Nucleotide sequence of the kanamycin resistance transposon Tn903. J Mol Biol **147:** 217-226.

ONODA, F., M. SEKI, A. MIYAJIMA and T. ENOMOTO, 2000 Elevation of sister chromatid exchange in Saccharomyces cerevisiae sgs1 disruptants and the relevance of the disruptants as a system to evaluate mutations in Bloom's syndrome gene. Mutat Res **459:** 203-209.

ORR-WEAVER, T. L., J. W. SZOSTAK and R. J. ROTHSTEIN, 1981 Yeast transformation: a model system for the study of recombination. Proc Natl Acad Sci U S A **78:** 6354-6358.

ORR-WEAVER, T. L., J. W. SZOSTAK and R. J. ROTHSTEIN, 1983 Genetic applications of yeast transformation with linear and gapped plasmids. Methods Enzymol **101:** 228-245.

OSBORN, A. J., and S. J. ELLEDGE, 2003 Mrc1 is a replication fork component whose phosphorylation in response to DNA replication stress activates Rad53. Genes Dev **17:** 1755-1767.

PACIOTTI, V., M. CLERICI, G. LUCCHINI and M. P. LONGHESE, 2000 The checkpoint protein Ddc2, functionally related to S. pombe Rad26, interacts with Mec1 and is regulated by Mec1-dependent phosphorylation in budding yeast. Genes Dev **14:** 2046-2059.

PACIOTTI, V., G. LUCCHINI, P. PLEVANI and M. P. LONGHESE, 1998 Mec1p is essential for phosphorylation of the yeast DNA damage checkpoint protein Ddc1p, which physically interacts with Mec3p. EMBO J **17:** 4199-4209.

PANE, F., M. INTRIERI, C. QUINTARELLI, B. IZZO, G. C. MUCCIOLI *et al.*, 2002 BCR/ABL genes and leukemic phenotype: from molecular mechanisms to clinical correlations. Oncogene **21:** 8652-8667.

PARRY, E. M., and B. S. COX, 1970 The tolerance of aneuploidy in yeast. Genet Res **16:** 333-340.

PEARSON, C. E., K. NICHOL EDAMURA and J. D. CLEARY, 2005 Repeat instability: mechanisms of dynamic mutations. Nat Rev Genet **6:** 729-742.

PEDERSEN, B., J. M. NORGAARD, B. B. PEDERSEN, N. CLAUSEN, I. H. RASMUSSEN *et al.*, 2000 Many unbalanced translocations show duplication of a translocation participant. Clinical and cytogenetic implications in myeloid hematologic malignancies. Am J Hematol **64:** 161-169.

PENNANEACH, V., C. D. PUTNAM and R. D. KOLODNER, 2006 Chromosome healing by de novo telomere addition in Saccharomyces cerevisiae. Mol Microbiol **59:** 1357-1368.

PEREZ-ORTIN, J. E., A. QUEROL, S. PUIG and E. BARRIO, 2002 Molecular characterization of a chromosomal rearrangement involved in the adaptive evolution of yeast strains. Genome Res **12:** 1533-1539.

PERLMAN, D., H. O. HALVORSON and L. E. CANNON, 1982 Presecretory and cytoplasmic invertase polypeptides encoded by distinct mRNAs derived from the same structural gene differ by a signal sequence. Proc Natl Acad Sci U S A **79:** 781-785.

PETES, T. D., 1979 Yeast ribosomal DNA genes are located on chromosome XII. Proc Natl Acad Sci U S A **76:** 410-414.

PLESSIS, A., and B. DUJON, 1993 Multiple tandem integrations of transforming DNA sequences in yeast chromosomes suggest a mechanism for integrative transformation by homologous recombination. Gene **134:** 41-50.

POLAKOVA, S., C. BLUME, J. A. ZARATE, M. MENTEL, D. JORCK-RAMBERG *et al.*, 2009 Formation of new chromosomes as a virulence mechanism in yeast Candida glabrata. Proc Natl Acad Sci U S A **106:** 2688-2693.

POTIER, S., B. WINSOR and F. LACROUTE, 1982 Genetic selection for reciprocal translocation at chosen chromosomal sites in Saccharomyces cerevisiae. Mol Cell Biol **2:** 1025-1032.

PRADO, F., F. CORTES-LEDESMA, P. HUERTAS and A. AGUILERA, 2003 Mitotic recombination in Saccharomyces cerevisiae. Curr Genet **42:** 185-198.

PUIGVERT, J. C., H. DE BONT, B. VAN DE WATER and E. H. DANEN, 2010 High-throughput live cell imaging of apoptosis. Curr Protoc Cell Biol **Chapter 18:** Unit 18 10 11-13.

PUTNAM, C. D., T. K. HAYES and R. D. KOLODNER, 2009 Specific pathways prevent duplication-mediated genome rearrangements. Nature **460:** 984-989.

PUTNAM, C. D., V. PENNANEACH and R. D. KOLODNER, 2004 Chromosome healing through terminal deletions generated by de novo telomere additions in Saccharomyces cerevisiae. Proc Natl Acad Sci U S A **101:** 13262-13267.

ROEDER, G. S., P. J. FARABAUGH, D. T. CHALEFF and G. R. FINK, 1980 The origins of gene instability in yeast. Science **209:** 1375-1380.

ROEDER, G. S., and G. R. FINK, 1980 DNA rearrangements associated with a transposable element in yeast. Cell **21:** 239-249.

ROSSI, B., P. NOEL and C. V. BRUSCHI, 2010 Different Aneuploidies Arise From the Same Bridge-induced Chromosomal Translocation Event in Saccharomyces cerevisiae. Genetics **Epub ahead of print**.

ROWLEY, J. D., 2001 Chromosome translocations: dangerous liaisons revisited. Nat Rev Cancer **1:** 245-250.

SABATIER, L., M. RICOUL, G. POTTIER and J. P. MURNANE, 2005 The loss of a single telomere can result in instability of multiple chromosomes in a human tumor cell line. Mol Cancer Res **3:** 139-150.

SAMBROOK, J., E. F. FRITSCH and T. MANIATIS, 1989 *Molecular cloning, a laboratory manual.* Cold Spring Harbor Laboratory Press, Cold Spring Harbor, New York.

SAN FILIPPO, J., P. SUNG and H. KLEIN, 2008 Mechanism of eukaryotic homologous recombination. Annu Rev Biochem **77:** 229-257.

SANDELL, L. L., and V. A. ZAKIAN, 1993 Loss of a yeast telomere: arrest, recovery, and chromosome loss. Cell **75:** 729-739.

SAXE, D., A. DATTA and S. JINKS-ROBERTSON, 2000 Stimulation of mitotic recombination events by high levels of RNA polymerase II transcription in yeast. Mol Cell Biol **20:** 5404-5414.

SCHERER, S., and R. W. DAVIS, 1979 Replacement of chromosome segments with altered DNA sequences constructed in vitro. Proc Natl Acad Sci U S A **76:** 4951-4955.

SCHERER, S., and R. W. DAVIS, 1980 Recombination of dispersed repeated DNA sequences in yeast. Science **209:** 1380-1384.

SCHMIDT, K. H., J. WU and R. D. KOLODNER, 2006 Control of translocations between highly diverged genes by Sgs1, the Saccharomyces cerevisiae homolog of the Bloom's syndrome protein. Mol Cell Biol **26:** 5406-5420.

SHAFFER, B., I. BREARLEY, R. LITTLEWOOD and G. R. FINK, 1971 A stable aneuploid of Saccharomyces cerevisiae. Genetics **67:** 483-495.

SHAW, C. J., and J. R. LUPSKI, 2004 Implications of human genome architecture for rearrangement-based disorders: the genomic basis of disease. Hum Mol Genet **13 Spec No 1:** R57-64.

SMITH, C. E., B. LLORENTE and L. S. SYMINGTON, 2007 Template switching during break-induced replication. Nature **447:** 102-105.

SMITH, S., A. GUPTA, R. D. KOLODNER and K. MYUNG, 2005 Suppression of gross chromosomal rearrangements by the multiple functions of the Mre11-Rad50-Xrs2 complex in Saccharomyces cerevisiae. DNA Repair (Amst) **4:** 606-617.

SOGO, J. M., M. LOPES and M. FOIANI, 2002 Fork reversal and ssDNA accumulation at stalled replication forks owing to checkpoint defects. Science **297:** 599-602.

SPELL, R. M., and S. JINKS-ROBERTSON, 2003 Role of mismatch repair in the fidelity of RAD51- and RAD59-dependent recombination in Saccharomyces cerevisiae. Genetics **165:** 1733-1744.

STORICI, F., M. COGLIEVINA and C. V. BRUSCHI, 1999 A 2-microm DNA-based marker recycling system for multiple gene disruption in the yeast Saccharomyces cerevisiae. Yeast **15:** 271-283.

STORICI, F., L. K. LEWIS and M. A. RESNICK, 2001 In vivo site-directed mutagenesis using oligonucleotides. Nat Biotechnol **19:** 773-776.

SUGAWARA, N., and J. W. SZOSTAK, 1983a Construction of specific chromosomal rearrangements in yeast. Methods Enzymol **101:** 269-278.

SUGAWARA, N., and J. W. SZOSTAK, 1983b Recombination between sequences in nonhomologous positions. Proc Natl Acad Sci U S A **80:** 5675-5679.

SVETEC, I. K., A. STAFA and Z. ZGAGA, 2007 Genetic side effects accompanying gene targeting in yeast: the influence of short heterologous termini. Yeast **24:** 637-652.

SWEENEY, F. D., F. YANG, A. CHI, J. SHABANOWITZ, D. F. HUNT *et al.*, 2005 Saccharomyces cerevisiae Rad9 acts as a Mec1 adaptor to allow Rad53 activation. Curr Biol **15:** 1364-1375.

SYMINGTON, L. S., 2002 Role of RAD52 epistasis group genes in homologous recombination and double-strand break repair. Microbiol Mol Biol Rev **66:** 630-670, table of contents.

SZOSTAK, J. W., T. L. ORR-WEAVER, R. J. ROTHSTEIN and F. W. STAHL, 1983 The double-strand-break repair model for recombination. Cell **33:** 25-35.

TAUSSIG, R., and M. CARLSON, 1983 Nucleotide sequence of the yeast SUC2 gene for invertase. Nucleic Acids Res **11:** 1943-1954.

TORRES, E. M., T. SOKOLSKY, C. M. TUCKER, L. Y. CHAN, M. BOSELLI *et al.*, 2007 Effects of aneuploidy on cellular physiology and cell division in haploid yeast. Science **317:** 916-924.

TORRES, E. M., B. R. WILLIAMS and A. AMON, 2008 Aneuploidy: cells losing their balance. Genetics **179:** 737-746.

TOSATO, V., C. NICOLINI and C. V. BRUSCHI, 2009 DNA bridging of yeast chromosomes VIII leads to near-reciprocal translocation and loss of heterozygosity with minor cellular defects. Chromosoma **118:** 179-191.

TOSATO, V., S. K. WAGHMARE and C. V. BRUSCHI, 2005 Non-reciprocal chromosomal bridge-induced translocation (BIT) by targeted DNA integration in yeast. Chromosoma **114:** 15-27.

UMEZU, K., M. HIRAOKA, M. MORI and H. MAKI, 2002 Structural analysis of aberrant chromosomes that occur spontaneously in diploid Saccharomyces cerevisiae: retrotransposon Ty1 plays a crucial role in chromosomal rearrangements. Genetics **160:** 97-110.

VANHULLE, K., F. J. LEMOINE, V. NARAYANAN, B. DOWNING, K. HULL *et al.*, 2007 Inverted DNA repeats channel repair of distant double-strand breaks into chromatid fusions and chromosomal rearrangements. Mol Cell Biol **27:** 2601-2614.

VERSINI, G., I. COMET, M. WU, L. HOOPES, E. SCHWOB *et al.*, 2003 The yeast Sgs1 helicase is differentially required for genomic and ribosomal DNA replication. EMBO J **22:** 1939-1949.

VIZEACOUMAR, F. J., Y. CHONG, C. BOONE and B. J. ANDREWS, 2009 A picture is worth a thousand words: genomics to phenomics in the yeast Saccharomyces cerevisiae. FEBS Lett **583:** 1656-1661.

WACH, A., A. BRACHAT, R. POHLMANN and P. PHILIPPSEN, 1994 New heterologous modules for classical or PCR-based gene disruptions in Saccharomyces cerevisiae. Yeast **10:** 1793-1808.

WAGA, S., and B. STILLMAN, 1998 The DNA replication fork in eukaryotic cells. Annu Rev Biochem **67:** 721-751.

WAGHMARE, S. K., and C. V. BRUSCHI, 2005 Differential chromosome control of ploidy in the yeast Saccharomyces cerevisiae. Yeast **22:** 625-639.

WAGHMARE, S. K., V. CAPUTO, S. RADOVIC and C. V. BRUSCHI, 2003 Specific targeted integration of kanamycin resistance-associated nonselectable DNA in the genome of the yeast Saccharomyces cerevisiae. Biotechniques **34:** 1024-1028, 1033.

WATT, P. M., I. D. HICKSON, R. H. BORTS and E. J. LOUIS, 1996 SGS1, a homologue of the Bloom's and Werner's syndrome genes, is required for maintenance of genome stability in Saccharomyces cerevisiae. Genetics **144:** 935-945.

WATT, P. M., E. J. LOUIS, R. H. BORTS and I. D. HICKSON, 1995 Sgs1: a eukaryotic homolog of E. coli RecQ that interacts with topoisomerase II in vivo and is required for faithful chromosome segregation. Cell **81:** 253-260.

WEAVER, B. A., and D. W. CLEVELAND, 2006 Does aneuploidy cause cancer? Curr Opin Cell Biol **18:** 658-667.

WEINERT, T., 1998 DNA damage checkpoints update: getting molecular. Curr Opin Genet Dev **8:** 185-193.

WEINERT, T. A., and L. H. HARTWELL, 1988 The RAD9 gene controls the cell cycle response to DNA damage in Saccharomyces cerevisiae. Science **241:** 317-322.

WYMAN, C., and R. KANAAR, 2006 DNA double-strand break repair: all's well that ends well. Annu Rev Genet **40:** 363-383.

YAMAGATA, K., J. KATO, A. SHIMAMOTO, M. GOTO, Y. FURUICHI *et al.*, 1998 Bloom's and Werner's syndrome genes suppress hyperrecombination in yeast sgs1 mutant: implication for genomic instability in human diseases. Proc Natl Acad Sci U S A **95:** 8733-8738.

YAMANA, Y., T. MAEDA, H. OHBA, T. USUI, H. I. OGAWA *et al.*, 2005 Regulation of homologous integration in yeast by the DNA repair proteins Ku70 and RecQ. Mol Genet Genomics **273:** 167-176.

YEH, A., M. WEI, S. B. GOLUB, D. J. YAMASHIRO, V. V. MURTY *et al.*, 2002 Chromosome arm 16q in Wilms tumors: unbalanced chromosomal translocations, loss of heterozygosity, and assessment of the CTCF gene. Genes Chromosomes Cancer **35:** 156-163.

YU, X., and A. GABRIEL, 2004 Reciprocal translocations in Saccharomyces cerevisiae formed by nonhomologous end joining. Genetics **166:** 741-751.

ZHU, Z., W. H. CHUNG, E. Y. SHIM, S. E. LEE and G. IRA, 2008 Sgs1 helicase and two nucleases Dna2 and Exo1 resect DNA double-strand break ends. Cell **134:** 981-994.

ZOU, L., and S. J. ELLEDGE, 2003 Sensing DNA damage through ATRIP recognition of RPA-ssDNA complexes. Science **300:** 1542-1548.

ZOU, L., D. LIU and S. J. ELLEDGE, 2003 Replication protein A-mediated recruitment and activation of Rad17 complexes. Proc Natl Acad Sci U S A **100:** 13827-13832.

Strain background	*Translocant*	*Chromosome XV*	*Chromosome IX*	*Translocated Chr.*	*Fragment XV*	*Fragment IX*
SAN1	SAD #1	✓	✗	✓	WT	✗
SAN1	SAD #16	✓	✓	✓	WT✓ and ✪	WT
SAN1	SAD #17	✓	✓	✓	WT	WT
SAN1	SAD #18	✓	✓	✓	WT	WT
SAN1	SAD #31	✓	✓	✓	WT	WT
SAN1	SAD #59	✓	✓	✓	WT	WT
SAN1	SAD #802	✓	✓	✓	WT	WT
PAW1	SAD #3	✓	✓	✓	WT	WT
PAW1	SAD #33	✓	✗	✓	WT	✗
PAW1	SAD #801	✓	✗	✓	WT	✗
mre11Δ/Δ	MR3	✓	✓	✓	WT	WT
mre11Δ/Δ	MR30	✓	✓	✓	WT	WT
tel1Δ/Δ	TL8	✓	✓	✓	WT	WT
tel1Δ/Δ	TL39	✓	✓	✓	WT	WT
ku70Δ/Δ	K53	✓	✓	✓	WT	WT
ku70Δ/Δ	K54	✓	✗	✓	WT	✗
ku70Δ/Δ	K60	✓	✗	✪	WT	✗
ku70Δ/Δ	K82	✓	✗	✓	WT	✗
ku70Δ/Δ	K85	✓	✓	✓	WT	WT
ku70Δ/Δ	K102	✓	✗	✓	WT	✗
sgs1Δ/Δ	S125	✓	✗	✓	WT	✗
sgs1Δ/Δ	S126	✓	✗	✓	WT	✗
sgs1Δ/Δ	S171	✓	✗	✓	WT	✗
sgs1Δ/Δ	S174	✓	✗	✓	WT	✗
sgs1Δ/Δ	S177	✓	✓	✓	WT	WT
sgs1Δ/Δ	S179	✓	✓	✓	WT	WT
sgs1Δ/Δ	S191	✓	✗	✓	WT	✗
sgs1Δ/Δ	S192	✓	✓	✓ and ✪	WT	
					WT	
elg1Δ/Δ	E194	✓	✓	✓	WT	WT
esc2Δ/Δ	EC18	✓	✗	✓	WT	✗
esc2Δ/Δ	EC57	✓	✗	✓	WT	✗
esc2Δ/Δ	EC70	✓	✗	✓	WT	✗
mrc1Δ/Δ	MC7	✓	✓	✗	WT	WT
mrc1Δ/Δ	MC55	✓	✓	✓	WT	WT and ✪
tel1Δ/Δ sgs1Δ/Δ	TS2-13	✓	✓	✓	WT	WT
tel1Δ/Δ sgs1Δ/Δ	TS2-14	✓	✓	✓	WT	WT

Appendix 1. A list of all the translocants described in Results Chapter 4 and Discussions 6.2. Relevant genetic backgrounds and translocant names are mentioned on the right, followed by a summary of southern hybridization based, detected (✓) or undetected (✗) chromosomes and/or chromosomal fragments. WT is wild type chromosome configuration; ✪ represents any unusual secondary rearrangements noticed. Shaded in green are representative examples from each mutant background that were also analysed for gene copy number via QPCR.

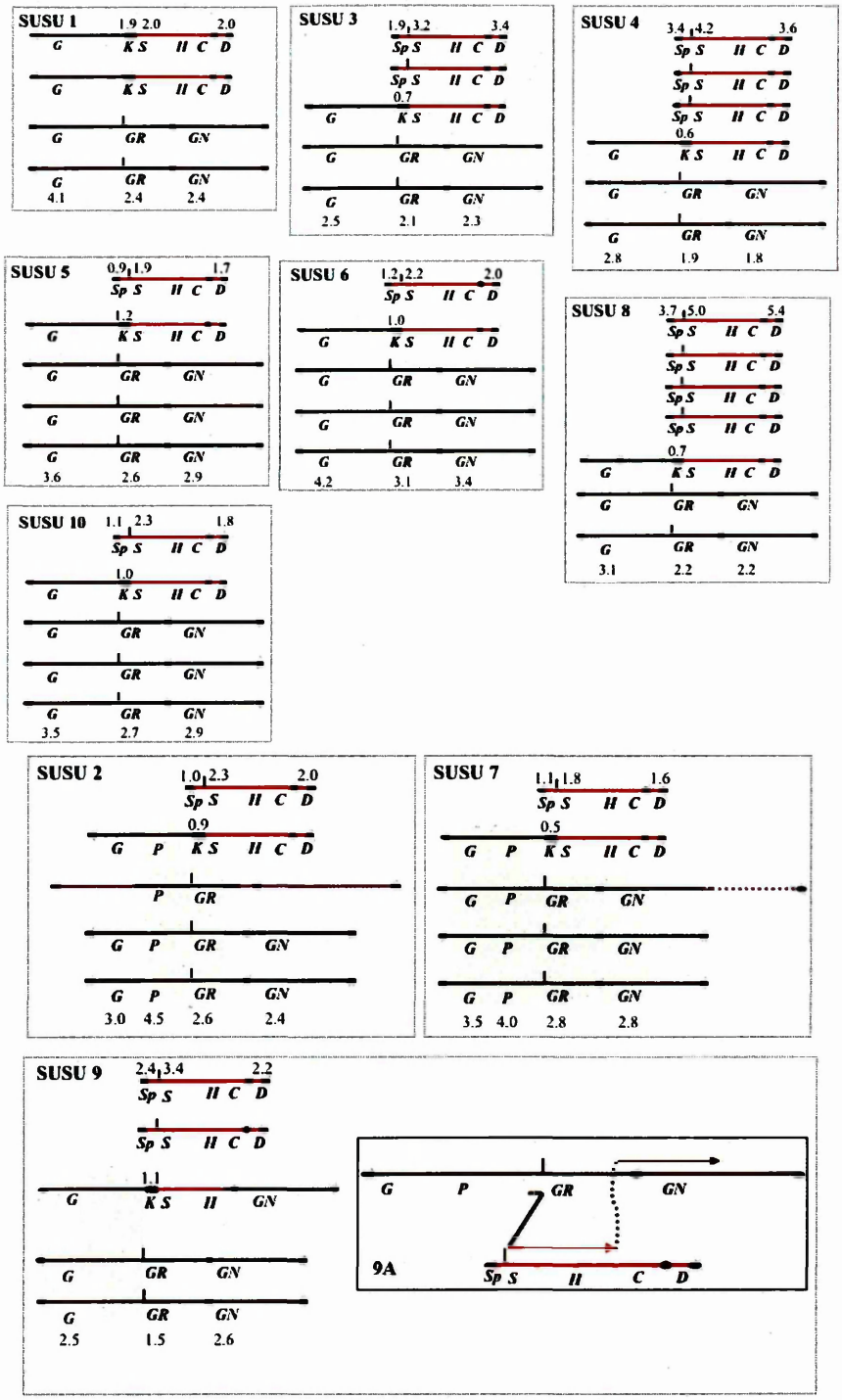

Appendix 2. Schematic representation of the genotypic situation for chromosomes XVI and IX, in SUSU translocants. The genes analyzed in the Southern hybridization and gene copy number experiments are reported. Gene copy number values are numerically indicated. **G**: *GAL4*; **GR**: *GLR1*, **GN**: *GLN1*, **S**: *SUC2*, **H**: *HIS5*, **C**: *CFD1*, **D**: *DAL4*, **K**: *KANMX4*. The scheme contained in panel 9A shows a putative template switching-like mechanism that might be responsible for the rearrangement observed in SUSU9.